CCRIF SPC
The Caribbean Catastrophe Risk Insurance Facility

Technical Workshop on CCRIF Models

March 14 & 15 2019
Caribbean Development Bank
Barbados

www.ccrif.org
ccrif spc
pr@ccrif.org
@ccrif_pr

TECHNICAL STAKEHOLDER WORKSHOP ON NEW CCRIF MODELS

MAIN OBJECTIVES

- To provide an in-depth overview and facilitate a comprehensive understanding of the new CCRIF models including information on the data underpinning the models
- Understand the rationale for updating the models
- A review of the country risk profiles, how these were developed, the data used and the rationale for the use of specific data sources; including brainstorming on ways in which the risk profiles can be used by countries for development planning, physical planning, policy development among other purposes; and how regional organizations could make use of the risk profiles in their own programming and in projects being developed and implemented by them
- To obtain feedback from stakeholders that may be critical in the policy renewal process for 2019/20
- To receive information from regional organizations that may inform CCRIF's models, products and services
- To present information related to the development of new models for agriculture, utilities etc. and the demand for these products
- Demonstration of web application tool for rainfall and discussion on its use
- Enhanced understanding of CCRIF and the products and services its provides
- To foster improved stakeholder engagement and enhanced relationships between CCRIF and regional organizations

Participating Organizations

- CIMH
- CDEMA
- CDB
- OECS
- CARICOM Secretariat
- ACS
- SRC (UWI St. Augustine)
- CERMES (UWI Cave Hill)
- Climate Studies Group (UWI Mona)
- CARICAD
- CCCCC
- CRFM
- Barbados Met Service
- Trinidad and Tobago Met Service
- Trinidad and Tobago ODPM
- UNECLAC
- CARDI
- CMO
- MCII
- World Bank

PARAMETRIC INSURANCE AND THE CCRIF CATASTROPHE MODEL

CCRIF policies were designed as parametric insurance instruments. Parametric insurance products are insurance contracts that make payments based on the intensity of an event (for example, hurricane wind speed, earthquake intensity, volume of rainfall) and the amount of loss calculated in a pre-agreed model caused by these events.

Parametric insurance disburses funds based on the occurrence of a pre-defined level of hazard and impact	Policy triggered on the basis of exceeding a pre-established trigger event loss
	Estimated based on wind speed and storm surge (tropical cyclones) or ground shaking (earthquakes) or volume of rainfall (excess rainfall)
	Hazard levels applied to pre-defined government exposure to produce a loss estimate
	Payout amounts increase with the level of modelled loss, up to a pre-defined coverage limit

The selection of a parametric instrument as a basis for the CCRIF policies was largely driven by the fact that parametric insurance is generally less expensive than an equivalent traditional indemnity insurance product as it does not require a loss assessment procedure in case of a disaster. Parametric insurance also allows for claims to be settled quickly. This is an important feature considering the urgent need for liquidity after a catastrophe.

However, despite the many benefits to parametric insurance, parametric products are exposed to basis risk, i.e., the possibility that calculated or modelled losses may be higher or lower than actual losses on the ground. Although this is a significant challenge in terms of the development of a parametric instrument, careful design of input parameters (identified in specially prepared country risk profiles) and the loss model as undertaken by CCRIF helps reduce the basis risk.

The CCRIF catastrophe models and their use in underpinning country policies

The objective of the loss modelling approach is to equip CCRIF with the capacity to estimate loss probabilities for individual countries, price contracts for specific countries, and estimate site-specific hazard levels and losses for specific events during the contract period.

In undertaking the development of the CCRIF parametric insurance coverage, significant investment has gone into developing the underlying catastrophe models. Catastrophe models are essential tools in assessing the risk associated with catastrophe events. The CCRIF model is based on robust datasets all developed within the context of the particular hazards of relevance to the client countries.

- TC is modelled using wind and storm surge data from the US National Oceanic and Atmospheric Administration (NOAA)

- EQ is modelled using source magnitude and hypocentre (location and depth) data obtained from the United States Geological Survey
- XSR is modelled using data from the Global Forecasting System (GFS) and CPC Morphing Technique (CMORPH) models produced by the US National Centers for Environmental Prediction (NCEP) and Climate Prediction Center (CPC)

The use of external public data sources, such as the ones mentioned above, provides a uniform model input for all member countries; guarantees real-time information to run the pre-agreed models; determines in the least possible amount of time whether a payout has been triggered; and eliminates the risk of not being able to collect information from local agencies due to a malfunction caused by the hazard event itself.

CCRIF strives to improve continuously the quality of the models used to underpin the country policies according to the most recent state of the art. The models are based on the latest scientific findings and the most updated hazard datasets.

Models for Tropical Cyclone and Earthquake

Starting in 2019/20 CCRIF will be using a new earthquake and tropical cyclone risk model, which is part of the platform called SPHERA (System for Probabilistic Hazard Evaluation and Risk Assessment). This replaces the Multi-Peril Risk Evaluation System (MPRES) model, used since 2011. The Tropical Cyclone and Earthquake models in SPHERA are last-generation state-of-the-art models that incorporate the most recent technical and scientific improvements and helps strengthen the financial resilience of CCRIF by estimating tropical cyclone and earthquake frequencies and intensities with a greater level of accuracy compared to other tools available for the region. The SPHERA suite of models has been reviewed by international experts, who have acknowledged it to be robust and reliable.

Model for Excess Rainfall

The current excess rainfall model – the CCRIF Excess Rainfall Model 2 (XSR 2) is based on public and internationally recognized precipitation datasets and meteorological models, which provide data from 1998. In 2015, CCRIF modified the existing rainfall model to improve the model estimates and the structure of the excess rainfall policy. XSR 2 is based on data from the Global Forecasting System (GFS) and CPC Morphing Technique (CMORPH) models produced by the US National Centers for Environmental Prediction (NCEP) and Climate Prediction Center (CPC). This weather models assimilate, when available, data such as rain, temperature, wind speed, humidity and pressure to improve modelled rain estimates. The final datasets provide accurate and reliable future daily rainfall estimates and have available a relatively long period of past data, which is necessary to fine-tune a forecasting rainfall model.

The first version of the XSR 2 model (XSR 2.0) was updated in 2017. Given the intense activity of the 2017 hurricane season, XSR 2.0 was updated by including data on several important rainfall events that occurred in 2016 and 2017, such as tropical cyclones Earl, Matthew, Irma and Maria and other rainfall events not induced by tropical cyclones. For the updated model, known as XSR 2.1, the inclusion of these events within the risk analysis of the countries provide a significant improvement in the assessment of the precipitation hazard in the region and allowed more accurate policies to be designed for member countries starting in the 2018/19 policy year. Along with the precipitation datasets used in the hazard module of the XSR model, the exposure and vulnerability modules also were updated to include additional exposure data on some additional assets and infrastructure. These data included mainly road networks and infrastructure, which improved the representation of distribution of the assets at risk in Caribbean and Central American countries. These revisions allowed for a more robust risk analysis and a reduction of the basis risk in the excess rainfall policy product.

The XSR 2.1 model has been upgraded to XSR 2.5 and this new model will be used to underpin the 2019/20 policies. Improvements and new features in the XSR 2.5 model include the consideration of soil saturation in addition to the pure rainfall in the loss calculation, as well as a multi-trigger CARE based on additional WRF configurations. These changes have been made to better represent smaller and/or localized severe rainfall events in the model.

SPHERA

A TROPICAL CYCLONE AND EARTHQUAKE LOSS MODEL FOR THE CARIBBEAN AND CENTRAL AMERICA

MODEL DESCRIPTION

THE SPHERA TROPICAL CYCLONE MODEL

CCRIF has recently developed a new in-house tropical cyclone risk model, called System for Probabilistic Hazard Evaluation and Risk Assessment (SPHERA). This new development was intended to provide CCRIF with the best technology available for the area it operates, according to the state of the art of the tropical cyclone risk assessment sector. The model was developed in collaboration with RED (Risk, Engineering and Development, Italy) and ERN (Evaluación de Riesgos Naturales, Mexico). The SPHERA tropical cyclone risk model estimates the probability of damages caused by tropical cyclone-induced winds and storm surge and will be used in the following policy years to underpin the tropical cyclone parametric insurance products offered by CCRIF.

The conceptual structure of the SPHERA model is composed by the three classic elements of the risk analysis: hazard, vulnerability and exposure. The hazard module computes the likelihood of the occurrence of an event and its intensity, the vulnerability module estimates the response of the country's assets to various levels of event intensity and the exposure module quantify the value, or replacement cost, of the country's assets. Furthermore, a loss computation module is used to combine these three components to estimate the damages caused by an event (or a set of events).

Hazard Module

The tropical cyclone hazard of the SPHERA loss model has two components: maximum wind speed and maximum storm surge. "Maximum wind speed" is the maximum velocity reached by the wind in a specific point during a tropical cyclone. The measure of wind speed used by the SPHERA model is the maximum averaged 1-minutes wind speed, in km/h. "Maximum storm surge" is the maximum level of water caused by the combined effect of a tropical cyclone (pressure drop and wind friction) and the astronomical tide at a specific location during a tropical cyclone, in m[1]. Both hazard measures are computed for a large set of locations through the use of mathematical models. The locations represent sites where one or more assets are located according to the exposure database.

Wind hazard model

A tropical cyclone is a rotating storm system characterized by a low-pressure centre and strong winds. Several types of mathematical models are available to reproduce this complex phenomenon and compute wind speed values over a large geographical domain, ranging from complex numerical weather model to simpler and faster parametric models. The wind component of the SPHERA model is based on a modified version of a parametric wind model published by Silva et al. (2002) . This model

[1] Note: in general, the term "storm surge" usually indicates the sea level rise due exclusively to a storm, not including the astronomical tide effect. However, in this document, to avoid excessive repetitions, the term "storm surge" is referred to the sum of both effects, unless specifically indicated.

is a modification of the Holland model, widely used in the field of tropical cyclone risk modelling. The model computes wind speed (and pressure) over a large domain, on the basis of input parameter values that can be usually found in the tropical cyclone best track database provided by all major national oceanographic agencies. These data include cyclone position, minimum sea level pressure, maximum wind speed and radius of maximum wind. The wind is computed as a function of the distance from the eye, the maximum wind speed and the Coriolis force parameter (dependent upon the latitude), and it is computed at every location of the domain. Then, the forward speed of the cyclone is also taken into account, as well as the rotational component of the cyclone movement. This operation is repeated at every time step of the cyclone, or at least at the time steps for which input information is available (usually every six hours), and at the end the maximum wind speed at every location over the domain is retained and used for loss computation purposes.

This model was chosen because of the following reasons:

- Its computational times are much shorter than those of numerical weather models, thus allowing fast real-time calculations and the simulation of a large dataset of events.
- It is a recent development of a very well established parametric model;
- It was developed specifically for the study area (while most of the parametric models available in the literature were developed for the US coasts).

Storm surge hazard model

Storm surge is a natural phenomenon that occurs on the coasts when the atmospheric conditions cause water level oscillations in the time range of a few minutes to a few days (excluding wind-generated waves), as shown in Figure .

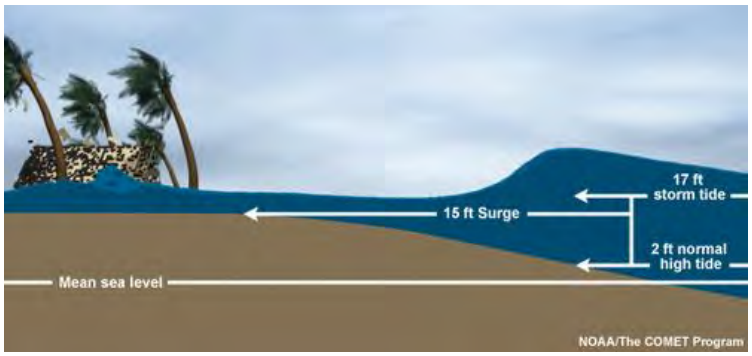

FIGURE 1 – SCHEME OF THE STORM SURGE PHENOMENON (HTTP://METED.UCAR.EDU/).

The generation of a storm surge arises from the interaction between air and sea. The atmospheric forcing is due to the atmospheric pressure gradient normal to the water body surface and to the tangential wind stress over the water surface. The pressure forcing is also called “inverse barometric effect”. The wind field associated with the storm pushes the water towards the coast, thereby causing a pile-up of water at the coast and it is the main driving force of the storm surge.

The model used for storm surge modelling in SPHERA is GeoClaw, which belongs to the ClawPack 5.4.1 software suite. This model was chosen for the following reasons:

- It is a well-established model (by UniWashington/Columbia) with a large user community for storm surge, tsunami, dam break and other geophysical flows.
- It is part of the well-known ClawPack package, a collection of state-of-the-art finite volume methods for resolving conservation laws.
- It is free and open source (thus it can be easily modified, customized and adapted to every context).
- It has no licence limitations for commercial purposes.
- It is very fast, and thus especially suitable for large domains, due to:

    - Parallel computation: It uses openMP parallelization;
    - Adaptive Mesh Refinement algorithm: the space and time resolution is automatically changed during the simulation to minimize the computational times while maximizing the accuracy. This also avoids the need for running the model on several nested domains, thus reducing the complexity of implementation.
- It runs on Linux Operative System and thus it can be run on High Performance Computing facilities, in case many simulations need to be run.

The storm surge model provides sea level variations responding to a tropical cyclone forcing (pressure and wind) but does not include any tidal forcing or tidal boundary conditions. Therefore, the astronomical tide needs to be accounted for externally. For this reason, the FES2014 tidal model was employed.

Exposure Module

Any risk model developed for parametric insurance purposes requires an Industry Exposure Database (IED), which allows estimating the economic losses caused by natural hazards in a reliable way. The exposure database for the SPHERA model was developed based on several data sources related to the built-up environment, the agriculture and the surrounding topography. These datasets included national building census surveys, land use/land cover maps, night-time lights imagery, population censuses, Digital Elevation Models (DEMs) and satellite imageries, among others.

The final exposure database includes information about to the number of assets of several lines of business, their spatial location, area, replacement value and physical characteristics, such as construction type and material, and height classification, and the location and expected annual production of the main crops. The structure replacement value is used in the loss calculation. In particular, the SPHERA exposure database contains information about:

- Building stock:
    - Residential building stock
    - Commercial and industrial building stock
    - Hotels, education and healthcare building stock
    - Public building stock
- Infrastructure:
    - Airports
    - Ports
    - Power facilities
    - Road Network
- Crops

With the exception of airports and ports, whose exact location is known, all other assets were distributed in space within each administrative division. This distribution was performed considering a wide range of datasets. The SPHERA database was aggregated at the same level of granularity used in the computation of the losses. The granularity was selected as a trade-off between computational times and precision of the model and it is not homogeneous across different countries or within the same country. The exposure database provides estimates of the asset count and replacement cost for each structure class at a 30 arc second resolution (approximately 1 km) for inland areas and at a higher resolution (approximately from 120m to 250m) for coastal areas. Figure shows an example of the SPHERA exposure grid in Trinidad and Tobago and in Turks and Caicos.

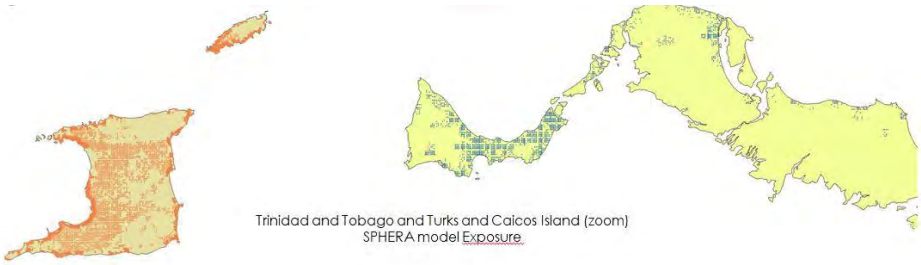

FIGURE 2 – DISTRIBUTION OF THE SPHERA EXPOSURE ASSETS IN TRINIDAD AND TOBAGO AND TURKS AND CAICOS.

Vulnerability Module

A vulnerability function is a curve that relates a given level of intensity caused by an event (here a tropical cyclone) at a given location with the economic cost or repairing the physical damage suffered by an asset at risk (building or infrastructure), expressed in terms of relative damage between 0 and 1, where 1 indicates a damage equal to the total replacement cost of the asset (Figure 3).

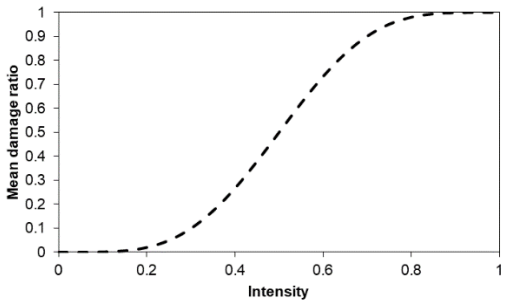

FIGURE 3– CONCEPTUAL EXAMPLE OF VULNERABILITY CURVE.

Two different sets of vulnerability functions were developed, one for wind losses and one for storm surge losses.

Wind vulnerability

The wind vulnerability module provides a probabilistic relationship between the wind speed at a site and the loss ratio suffered by a specific building at that site. The model reflects the large size of the structure inventory and the lack of data to fully characterize each building individually by considering classes of structures rather than individual buildings. These classes cover all the structures of the building exposure database.

Construction typologies, occupancy classes, building code requirements, construction practices and other parameters affecting the wind vulnerability of the physical assets present in the exposure model of the Central American and Caribbean countries were evaluated. The vulnerability model includes up-to-date empirical, expert opinion-based, analytical and hybrid fragility and vulnerability functions collected during an exhaustive search of peer-reviewed publications, public and private reports, conference proceeding, among other sources.

The vulnerability functions are specific for the different classes of assets located in the different countries and are defined as function of structural system, height and occupancy. Other building characteristics such as roof shape and roof material that are not explicitly considered in the exposure database are accounted for with the use of country-specific modifiers that generate a country-specific function for every class of structure. Given the uncertainty associated with the estimation of losses for classes of assets, the vulnerability functions provide the mean loss ratio and its associated uncertainty for varying levels of wind speed.

Storm surge vulnerability

The storm surge vulnerability functions were developed using RED's in-house damage model for residential buildings. The model is based on a synthetic approach, which takes into account hazard properties at the building locations (e.g., water depth), the characteristics of the exposed buildings (e.g., structural type) and the replacement costs of its components, in order to compute damage values. The damage mechanisms of each building component were described through a what-if analysis, which depends on hazard and exposure variables.

The impact of different exposure characteristics on the storm surge flood vulnerability of residential buildings was taken into account in the development of the vulnerability module. More specifically, material, presence of basement, number of stories in the building, and ground level height (i.e. whether the ground floor is more elevated than the street or the surrounding environment) were adopted as the main characteristics that define the storm surge vulnerability of buildings.

The curves obtained with the above methodology were then aggregated to obtain curves for the categories of building used in the exposure database. Vulnerability curves for infrastructure were also developed, based on literature information for:

- Ports;
- Airports;
- Power plants;
- Roads.

Furthermore, the storm surge vulnerability curves were customized for every stretch of coast within the domain of study to reproduce the effect of tidal defence, by estimating a low-probability astronomical tide level through the use of the software FES2014 and then correcting the vulnerability curve to take into account the protection from such astronomical tide oscillation.

Loss Module

Once the effects (wind and surge) caused by a tropical cyclone have been computed an estimate of the economic losses is computed by the SPHERA using the classical approach shown below. For a single asset *i*:

$$L_i = V_i(H_i) \times E_i$$

Where:

L: losses (USD);

H: hazard (maximum wind – km/h, maximum storm surge – m);

V(H): vulnerability as a function of the hazard (-) [0-1];

E: exposure, or asset value (USD).

The economic losses caused by a tropical cyclone on the asset *i* are computed as a fraction of the total value of the asset E_i, defined by a specific vulnerability function V_i given a level of the intensity of the storm effects, H_i. In the case of tropical cyclone hazard, H_i is bi-dimensional, i.e., it is defined by two variables, wind speed and storm surge. In this model, two separate sets of vulnerability curves were developed, for wind and storm surge. Therefore:

$$L_{w,i} = V_{w,i}\left(H_{w,i}\right) \times E_i$$
$$L_{s,i} = V_{s,i}\left(H_{s,i}\right) \times E_i$$

Where the subscript *w* refers to wind losses, hazard and vulnerability and the subscript *s* refers to storm surge losses, hazard and vulnerability. The losses are then computed using a combined approach. The losses are then aggregated at the country scale to obtain the damages caused by an event to a single country.

Risk Assessment

The SPHERA model is used for two different purposes:

1. Long-term risk assessment.
2. Real-time damage assessment.

Long term risk assessment

The long-term risk assessment is the estimation of the distribution of the losses caused by tropical cyclones to a country, i.e. the assessment of the likelihood losses will exceed a threshold. In order to estimate the long-term risk of a country, the historical record of events needs to be analyzed. However, reliable data on cyclone tracks is only available for a relatively short period of time and it is not sufficient to make a risk assessment based solely on historical storm tracks. To overcome this limitation, large sets of synthetic cyclones, or stochastic cyclones, can be generated. The theoretical cyclones, also called stochastic cyclones, are statistically similar to the real, or observed, cyclones, but their large number can help estimate more precisely and robustly the tropical cyclone risk in a specific area.

This approach has been used frequently in the past decade. A stochastic approach was used, based on the following steps:

1. Synthetic tracks were generated based on the historical tracks, applying random perturbations to the changes in direction of the observed tracks. The genesis of the synthetic cyclones was based on the genesis of the historical cyclones.
2. The minimum sea level pressure was computed based on an autoregressive model (AR2) fitted on observed data, with a random term representing the natural variability of the process.
3. The maximum wind speed and the radius of maximum wind were generated depending on the minimum sea level pressure based on regression fitted on observed data, with a random term.
4. The filling effect, i.e. the decay in cyclone intensity when the cyclone eye makes landfall, was modelled with an exponential model, whose exponential decay was calibrated on observed data, with a random term.

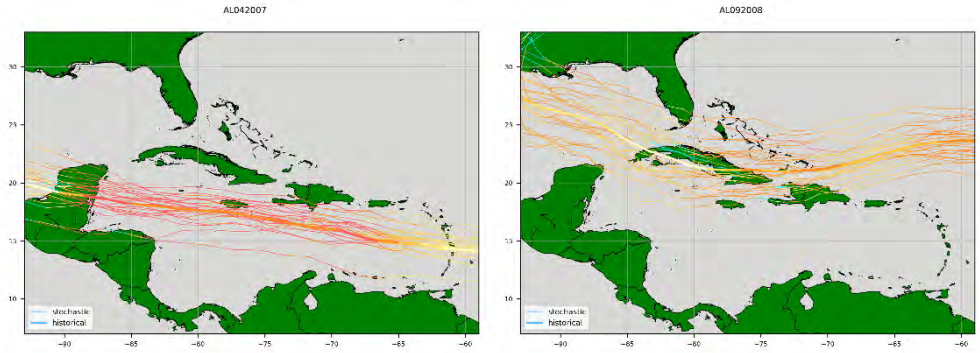

FIGURE 4 – EXAMPLES OF PARENT OBSERVED HURRICANE TRACK AND DERIVED PERTURBED TRACKS. THE COLOUR SCALE INDICATE HURRICANE INTENSITY – SEE FOLLOWING SECTIONS FOR MORE INFO ON HOW THIS WAS GENERATED. THE THICKEST TRACK REPRESENTS THE HISTORICAL CYCLONE THAT WAS USED TO GENERATE THE PERTURBED TRACKS.

The wind and storm surge models were set up to obtain the maximum wind speed field and the maximum surge field caused by both historical and stochastic hurricanes. The SPHERA model was used to compute economic losses due to all stochastic cyclones included in the catalogue. The results of the stochastic catalogue simulations aggregated by country form the so-called Event Loss Table (ELT). Then, the results were used to estimate the empirical distributions of losses.

Real-time damage assessment

The aim of the real time hazard calculation is to compute the losses caused by a developing cyclone. The calculation is triggered whenever the US National Oceanic and Atmospheric Administration (NOAA) communicates the development of a tropical cyclone on its web page. The input data for real-time tropical cyclone loss estimation is the a-deck format best track file provided by NOAA. This file contains data regarding the ongoing cyclone, including:

- position of the eye
- minimum sea level pressure
- maximum wind speed
- radius of maximum wind
- radii at different wind speeds and in different quadrants

Losses are also computed for all countries in real time, as the cyclone develops, following a pre-established protocol. Once the cyclone eye is in a position such that it cannot cause further damage to a country, the value of computed losses is considered as final. If the country has subscribed an insurance policy, the loss estimate is used to compute a potential payout, based on the policy parameters.

The methodology implemented for the real-time loss assessment is the same already described for the long-term assessment, since a complete consistency is needed between the two configurations of the SPHERA model. The main difference between the two cases is that in the near real-time configuration, the loss assessment module computes the economic losses caused by a single event rather than considering those caused by an entire catalogue of stochastically simulated events, such as in the long-term configuration.

Cornell, C.A., 1968. Engineering seismic risk analysis. Bull. Seismol. Soc. Am. 58, 1583–1606.
Esteva, L., 1970. Regionalización sísmica de México para fines de ingeniería. Instituto de Ingeniería, Universidad Nacional Autónoma de México.

THE SPHERA EARTHQUAKE MODEL

CCRIF has recently developed a new in-house earthquake risk model, called System for Probabilistic Hazard Evaluation and Risk Assessment (SPHERA). This new development was intended to provide CCRIF with the best technology available for the area it operates, according to the state of the art of the seismic risk assessment sector. The model was developed in collaboration with RED (Risk, Engineering and Development, Italy) and ERN (Evaluación de Riesgos Naturales, Mexico). The SPHERA earthquake risk model estimates the probability of damages caused by seismic events and will be used in the following policy years to underpin the earthquake parametric insurance programmes offered by CCRIF.

The conceptual structure of the SPHERA model is composed by the three classic elements of the risk analysis: hazard, vulnerability and exposure. The hazard module computes the likelihood of the occurrence of an event and its intensity, the vulnerability module estimates the response of the country's assets to various levels of event intensity and the exposure module quantify the value, or replacement cost, of the country's assets. Furthermore, a loss computation module is used to combine these three components to estimate the damages caused by an event (or a set of events).

Hazard Module

The long-term seismic hazard module was designed to model the occurrence of earthquakes to be statistically consistent in time and space with the historical seismicity in the region covered by the SPHERA model. It allows characterizing the occurrence of future earthquakes and determining the

relationship between seismic hazard intensities (e.g. spectral accelerations) and their exceedance rates in all the sites covered by the model, by the means of probabilistic seismic hazard analyses (PSHAs). The methodological framework to build a seismic hazard model, even using the state-of-the-art tools, in its essence is still based on the approaches first proposed by Cornell (1968) and Esteva (1970).

As first step, an updated and complete historical earthquake catalogue has to be compiled. Then, the region of study has to be divided in sub-regions in which the occurrence of earthquakes can be assumed to be uniform in time and space and to present similar characteristics (e.g. crustal or subduction seismicity). The future earthquake occurrence process for each of these regions is statistically modelled using the information collected about the historical seismicity (earthquake catalogues). In each sub-region is then possible to simulate possible future earthquakes compatible with the historical seismicity. Finally, for each of these simulated events ground motion prediction equations (GMPEs) allow obtaining quantitative measures of ground motion intensities such as peak ground accelerations at the sites of interest.

Tectonic zonation and seismicity characterization

Based on different tectonic and geological studies previously performed in the region, a tectonic zonation was carried out for the area of study, with the aim of identifying regions on which the seismic activity can be considered as uniform in time and space. Depending on the characteristic of the sources and the faulting mechanisms, different geometrical models were employed. This is because, for example, earthquakes occurring in subduction zones have very different characteristics than those that occur with strike-slip mechanisms in intraplate areas. Figure 5 summarizes the geometry of the sources considered in this PSHA together with the description of the geometrical model employed for the representation of each of them. A total of 146 seismic sources are included in the model. Four correspond to background sources included to consider the occurrence of future events at locations on which no historical earthquake records exist.

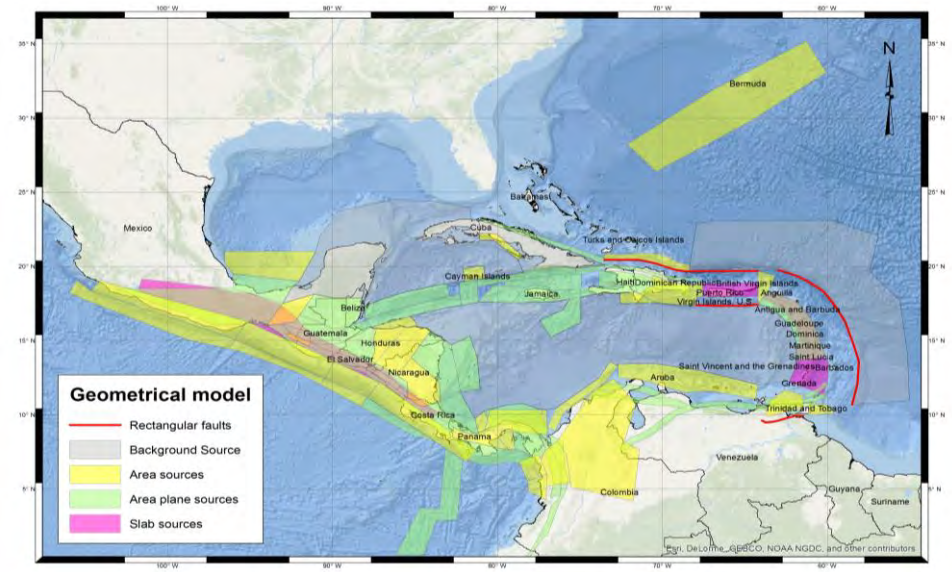

FIGURE 5 – SEISMIC SOURCES AND ASSIGNED GEOMETRICAL MODEL

Once the geometries and boundaries of each of the seismic sources have been defined, every single event included in the earthquake catalogue needs to be assigned to only one of them. The earthquake catalogue, in order to be consistent with the Poissonian seismicity models, was declustered with the objective of removing aftershocks and foreshocks. The occurrence of earthquakes within the different seismic sources was then characterized by means of magnitude-recurrence relationships (i.e. seismicity models). The analysis of the historical events assigned to each source allowed defining the

parameters of these relationships. The magnitude-recurrence relationships were limited defining a minimum magnitude threshold M_0 equal to 4.0 (M_W) for all the seismic sources and a maximum magnitude threshold M_u different for each source that was was assigned using several criteria.

The two Poissonian seismicity models used here were:

- The modified Gutenberg-Richter model;
- The characteristic earthquake model.

Ground motion prediction equations

To quantify the hazard in terms of ground motion intensity measures, in this case spectral accelerations, a GMPE needs to be assigned to each of the seismic sources. GMPEs are relationships between ground motion intensity measures and magnitude, distance, and other parameters of the source and the site. GMPEs have the form of the schematic plot shown in Figure .

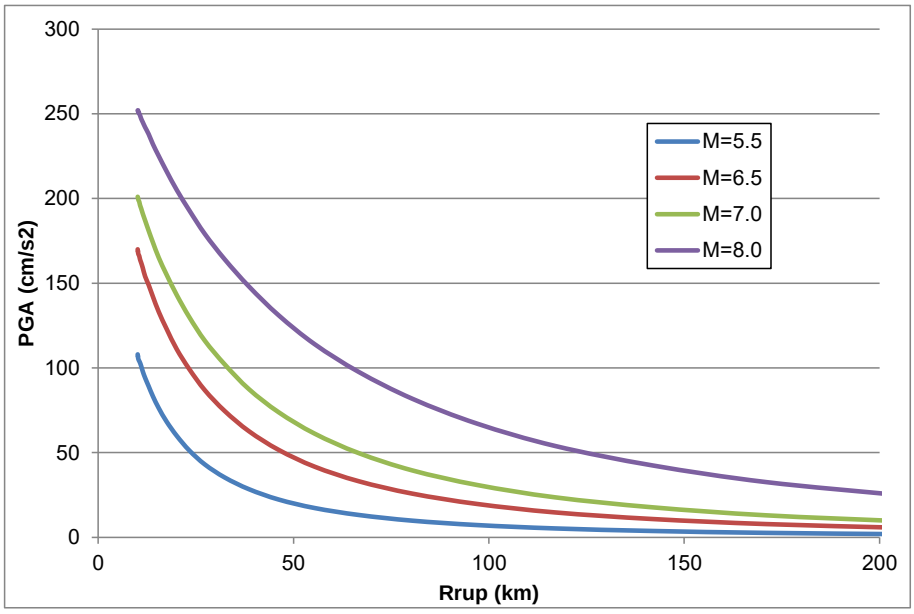

FIGURE 6 – SCHEMATIC PLOT FOR PEAK GROUND ACCELERATION AS PREDICTED BY A GENERIC GMPE FOR FOUR DIFFERENT MAGNITUDE EVENTS

A review of previous studies was performed for the region of interest, complemented with the consideration of ground motion attenuation models developed using regional records (for Mexico and the Northern Andes).

Since the number of GMPEs developed for the region is small, a combination of them was assembled for each tectonic environment in the form of a composite (or hybrid) GMPE. These composite GMPEs are a combination of applicable existing ground motion models that use subjective weights in a very similar manner to the logic-tree approach commonly used in PSHA. The hybrid approach, however, is much more efficient than the logic tree approach and, therefore, it is usually preferred in loss estimation models where the computations are very heavy. Table 1 summarizes the GMPEs used for each composite model, classified by region and tectonic environment. The soil parameter was set equal to rock conditions for all the GMPEs, since the soil amplification effects were treated in a separate manner, as explained in more detail in the following section.

TABLE 1 – GMPES ADOPTED FOR EACH TECTONIC ENVIRONMENT AND BY REGION/COUNTRY

Region/Country	Tectonic environment	Base GMPEs	Weights
Mexico	Crustal	Chiou-Youngs (2014) - Abrahamson et al. (2014) - Zhao et al. (2006)	0.33 - 0.33 - 0.34
	Interface	Zhao et al. (2006) - Youngs et al. (1997) - Lin and Lee (2008) - Arroyo et al. (2010)	0.25 - 0.25 - 0.25 - 0.25
	Intraslab	Zhao et al. (2006) - Youngs et al. (1997) - Kanno et al. (2006) - García et al. (2005)	0.25 - 0.25 - 0.25 - 0.25
Central America and the Caribbean	Interface	Zhao et al. (2006) - Youngs et al. (1997) - Lin and Lee (2008)	0.33 - 0.33 - 0.34
	Intraslab	Zhao et al. (2006) - Youngs et al. (1997) - Kanno et al. (2006)	0.33 - 0.33 - 0.34
	Outer-rise	Chiou-Youngs (2014)	1.0
	Crustal	Chiou-Youngs (2014) - Abrahamson et al. (2014) - Zhao et al. (2006)	0.33 - 0.33 - 0.34
Northern Andes	Interface	Zhao et al. (2006) - Youngs et al. (1997) - Lin and Lee (2008) - Bernal (2014)	0.25 - 0.25 - 0.25 - 0.25
	Intraslab	Zhao et al. (2006) - Youngs et al. (1997) - Kanno et al. (2006) - Bernal (20014)	0.25 - 0.25 - 0.25 - 0.25
	Crustal	Chiou-Youngs (2014) - Abrahamson et al. (2014) - Zhao et al. (2006) - Bernal (2014)	0.25 - 0.25 - 0.25 - 0.25

Local effects

Local soil amplification effects were considered in the model by estimating an amplification factor, *AF*, using the methodology proposed by Chiou and Youngs. This methodology requires information about the Vs30 parameter (namely the average shear wave velocity in the top 30m of soil), which was extracted from the USGS site. Vs30 data were available with a 30 arc-seconds resolution level and has coverage of the totality of the area under analysis as shown in Figure 7.

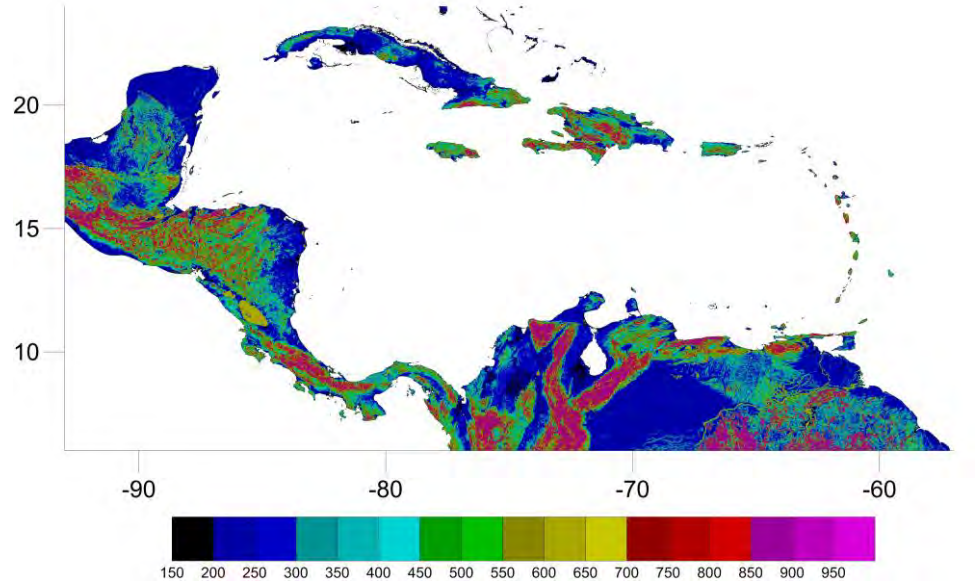

FIGURE 7 – VS_{30} VALUES (M/S) FOR THE AREA UNDER STUDY

Exposure Module

Any risk model developed for parametric insurance purposes requires an Industry Exposure Database (IED), which allows estimating the economic losses caused by natural hazards in a reliable way. The exposure database for the SPHERA model was developed based on several data sources related to the built-up environment and surrounding topography. These datasets included national building census surveys, land use/land cover maps, night-time lights imagery, population censuses, Digital Elevation Models (DEMs), and satellite imageries, among others.

The final exposure database includes information about to the number of assets of several lines of business, their spatial location, area, replacement value and physical characteristics, such as construction type and material, and height classification. The replacement value is used in the loss calculation. In particular, the SPHERA exposure database contains information about:

- Building stock:
  - Residential building stock
  - Commercial and industrial building stock
  - Hotels, education and healthcare building stock

    - Public building stock
- Infrastructure:
    - Airports
    - Ports
    - Power facilities
    - Road Network

With the exception of airports and ports, whose exact location is known, all other assets were distributed in space within each administrative division. This distribution was performed considering a wide range of datasets. The SPHERA database was aggregated at the same level of granularity used in the computation of the losses. The granularity was selected as a trade-off between computational times and precision of the model and it is not homogeneous across different countries or within the same country. The exposure database provides estimates of the asset count and replacement cost for each exposure class at a 30 arc second resolution (approximately 1 km) for inland areas and at a higher resolution (approximately from 120m to 250m) for coastal areas. Figure 8 shows an example of the SPHERA exposure grid in Trinidad and Tobago and in Turks and Caicos.

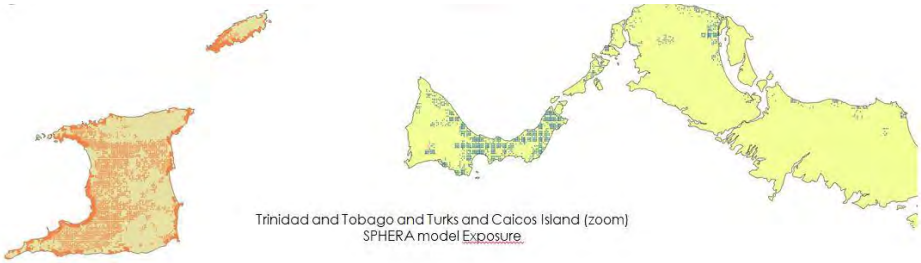

FIGURE 8 – DISTRIBUTION OF THE SPHERA EXPOSURE ASSETS IN TRINIDAD AND TOBAGO AND TURKS AND CAICOS.

Vulnerability Module

A vulnerability function is a curve that relates a given level of intensity caused by an event (here an earthquake) at a given location with the economic cost of repairing the physical damage suffered by an asset at risk (building or infrastructure), expressed in terms of relative damage between 0 and 1, where 1 indicates a damage equal to the total replacement cost of the asset (Figure 9).

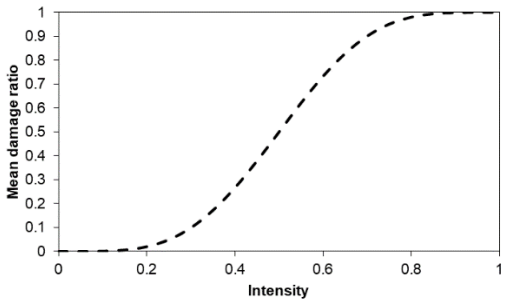

FIGURE 9 – CONCEPTUAL EXAMPLE OF VULNERABILITY CURVE.

An earthquake vulnerability function is assigned to each class of asset included in the Industry Exposure Database (IED). The vulnerability functions define the probability distribution of economic loss for different levels of ground motion intensity induced by an earthquake.

The SPHERA model includes a database of vulnerability functions derived for buildings and the different types of infrastructure in all the countries covered by the model. More details about the derivation of the vulnerability model can be found in the “Earthquake Vulnerability Technical Report”. Figure 10 shows some earthquake vulnerability functions developed for the SPHERA model.

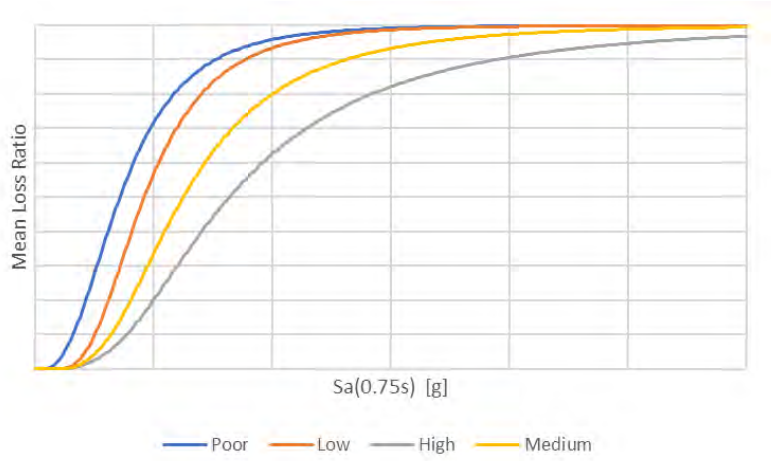

FIGURE 10 VULNERABILITY CURVES RELATED TO REINFORCED CONCRETE MID-RISE INFILLED FRAMES FOR DIFFERENT QUALITY OF BUILDING STOCK

Loss Module

Once the effects (ground motion intensity) caused by an earthquake have been computed an estimate of the economic losses is computed by the SPHERA model using the classical approach shown below. For a single asset *i*:

$$L_i = V_i(H_i) \times E_i$$

Where:
L: losses (USD);
H: hazard (spectral acceleration);
V(H): vulnerability as a function of the hazard (-) [0-1];
E: exposure, or asset value (USD).

The economic losses caused by an earthquake on the asset *i* are computed as a fraction of the total value of the asset E_i, defined by a specific vulnerability function V_i given a level of the intensity of the seismic effects, H_i. The losses computed for all the assets in the exposure database are then aggregated at the country scale to obtain the damages caused by an event to a single country.

Risk assessment

The SPHERA model is used for two different purposes:

3. Long-term risk assessment.
4. Real-time damage assessment.

Long-term risk assessment

The long-term risk assessment is the estimation of the distribution of the losses caused by earthquakes to a country, i.e. the assessment of the likelihood losses will exceed a threshold. In order to estimate the long-term risk of a country, the historical record of events needs to be analyzed. However, reliable data on seismic events is only available for a relatively short period of time and it is not sufficient to make a risk assessment based solely on historical earthquakes. To overcome this limitation, large sets of synthetic earthquakes, or stochastic earthquakes, can be generated. The theoretical earthquakes, also called stochastic earthquakes, are statistically similar to the real, or observed, earthquakes, but their large number can help estimate more precisely and robustly the seismic risk in a specific area. A stochastic approach was used, based on the following two steps.

1. Probabilistic seismic hazard analysis: Once the seismicity parameters were defined for each one of the sources, and appropriate GMPEs were assigned to each source, the seismic hazard at each site of interest can be computed by integrating the contribution of all the earthquakes that may occur in each source. For the computation of the ground motion affecting any given

site only the events within 300km were considered. The hazard was computed for uniformly spaced calculation grid of sites with a resolution level compatible with all the PSHA input data. The grid covers the entire domain of study.

2. Stochastic event-set generation: The main objective of developing this PSHA is to obtain a stochastic event-set populated by simulated future earthquakes to be used for a fully probabilistic seismic loss assessment study of the assets in these countries. Using all the input data previously described, it is possible to generate a stochastic event-set after the definition of several parameter values. First of all, a minimum magnitude of 5.0 was selected for the event generation process. Earthquakes with lower magnitudes were deemed to cause losses of negligible amount for the purposes of this model. After this, 9 magnitude bins between the minimum and the maximum magnitude (which varies from source to source) were sampled. An average spacing of 15km was set in both orthogonal directions for the generation of epicentres of future earthquakes. Events that did not generate a peak ground acceleration exceeding 1 cm/s^2 anywhere in these countries were removed from the catalogue. Each event has unique rupture characteristics, an annual occurrence frequency and a probabilistic representation of the footprint associated to the ground motion intensities (spectral accelerations here) caused by that particular event. The footprints are represented by means of the first two statistical moments of the intensity measure at each site, compatible with the assumption of the hazard intensity being a random variable.

The final risk for a set of assets (e.g., the building stock and infrastructure inventory of a country) is usually described in terms of a so-called exceedance probability curve of losses, which provides the annual frequency (or probability) of exceedance of different loss values. The annual loss exceedance rate can be calculated using the following equation:

$$v(p) = \sum_{i=1}^{Events} \Pr(P > p | Event_i)\, F_A(Event_i)$$

In this equation, which is one of the many ways the total probability theorem can adopt, *v(p)* is the loss exceedance rate of loss *p*, and $F_A(Event\ i)$ is the annual frequency of occurrence of the *Event i*, while *Pr(P>p(Event i)* is the probability that the loss will be higher than *p,* given that the *i*-th event has occurred. The sum in the equation is made for all potentially damaging events included in the stochastic event set. The inverse of the annual rate of the loss corresponds to its expected return period. The loss exceedance curve contains all the necessary information for describing the process of loss occurrence considering the associated uncertainties in the analysis process.

Real-time damage assessment

The aim of the real-time seismic risk assessment is to evaluate economic losses due to a single earthquake, with the aim of computing whether a payout is due or not, depending on the policy parameters computed in the long-term risk assessment, for the countries considered. The “real-time” term refers to the characterization of the economic losses due to a single earthquake that has occurred shortly before the beginning of the loss computation.

The near-real time loss assessment module of SPHERA relies on a reputable third-party data source to define the main parameters of an earthquake almost immediately after its occurrence. This is the USGS database of real-time earthquake data. The USGS assigns a unique identifier to each event. The identifier allows associating each event with parameters such as its magnitude (M_W), location and depth, as well as, for most of events with moderate-to-high magnitude ($M_W > 5.5$), the moment tensor data. This last parameter allows a more precise identification of the fault plane and modelling of the rupture needed to estimate the ground motion field.

The methodology implemented for the real-time loss assessment is the same already described for the long-term assessment, since a complete consistency is needed between the two configurations of the SPHERA model. The main difference between the two cases is that in the near real-time configuration, the loss assessment module computes the economic losses caused by a single event rather than considering those caused by an entire catalogue of stochastically simulated events, such as in the long-term configuration.

In the near real time, the loss assessment is carried out by gathering the base data to characterize the event by USGS and computing the ground motion intensity field associated with it (as described in Section above). The economic losses computed in each of the countries affected by the event and covered by the model are then computed by the loss module using as input the ground motion field, the database of exposed assets and the earthquake vulnerability models. The model in real-time configuration estimates the economic losses considering the same uncertainties taken into account for long-term loss assessment.

The final output of the real-time loss assessment is the expected loss experienced by each country affected by the event under analysis and corresponding uncertainty.

Appendices 1 and 2 provide additional details about the SPHERA TC and EQ Models.

EXCESS RAINFALL LOSS MODEL FOR THE CARIBBEAN AND CENTRAL AMERICA

MODEL DESCRIPTION

THE XSR 2.5 MODEL FOR EXCESS RAINFALL

This model[2] features the probabilistic evaluation of the effects of Excess Rainfall (XSR) on residential, commercial, public and industrial buildings in the Caribbean Region and in Central America. This model (XSR 2.5) was developed with the intention of updating the previous XSR 2.0 model. XSR 2.5 model computes the country aggregated losses due to excess rainfall on a daily basis. Once the excess rainfall exceeds a threshold level across a sufficiently large portion of a country, the losses and corresponding insurance payout are calculated according to the pre-defined policy parameters. The overall performance of the model was validated using loss and damage data from various historical events.

The two primary applications of the XSR model are as:

1. An operational real-time model to compute the loss and relative country-by-country payout due to an excess rainfall event;
2. A model to coherently estimate the financial risk and perform the financial analysis necessary to compute and quote equitable insurance policy premiums.

The XSR 2.5 model covers quite a large geographic area; hence it was developed in three phases. The first delivery targets countries (Group 1) that are existing members of CCRIF, including those that have not previously purchased XSR coverage. The second delivery targets the Central American countries (Group 2), while the third delivery comprises the Caribbean countries (Group 3) that are not currently members of CCRIF.

The complete list of countries in each group is reported below and shown in Figure 11:

- **Group 1:** Anguilla, Antigua and Barbuda, Bahamas, Barbados, Belize, Bermuda, Cayman Islands, Dominica, Grenada, Haiti, Jamaica, St. Kitts and Nevis, St. Lucia, St. Vincent & the Grenadines, Trinidad and Tobago, Turks and Caicos Islands.
- **Group 2:** Costa Rica, El Salvador, Guatemala, Honduras, Nicaragua, Panama.
- **Group 3:** Aruba, Curaçao, Dominican Republic, Guadeloupe, Guyana, Martinique, Montserrat, Netherlands Antilles, Puerto Rico, Suriname.

All these countries are characterized by very frequent and destructive climatic events as shown in Figures 12 and 13

[2] Developed by RED - Risk Engineering and Design, and ERN – Evaluación de Riesgos Naturales for CCRIF SPC

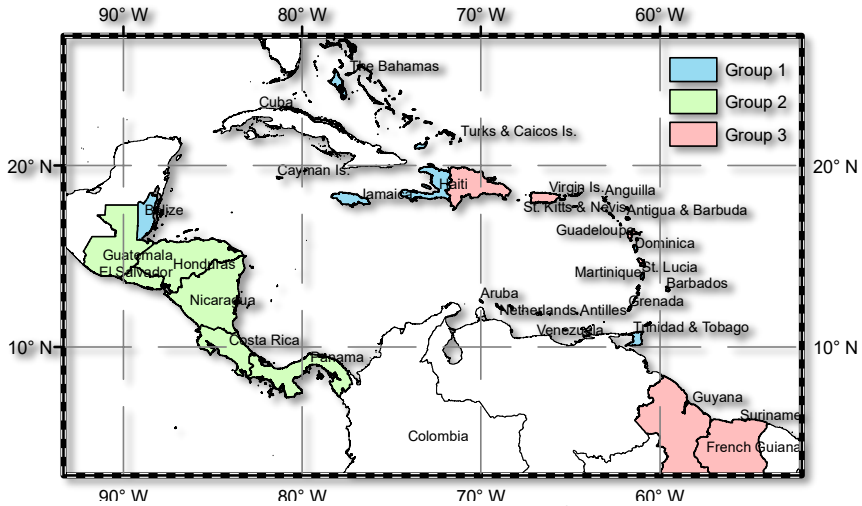

FIGURE 11 – LOCATION OF THE THREE GROUPS OF COUNTRIES COVERED BY XSR 2.5 (WITH THE EXCEPTION OF BERMUDA, LOCATED OUTSIDE OF THIS IMAGE)

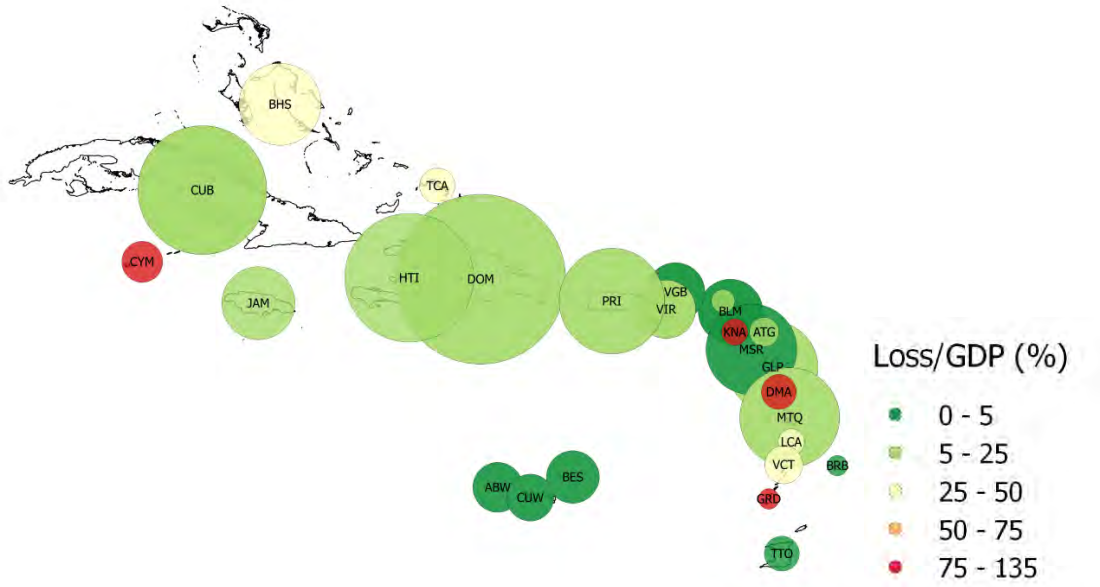

FIGURE 12 – RELATIVE FREQUENCY OF CLIMATIC EVENTS (SIZE OF THE CIRCLE) AND LOSS PER UNIT GDP (COLOR OF THE CIRCLE) FOR CARIBBEAN COUNTRIES COVERING EVENTS FROM 1998 TO 2014 INCLUSIVE

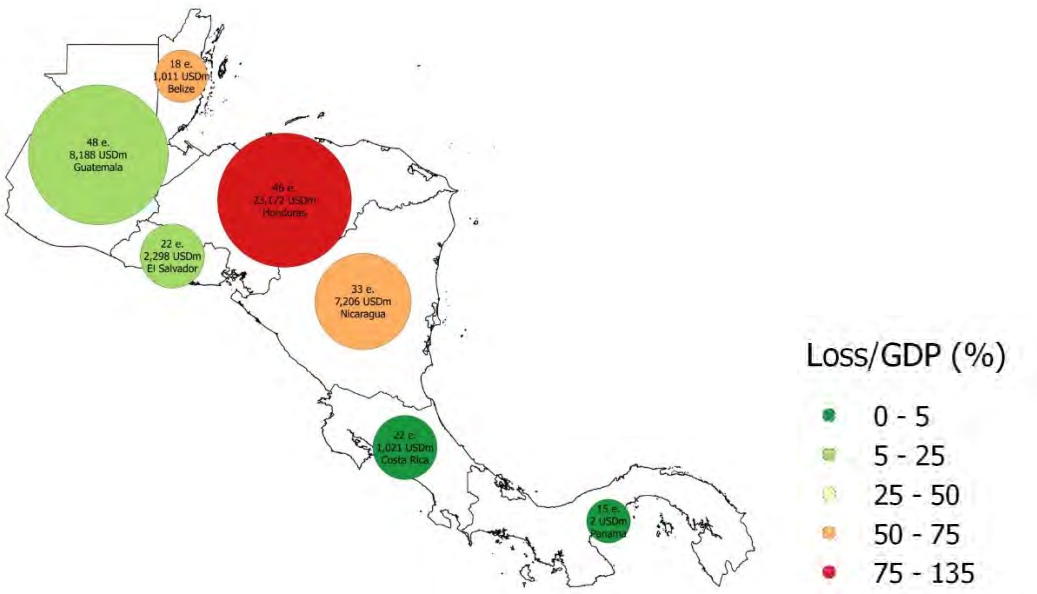

FIGURE 13 – NUMBER OF CLIMATIC EVENTS (SIZE OF THE CIRCLE), LOSS PER UNIT GDP (COLOR OF THE CIRCLE) AND TOTAL LOSS IN MILLIONS USD FOR EACH CENTRAL AMERICAN COUNTRY FROM 1998 TO 2014 INCLUSIVE

Modeled Peril

The Caribbean and Central American countries covered by the XSR 2.5 model are affected by extreme precipitation events that are often, but not always, induced by tropical cyclones. The consequent losses are mostly caused by the accumulation of water over the land followed by the high velocity of water impacting assets and infrastructure lying in its path. The most robust model to compute the damage and losses from such events would be a distributed flood loss model that explicitly considers all of the physical processes related to water runoff mechanisms (e.g., infiltration of water into the soil, overland and subsurface water flow, inland riverine flow, flood generation) and the physical damage caused by water breach to buildings and their contents, and to infrastructure assets (e.g., roads and bridges). However the XSR 2.5 model only accounts for the quantification of excess rainfall and its corresponding local impacts, while a possible future version of the model could account for hydrological runoff and hydraulic effects. Notwithstanding the runoff and damage mechanisms, ultimately excess rainfall is the main physical trigger of flood losses, and the XSR 2.5 model will be shown to simulate plausible rainfall events and realistic damage and loss.

The General Framework of the Model

The XSR model can be conceptually divided into five components:

- **Hazard module:** by means of climatic and meteorological data, the hazard model produces an estimate of the *physical trigger* (i.e., accumulated rainfall amount).
- **Exposure module:** by leveraging several sources of information concerning the built-up environment and surrounding topography, the exposure model provides quantification of *building count*, *replacement cost* and *vulnerability classification* of various building classes and infrastructure assets at a granularity of $1km^2$.
- **Vulnerability module:** based on available data on the exposure, the vulnerability module comprises the model's damage functions (DFs).
- **Loss module:** as a function of the physical trigger, the exposure at risk and the damage functions, the loss module computes an estimate of flood losses.
- **Insurance module:** based on the policy parameters, the insurance module provides the quantification of payouts for each country affected.

The framework of the XSR 2.5 model is shown in the flowchart in Figure 14. These components will be discussed in the following sections.

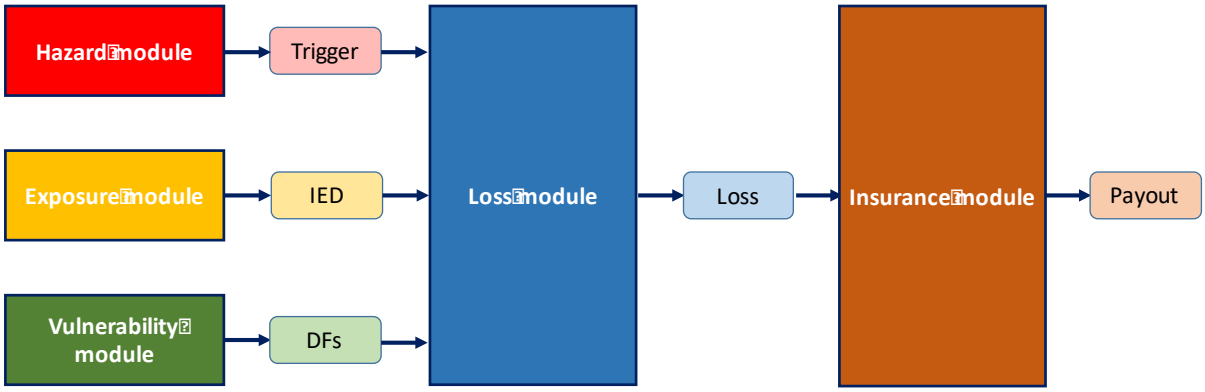

FIGURE 14 – GENERAL FRAMEWORK OF THE XSR 2.5 MODEL

Legend: IED=Industry Exposure Database; DFs: damage functions (i.e., relationships between accumulated rainfall and expected loss).

Hazard Module

The hazard module provides an estimate of the physical trigger (daily accumulated precipitation) to the loss module. The precipitation is computed on a grid covering the Caribbean and the Central American countries (see Figure) with a 24-hour time resolution and 1 km^2 spatial resolution. The XSR 2.5 hazard module makes use of two input datasets: the first consisting of a rainfall rate estimation from satellite images elaborated by NOAA (National Oceanic and Atmospheric Administration); the second consisting of a rainfall rate estimation provided by a numerical weather prediction (NWP) model called WRF (Weather Research and Forecast model) developed at the National Center for Atmospheric Research (NCAR) and initialized by a global climate model called GFS-FNL (Global Forecast System, Final) developed at the National Centers for Environmental Prediction (NCEP).

The hazard module provides the estimation of rainfall using a combination of remotely-sensed (satellite-derived) and modeled data. The satellite-based data allows for the accurate positioning of storms (such as tropical cyclones) while the NWP model provides robust estimates of local rainfall intensity, especially in the case of extreme events. Furthermore, the NWP model is run into two configurations (differing in their treatment of cumulus cloud generation), thus allowing for two realistic estimates of rain accumulations.

The module produces three distinct rainfall estimates (one satellite based and two model based) constituting a small (near real-time) “forecast ensemble” which in turn allows for probabilistic loss analysis (as described in subsequent sections). As explained in the loss module, the availability of three rainfall estimates allows for a more refined and reliable assessment of damage and loss, and in the reduction of prediction error such as undetected and false-positive events.

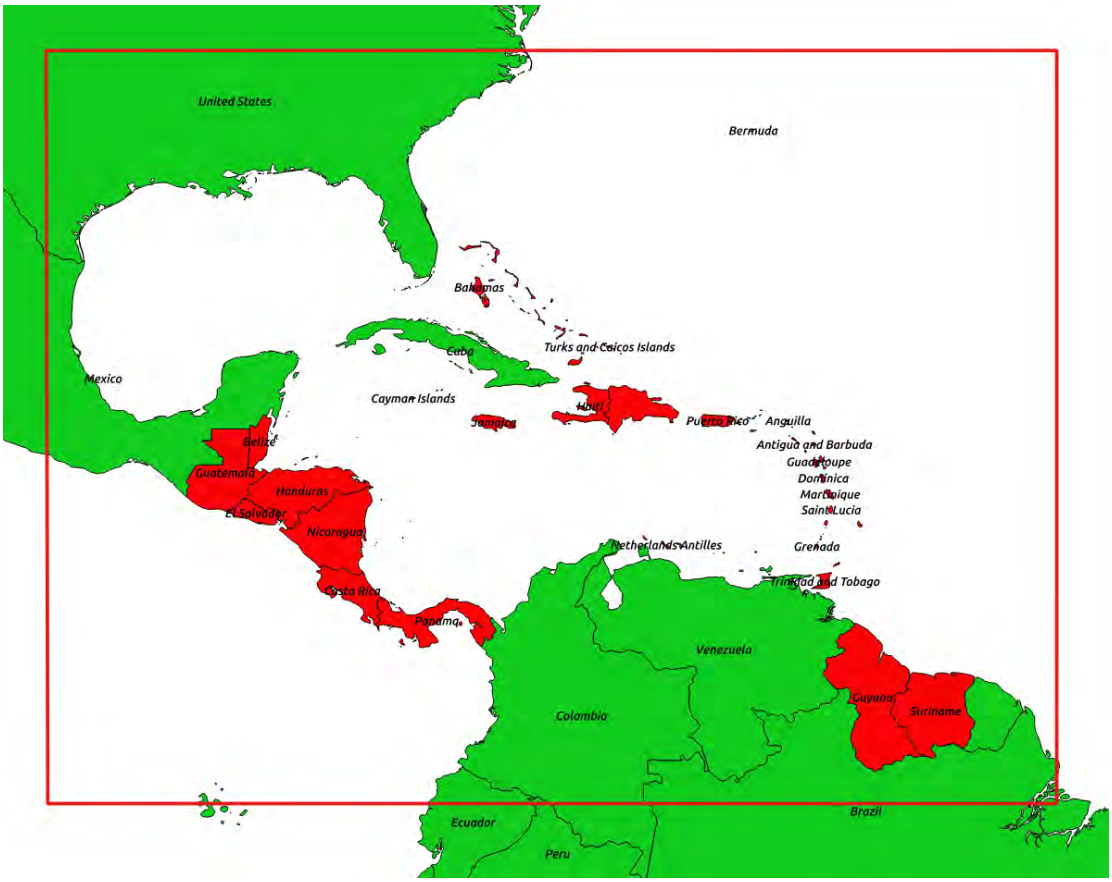

FIGURE 15 – THE XSR 2.5 MODEL DOMAIN

Exposure Module

The exposure module provides the monetary value of modeled assets, such as residential, commercial, and industrial buildings, and public infrastructure. Exposure modeling is the process necessary to develop a database of these assets at risk, organized in terms of vulnerability classes and characterized in terms of replacement values. Elements at risk include residential, commercial, public and industrial buildings that are significantly heterogeneous in terms of construction practices and hence their vulnerability to flood damage.

Building stock quantification, their spatial location, and structural characterization are essential steps towards the definition of building exposure. In catastrophe risk models, building characteristics such as the size, shape, configuration, architecture, material strength, structural strength, and stiffness can help describe unique qualities. To systematically characterize various construction classes, it is essential to compile the data related to building attributes and features and the vulnerabilities of each, which in turn helps describe the asset's susceptibility to damage and loss from perils such as wind and flood.

Detailed data describing the attributes of each and every building in a country is seldom practical and rarely possible. In addition, the potential applications of these detailed datasets may be limited, owing to the difficulty of quantifying the vulnerability of assets for which little data exists. Given these practical challenges, the engineering and loss modeling communities often rely on regional loss estimation strategies that make use of aggregated statistical data on building stock and 'archetype-based' structural vulnerability models to offer realistic solutions for risk management. Nonetheless, it is crucial to compile an inventory of building stock with structural characteristics and population distribution in order to perform meaningful risk analyses for the extreme rainfall hazard.

The final outcome of the exposure module is a monetary exposure value in its disaggregated form (i.e. the estimated replacement value of the inventory of elements at risk, at the desired spatial resolution); which, in combination with the vulnerability, hazard and financial modules, is used for the quantification of ground-up and insured losses.

Vulnerability Module

The vulnerability module provides for each 1km x 1km grid cell the expected "loss ratio" equal to the proportion of the asset's replacement value damaged by the hazard. For example, an asset with a replacement value of US$1M having an excess rainfall loss ratio of 1% is estimated to have suffered a loss of $10,000. In XSR 2.5, vulnerability is represented by means of a curve known as a damage function (see for instance Figure 16). In contrast to the previous version of the XSR model, the vulnerability curves vary by class of vulnerability. In XSR 2.5 the damage functions vary by time aggregation period, by class of vulnerability and by country. Research leading to the development of XSR 2.5 have shown that the damage mechanisms for rainfall induced flood are substantially the same in the countries contained in the XSR 2.5 model domain.

The vulnerability module is the link between the physical component (hazard) and the economic component (loss), thus allowing for the translation of rainfall intensity into an expected consequences and impact quantification. By means of the vulnerability curves, it is possible to distinguish between negligible rainfall events and damaging ones.

The vulnerability curve is represented by a parametric mathematical function and its parameters are selected in the calibration procedure based on historically recorded rainfall accumulation and corresponding losses.

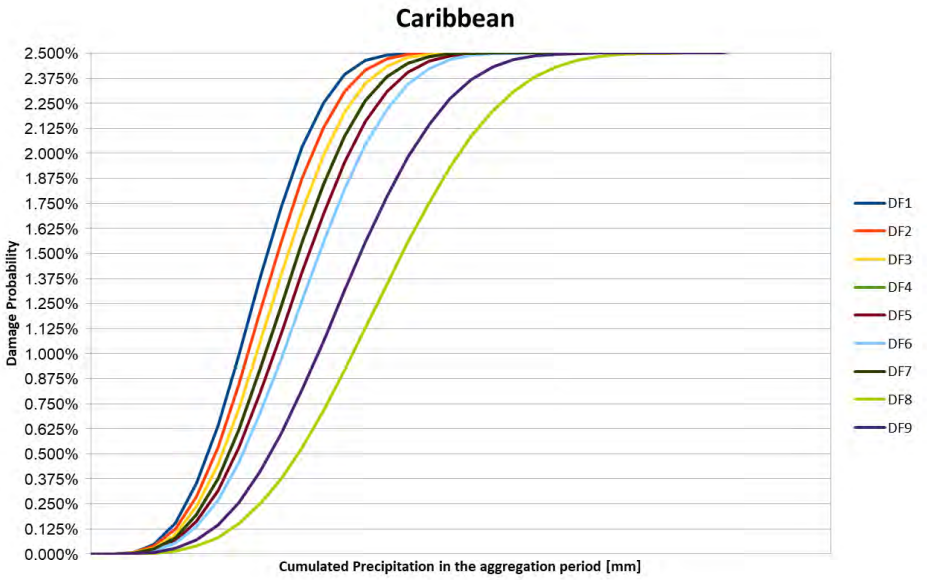

FIGURE 16 – EXAMPLE OF VULNERABILITY CURVES

Loss Module

The loss module provides estimates of total ground-up loss, aggregated on a country-by-country basis, that are then provided as input to the insurance module to determine country payouts. It also provides the temporal definition of an event (start date and end date) as per the policy conditions necessary to compute the final payout.

The loss module can be divided into two steps:

1. Identification of a CARE
2. Computation of the ground-up loss

The first step identifies a CARE (Covered Area Rainfall Event) based on the Climate Prediction Center's Morphing Technique (CMORPH) for estimating rainfall accumulation along with four additional parameters, as follows:

a. The *aggregation period* is the number of hours the rainfall intensity is aggregated in order to be considered for the loss computation. The aggregation is necessary because flood damage is caused by the sustained accumulation of rainfall over time rather than by the peak rainfall intensity (maximum intensity) alone.
b. The *rainfall threshold* is the value of rainfall intensity (averaged over the aggregation period) that must be exceeded to activate a grid cell with non-zero rainfall. That is, rainfall intensity below the rainfall threshold is considered to produce negligible losses and is therefore excluded from the total loss computation.
c. The *active cell fraction threshold* is the percentage of exposure cells having average rainfall intensity over the aggregation period (from [a]) greater than the rainfall threshold (from [b]).
d. The *tolerance period* is the maximum number of days that active cell fractions can drop below the threshold without interrupting a CARE.

A CARE in a modeled country is identified when the active cell fraction threshold is exceeded. A CARE is always reported with a start date and end date, and the computation of loss refers only to this time period.

The computation of loss depends on:

- the rainfall intensity computed by the hazard module by each dataset (CMORPH and two configurations of the Weather Research Forecasting [WRF] model)
- a Disaster Alert posted on the website by ReliefWeb[3], a specialized digital service of the United Nations Office for the Coordination of Humanitarian Affairs (OCHA)
- the vulnerability curve
- the exposure value for each cell
- and the loss threshold (LT)

In case of a Disaster Alert, a loss event is generated by the modeling system if the Rainfall Index Loss (RIL) computed from one of the rainfall datasets exceeds the LT; otherwise the RIL from at least two of the three hazard estimates must exceed the LT to qualify as a loss event.

Therefore, the loss module consists of two triggers: the primary trigger is the rainfall intensity (as in the previous version of the model) and the secondary trigger is the issuing of a Disaster Alert. This approach drastically reduces the number of false positives (i.e. cases in which no significant losses were caused, but the model computes a payout).

[3] http://reliefweb.int/

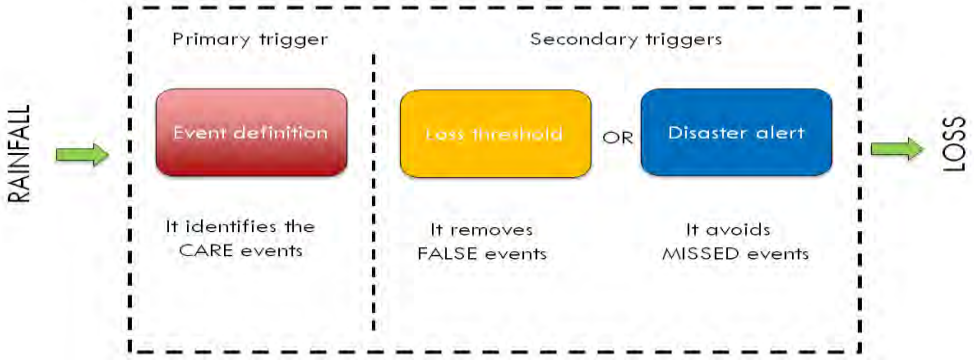

FIGURE 2.17: RAINFALL TRIGGERS

The output of the loss module is the final RIL, computed as the average of the RILs above the loss threshold, which in turn is used by the Insurance Module to compute the country payouts.

Insurance Module

The aim of the insurance module is to compute the payouts due for an insured event on the basis of the policy conditions and the final Rainfall Index Loss (RIL). In fact, the insured loss calculation is parametric, which means that the payout is dependent on the modeled loss (RIL) rather than the actual loss suffered by a country.

A few parameters define the payout, as follows:

- Attachment Point (AP): represents the loss that a country decides to retain before any insurance payout begins and is in principal similar to the "deductible" in a standard insurance policy;
- Exhaustion Point (EP): represents the loss value at which the full insurance payout is due;
- Ceding Percentage (CP): represents the fraction of the difference between the EP loss and the AP loss that the insured country transfers to CCRIF;
- Coverage Limit (CL): represents the maximum amount that can be paid to an insured country in any one year of coverage.

The payout computation is rather simple:

$$payout = \frac{RIL - AP}{EP - AP} * CP$$

The Coverage Limit is both the claim limit and the annual aggregate limit. Thus, the payout and the annual aggregate payout cannot exceed the CL.

The AP and EP losses are estimated based on the loss exceedance probability curve and correspond to a previously agreed-to return period. The CP is determined by the insured country.

Calibration Procedure

As illustrated above, the XSR 2.5 is a complex model, which allows for flexibility and adaptability. These features have been obtained by means of a rigorous calibration procedure. Considering the model as a whole, the parameters to be calibrated are:

- *Hazard module*: aggregated period, rainfall threshold, active cell fraction, tolerance period
- *Vulnerability module*: parameters of the vulnerability curve, namely alpha and beta
- *Loss module*: loss threshold

The other parameters of the insurance module are identified by means of a financial analysis and are based on the needs of the insured.

The objectives of the calibration procedure are:

- to maximize the capability of the model to identify the loss events
- to minimize the errors between modeled loss and actual loss
- to estimate coherently the model loss frequency as a basis for a financial analysis

Operational use of the XSR 2.5 model

The XSR 2.5 model is both a risk model to make quotations and assist underwriting of the insurance policy. It also acts as an operational model providing near real-time calculation of the loss and relative payouts due to excess rainfall in modeled countries.

In order to provide the computation of loss and the relative payout within a short time frame (14 days), the XSR model is designed for real-time loss assessment. When run in this mode, the input data of the model (i.e. the satellite-based rainfall estimates and the initial conditions from the climate model) are collected automatically every 24 hours. Once per day, the chain of XSR modules runs and produces the losses for all of the countries in the domain. Model output includes the payout for each CCRIF member country.

The conceptual framework of the operational use of the XSR 2.5 model for post-event rainfall payout computations is depicted in Figure 18. During each monitored day, every country can be found in one of five states (see Figure 19): normal conditions (green), ongoing CARE (red), CARE temporarily closed but tolerance period still ongoing (orange), CARE definitely closed but waiting period for Disaster Alert issuance still ongoing, (purple), and CARE closed (yellow). Note that Figure 9 is a simplification of the procedure as regulated by the CCRIF XSR protocol and is reported here for illustration purposes only.

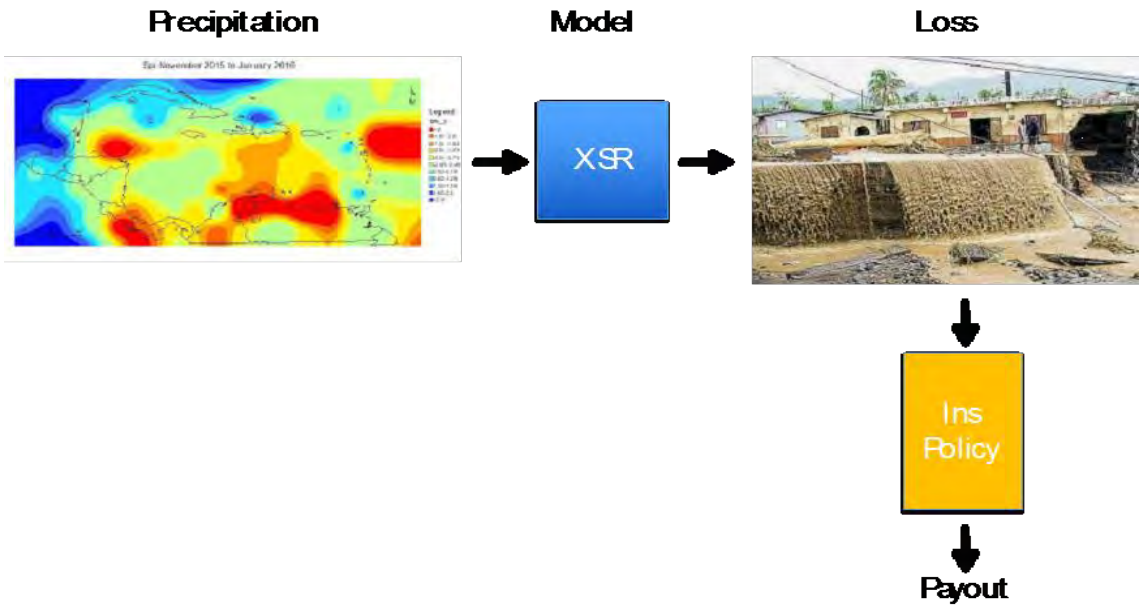

FIGURE 18 – CONCEPTUAL FRAMEWORK SHOWING OF THE OPERATIONAL USE OF XSR MODEL

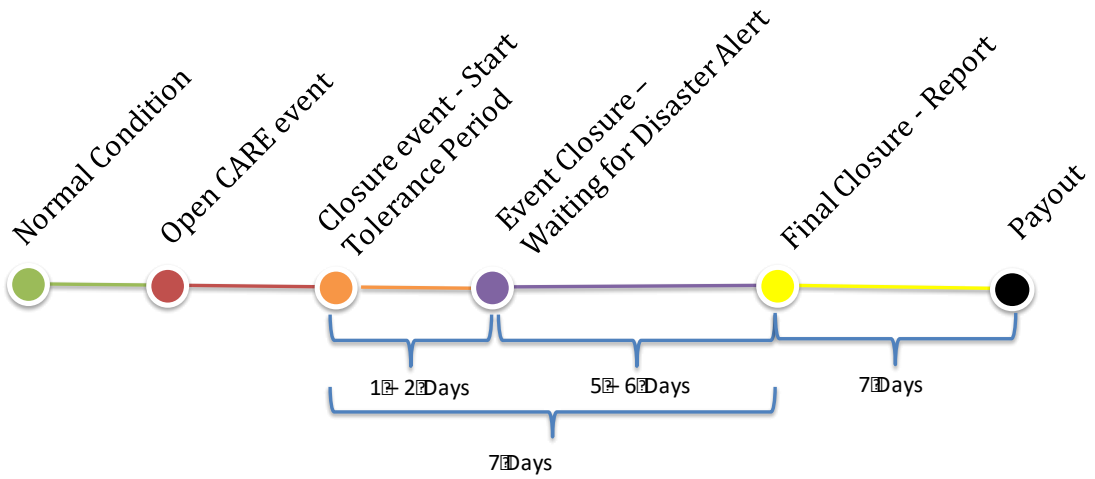

FIGURE 19 – CONCEPTUAL SCHEME SHOWING THE REAL-TIME OPERATIONAL USE OF THE XSR MODEL

Excess Rainfall (XSR) Run-Off Model

An additional activity currently undertaken by CCRIF is the development of a dedicated module within the XSR model for flood events. In many cases, and in particular in countries with a bigger land mass, damage caused by rain manifests itself in the form of riverine floods, often downstream of the area where the rain was observed. For these forms of water-related damage, a new run-off module will be created. This additional feature will not be available for the 2019/2020 policy year, but will be presented in the course of the year to CCRIF's members.

COUNTRY RISK PROFILES

CCRIF prepares Country Risk Profiles for the three perils currently covered: TC, EQ and XSR for each member country. These profiles provide an outline of the earthquake, tropical cyclone and rainfall characteristics and risks for the country as well as economic loss information used by the models. The profiles are reviewed and approved by the member government. New profiles are created when there is a change in the underlying model. Similarly, new profiles are created for new perils e.g. drought or economic sectors e.g. agriculture when those products are developed.

The profiles are aimed at providing decision makers with a clear picture of the key risks which the country faces in order to guide national catastrophe risk management and inform decision making for both risk reduction and risk transfer (via CCRIF coverage and other mechanisms which may be available). The risk profiles provide the basis for CCRIF to discuss coverage options with each country individually and to underwrite country policies once coverage levels have been agreed.

The development of the CCRIF catastrophe risk model is an important contribution to national and regional risk management institutions through its collection of a significant set of detailed databases on national catastrophe risk exposures in its member states. This is important specifically because prior to this initiative most member countries had for the most part never undertaken any major effort to collate this information which is critical in understanding the catastrophe risks faced at a national and regional level. These risk profiles facilitate increased knowledge of the extent of catastrophic risk facing CCRIF member countries and the risk modeling can help governments better adapt to known threats and mitigate against future threats.

The country risk profiles and accompanying annexes provide the following information:

- Details about the risk modelling platforms which are used to underpin the associated policies
- Regional Hazard Profile
- Basic demographic/economic/geographic information about the country
- The country-specific profile: hazard, exposure and risk for the country
- The most severe historical scenarios and their estimated economic losses

COUNTRY RISK PROFILE (SPHERA) – TROPICAL CYCLONE

Hazard

The hazard module of the SPHERA TC model provides a stochastic catalogue of potential future tropical cyclones that are statistically consistent with the historical tropical cyclone activity in the region. Records of cyclones in the region start in 1850. The catalogue is based on statistics of past events. From this catalogue it is possible to estimate the level of wind speed and storm surge expected in the region with different annual rates of exceedance.

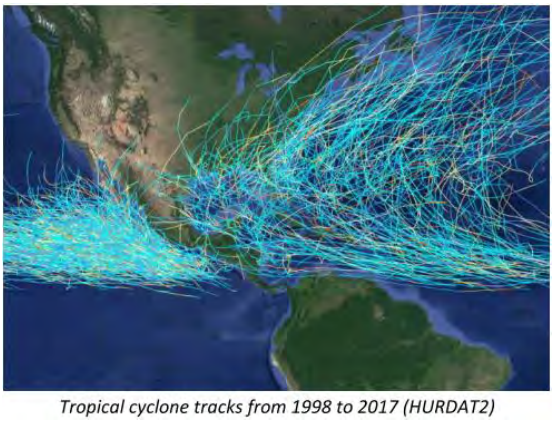

Tropical cyclone tracks from 1998 to 2017 (HURDAT2)

The profile provides maps that show the maximum wind speeds and the maximum sea level generated by tropical cyclones that are expected to occur in the country with an average frequency of once every 50 and once every 250 years.

Exposure

The exposure database provides count, replacement cost and vulnerability classification of different building classes and infrastructure assets. It has been developed by collating several sources of data up to 2017 related to the built environment and the surrounding topography. The resolution is 1 km^2 for inland areas and from approximately 250 m^2 to 120 m^2 for coastal areas. The profile provides graphs that show the breakdown of the replacement value of the assets at risk, classified by occupancy class, in terms of percentage and absolute value. The profile also includes a map with the spatial distribution of the assets in terms of Replacement Value exposed to tropical cyclones.

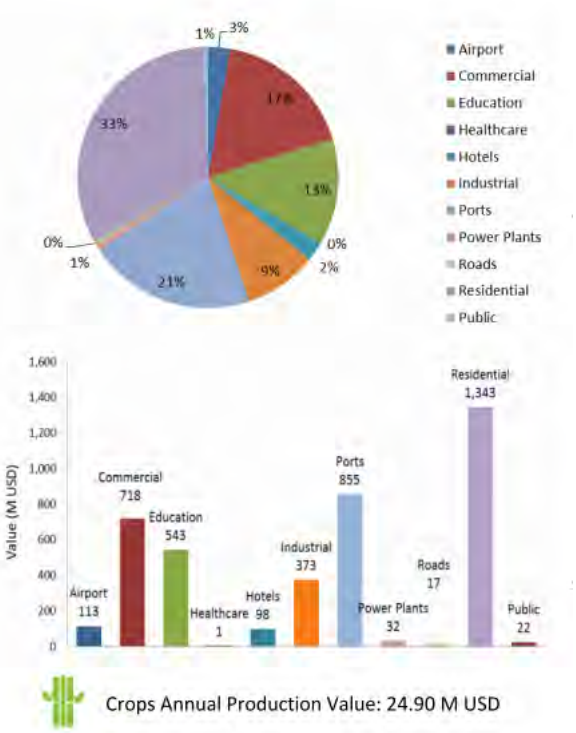

Vulnerability

The vulnerability module estimates the possible consequences of a tropical cyclone on the different assets, described in the exposure database, that constitute the built environment. To do so the model makes use of relationships between the intensity of wind/surge and the repair cost of the exposed damaged assets. The profile presents the classification of country's vulnerability to TC (low, medium or high) based on the characteristics of the building stock, the age of the building stock, the local building codes, the characteristics of the roofs and shutters and the preparedness of the country to tropical cyclones

Historical Losses

The most severe events during the past 20 or so years are presented along with the associated human and economic losses.

Risk

The estimate of TC risk is based on the stochastic catalogue of potential future tropical cyclones that may affect the region and on the losses that they may cause to the exposed assets. The profile provides a graph which shows the tropical cyclone-induced ground-up losses (OEP) that are expected to be exceeded, on average, once every certain numbers of years (the return period). It also presents a table that reports the numerical values of the losses associated with five return periods extracted from the curve and the long-term average annual loss due to tropical cyclone events.

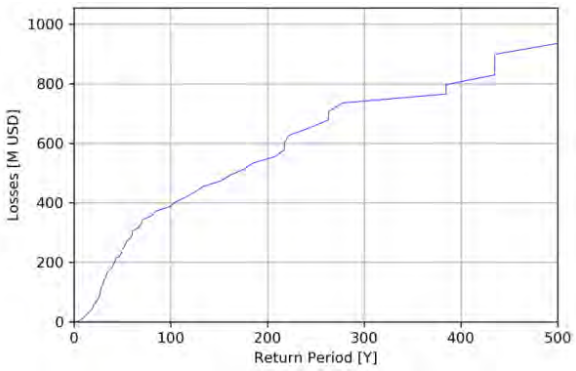

COUNTRY RISK PROFILE (SPHERA) – EARTHQUAKE

Hazard

The hazard module of the SPHERA EQ model provides a stochastic catalogue of potential future earthquakes that are statistically consistent with the historical seismicity in the region, displayed in the map at right. This catalogue is based on statistics of past events and on the knowledge about location, geometry and rate of activity of the earthquake sources (faults) present in the area of interest. From this catalogue it is possible to estimate the level of earthquake g round motion expected in the region with different annual rates of exceedance. The profile provides maps that show the Peak Ground Acceleration expected to occur in the country with an average frequency of once every 95 (left) and once every 475 years (right).

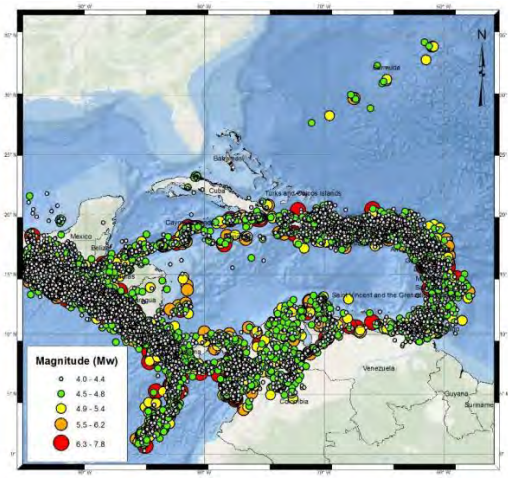

Exposure

The exposure database provides count, replacement cost and vulnerability classification of different building classes and infrastructure assets. It has been developed by collating several sources of data up to 2017 related to the built environment and the surrounding topography. The resolution is of 1 km^2 for inland areas and from approximately 250 m^2 to 120 m^2 for coastal areas. The profile presents a map that show the spatial distribution of the assets exposed to earthquakes in terms of Replacement Value and graphs that show the breakdown of the replacement value of the assets at risk, classified by occupancy class, in terms of percentage and absolute value.

Vulnerability

The vulnerability module estimates the possible consequences of an earthquake on the different assets, described in the exposure database, that constitute the built environment. To do so the model makes use of relationships between the intensity of ground motion generated by the given event and the repair cost of the exposed damaged assets. The profile presents the characteristics of the building stock of the country and the characterization of its vulnerability to ground shaking.

Historical Losses

The most severe earthquakes during the past 20 or so years (if any) are presented along with the associated human and economic losses.

Risk

The estimate of EQ risk is based on the stochastic catalogue of potential future earthquakes that may affect the region and on the losses that they may cause to the exposed assets. The profile provides a graph which shows the earthquake-induced ground-up losses (OEP) that are expected to be exceeded, on average, once every certain numbers of years (the return period). It also presents a table that reports the numerical values of the losses associated with five return periods extracted from the curve and the long-term average annual loss due to earthquake events.

COUNTRY RISK PROFILE (XSR 2) – EXCESS RAINFALL

Hazard

The hazard module of the excess rainfall model provides estimates of precipitation on a daily basis. These estimates are derived in near real time by a combination of both climatic-meteorological models and a satellite-based precipitation model. Maps show the amount of daily rainfall that is expected to

be observed in the country, on average, once every 5 and 25 years as well as graphs that show rainfall patterns in the country.

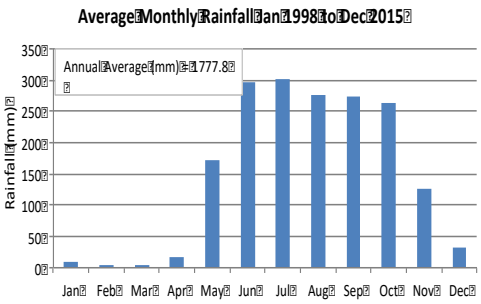

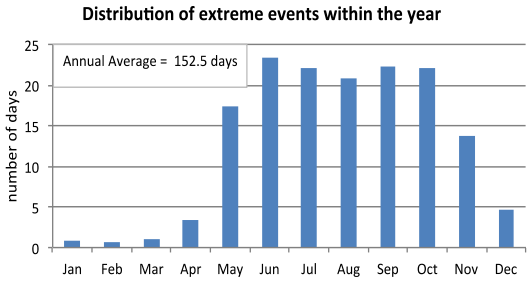

Exposure

This section presents graphs that show the breakdown of the value of the assets at risk by occupancy class and a map that shows the distribution across the country of the assets exposed to natural hazards. The representation is in terms of Replacement Value in millions USD.

Vulnerability

The vulnerability module estimates the possible consequences of an excess rainfall event on the different assets, described in the exposure database, that constitute the built environment. To do so the model makes use of relationships between the amount of rainfall and the repair cost of the exposed damaged assets.

Historical Losses

This section presents a record of historical losses from tropical cyclones and other significant rain events.

Risk

The risk profile presents a graph showing the rainfall-induced losses to public buildings that are expected to occur with a range of return periods and a table that shows the long-term average annual loss due to excess rainfall events.

NEW CCRIF PARAMETRIC PRODUCTS




DROUGHT

A new Drought product will be offered in 2019/20 as a pilot test to select CCRIF member countries. The purpose of the model is to identify agricultural drought events (i.e., droughts affecting crop production) occurring in Caribbean and Central American countries, and assessing the resulting losses due to reduced yield.

The model is designed to run on an annual basis, for CCRIF member countries and for six types of crops (banana, coffee, maize, rice, sugar cane and a generic category that is meant to be used for any other crop). Thus, a payout could occur at the end of a dry year to any insured country that has had a significant loss of crop yield or at the end of a severe dry spell before the end of the year. Given that the growing process for crops does not necessarily follow CCRIF's policy year, the Drought policy insurance period will likely run from January 2 to January 1 the next year.

FISHERIES AND AQUACULTURE

Currently, CCRIF is in the process of developing a product for the fisheries sector. Since 2015, CCRIF has been engaged in the Caribbean Oceans and Aquaculture Sustainability Facility (COAST) initiative with the United States Department of State, World Bank, the Food and Agriculture Organization (FAO) to develop parametric insurance products to be marketed in the Caribbean to promote the resilience of the fisheries sector against increasing climate change-related disaster risks.

The overall development objective of COAST is to foster country-led climate smart food security and develop and implement disaster risk management plans. A parametric insurance product for the fisheries and aquaculture sectors will be an essential tool to help address the impacts of natural hazards on food security and livelihoods of those working in the fisheries and aquaculture sectors.

Within the COAST initiative, CCRIF is developing a specific product for covering direct losses sustained by the fisheries sector due to high wind and storm surge caused by tropical cyclones. The parametric insurance coverage provided with this product will be underpinned by an adapted version of the SPHERA model called SPHERA4COAST. This adapted version of the model will consider only the portion of the exposure database related to the fisheries sector, paying particular attention to landing sites, piers, warehouses, waterfront structures, boats and storage buildings. The SPHERA4COAST model will be used to test the applicability of a parametric sovereign fisheries insurance policy in the Caribbean.

CCRIF is also considering the possibility of developing a microinsurance product aimed at compensating fisherfolk and fisher cooperatives for business interruption losses caused by inclement weather. This product will be based on an advanced version of the SPHERA4COAST model, which would also consider the intensity of wind and potentially waves within a certain distance from the coastline that may prevent fishing activities. It would also take into account information about best practices of storing fishing material, tying boats and other activities aimed at limiting damages.

AGRICULTURE

CCRIF continued discussions with development partners and member governments about the development of a model for agriculture. While the new drought product addresses one aspect of agricultural losses, and the existing tropical cyclone and excess rainfall products can provide coverage for the agriculture sector, governments in the region have been requesting a comprehensive product specifically for the sector (for farming activities and related processes) – one which addresses and includes different perils, such as extreme rainfall, tropical cyclone-induced extreme wind and coastal flooding, and drought. At the individual (microinsurance) level, the Livelihood Protection Policy developed under the Climate Risk Adaptation and Insurance in the Caribbean project (see below) provides insurance for the agriculture sector at the individual level – but based only on excess rainfall and wind.

MICROINSURANCE – THE CLIMATE RISK ADAPTATION AND INSURANCE IN THE CARIBBEAN PROJECT

During 2010 – 2014, CCRIF was a key partner in the Climate Risk Adaptation and Insurance in the Caribbean project. Under this project a parametric microinsurance product called the Livelihood Protection Policy (LPP) was developed and made available in the three pilot countries (Jamaica, Saint Lucia and Grenada). Targeted at individuals, the LPP is designed to help protect the livelihoods of vulnerable low-income individuals such as small farmers, tourism workers, fishers, market vendors and day labourers, by providing quick cash payouts following extreme weather events (specifically, high winds and heavy rainfall). The livelihood protection policy is designed to reduce vulnerability and sustain the livelihoods of low-income communities. Since the LPP was introduced, four rainfall events have triggered payouts of the LPP in Jamaica and Saint Lucia.

Launched in November 2017, Phase II is being implemented in collaboration with the Munich Climate Insurance Initiative, International Labour Organization's Impact Insurance Facility, DHI Water & Environment and GK Insurance. The project is funded by the International Climate Initiative of the German Federal Ministry for the Environment, Nature Conservation, and Nuclear Safety.

Phase II aims to expand access to the LPP within the three pilot countries and also in Belize and Trinidad and Tobago. The focus is on the introduction and commercial roll-out of the products to farmers, fishers, market vendors, small entrepreneurs among others via development/microfinance institutions and other entities such as trade associations. The ambition under Phase II includes the participation of a wide range of stakeholders in the process – acting on behalf of, or purchasing products on behalf of, their constituents. These stakeholders include government entities, local authorities, cooperatives and industry associations on behalf of their members.

Because the LPP is parametric, policy holders do not have to make a claim to the insurer – individual payouts are tied to a series of thresholds for wind speed and rainfall. If one of these thresholds is met, the client's policy is "triggered" and the client will receive an automatic payout within 7 days made to his or her bank account, the amount of the payout scaling upwards with the severity of the triggering event. Furthermore, the policy includes an information system that uses mobile text messages to inform clients quickly if their individual policy was triggered and to provide weather risk information such as storm warnings.

INTEGRATED SOVEREIGN RISK MANAGEMENT

In May 2017, the Caribbean Development Bank and CCRIF SPC launched the Integrated Sovereign Risk Management in the Caribbean project. This project seeks to enable all Caribbean countries to take a more proactive approach towards country risk management, moving beyond planning for natural disaster risks such as climate change and events like hurricanes and earthquakes and recognizing the intrinsic linkages between

disaster risk and other types such as economic, technological and financial risks and the impacts of these on socioeconomic development, especially.

The project is intended to enable the countries in the region to become more resilient, by enhancing the capacity of governments to take a portfolio view of risks and include all risk categories – technical, economic, natural and social risks – and their interdependence in a geographic context. A key part of this new integrated risk management framework will be to establish country risk officers or coordinators within countries – that is senior level positions that will be responsible for managing the overall risk landscape, taking a holistic approach to risks before events occur and ensuring that countries adopt a more proactive, precautionary approach to anticipating future challenges.

Introducing Sovereign Risk Management – the Rationale for the Initiative

With significant shifts in the frequency, impact and very nature of risks in the 21st century, governments are faced with a need to adjust their sovereign risk management strategies. The underlying changes which have taken place in many societies over the last 30 years have tremendously increased vulnerabilities. These vulnerabilities have not only increased due to socioeconomic factors, but also due to the technological and economic interconnectedness of communities across regions and globally. This has led to an increase in uncertainty regarding the beginning and end points of sovereign risks, as seemingly far away events could cascade into transnational shocks. Privatization in key industries also represents a growing economic trend over the last 20 years, which has created uncertainties regarding ownership and accountability for prevention and mitigation of associated risks.

The concept of risk governance and sovereign risk management covers a broad spectrum: not only does it include what has been termed 'risk management' or 'risk analysis' but it also focuses on how risk-related decision making unfolds when a range of actors is involved, and calls for a coordinated effort amongst stakeholders including the private sector.

Risk management at the national level considers sovereign risk beyond natural disasters and catastrophes and requires nations as a matter of duty to protect their people, assets and environment from a range of threats that they could potentially face. Apart from the risks created by climate change, Caribbean countries are subject to a myriad of others, including economic, geopolitical, environmental, societal and technological risks.

Whilst many national policies being developed by countries in the region are taking sustainability issues into account, there is still considerable scope for further work in integrating all the other categories of risks under a single broad umbrella.

Caribbean governments currently possess large amounts of information and data on a wide range of risks facing them. The key challenge is to effectively process and synthesize those data and aggregate them in a manner that would enable them to prioritize threats, design effective mitigation strategies and develop responsive policies that would address socioeconomic and developmental issues. There is the additional challenge of budgeting and allocating resources to support mitigation measures in a way that minimizes adverse threats.

Regional governments would also need to pay particular attention to two new developments in sovereign risk management: (a) all-hazards policy frameworks – integrating information from a diverse set of government bodies and the private sector and (b) national risk assessments, both of which are part of a broader framework of risk governance. Also, within this framework is the need to appoint dedicated country risk coordinators (CRCs) to act as custodians of the governance process.

The creation of a country risk office within each Caribbean country would serve to significantly aid in identifying risks at the national and regional level and also would formalize risk assessment, mitigation and adaptation, thereby reducing potential domestic, national and regional risks.

This initiative will allow for countries to adopt a more proactive approach towards country risk management. It moves beyond planning for disaster risks such as climate change and extreme events and recognizes the intrinsic linkages between disaster risk and other categories, including but not limited to economic, technological, financial, socioeconomic and green economy transition risks. It will enable the development of a standardized integrated risk management framework for use by all Caribbean countries. It will advance the institutionalization of CRCs within countries who would act as a central point of contact for the purposes of managing a comprehensive portfolio of sovereign risks.

Key Activities under this Initiative

The following activities are being or will be implemented:

- A Situational Analysis on Risk Management within CCRIF Member Countries and CDB Borrowing Member Countries (BMCs) – this analysis will form the basis for the development of a register of lessons learned and regional best practices that would become part of the standardized integrated risk management framework
- A Country Comparative Analysis of Integrated Risk Management Frameworks – this analysis will identify best practices in integrated risk management globally, and document lessons learned at the international level in both the public and private sectors
- A Gap Analysis – this analysis will be based on the comparative analysis and the situational analysis and will illustrate the key differences between the current situation of the countries assessed and international best practice. The gap analysis also will provide necessary information related to capacity development needs in risk management across countries
- Development of a standardized integrated risk management framework to be implemented across countries
- Development of terms of reference for CRCs
- Hosting of a regional training workshop and conference on integrated risk management frameworks for policy makers in June 2019

INTRODUCTION TO THE RTFS

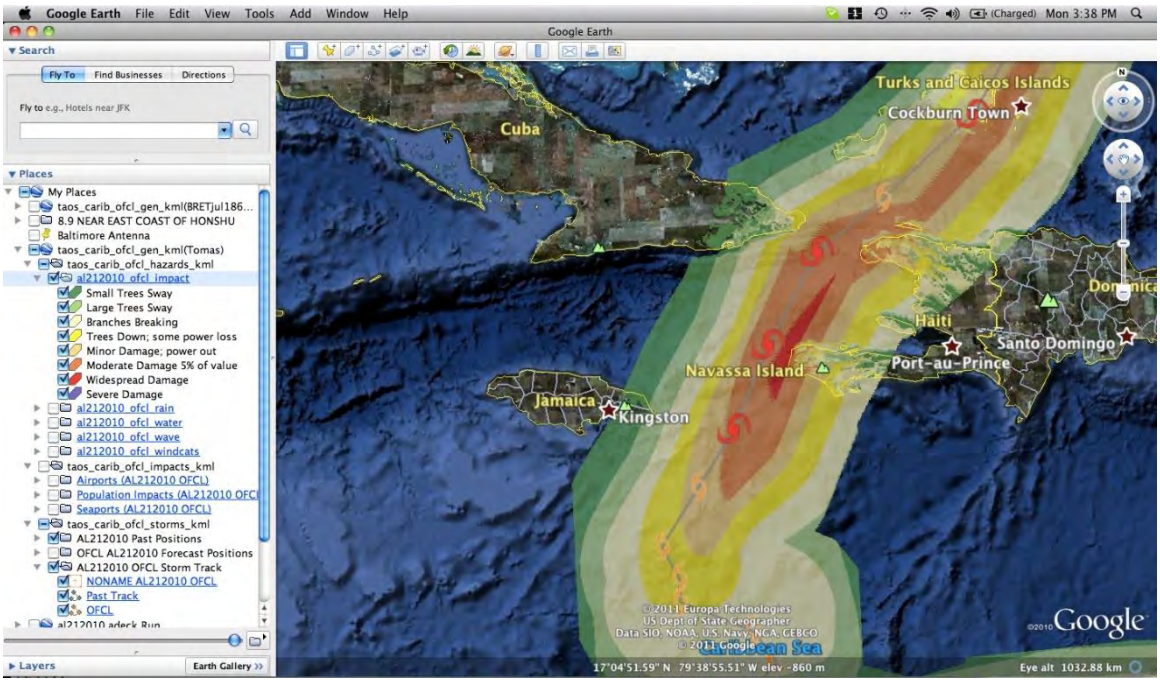

Knowledge of a storm's expected impacts helps with effective preparedness and response, aiding with evacuation decision making, planning for pre-positioning of equipment and supplies, activation of mutual assistance arrangements and asset management.

The Real-Time Impact Forecasting System (RTFS) is a storm impact forecast tool which provides users with real-time hurricane hazard and impact information to support intelligent risk management.

While typical hurricane weather sites tell the user where the storm is going, and how strong it is likely to be, the CCRIF RTFS tells the user what it is likely to do when it gets there - in terms of: wind speed over land, storm surge and wave heights along the coast, total expected rainfall, number of people affected by wind speed category, expected general damage levels, and expected down-time for ports and airports.

Utilizing a 3D high-resolution modelling platform, detailed information on the expected hazard levels and their impacts from tropical cyclones for the entire Caribbean region is produced. The RTFS therefore enables all CCRIF members to access real-time estimates of the expected hazard levels and impacts on population and infrastructure for all tropical cyclones during the hurricane season.

The Practical Importance of the RTFS to Policymakers

The main users of the RTFS product include disaster and emergency managers and meteorological officers. The RTFS outputs are of greatest benefit to governmental and non-governmental agencies involved in hurricane risk management.

Emergency managers can use the RTFS information as triggers for preparedness and alert procedures. For example, shelter management can be informed when the maximum wind speed is expected at a

specific location. The decision to evacuate a low-lying area can be informed by the maximum storm surge height expected just off the coast of that location.

Outputs can be used to produce reports, maps and other guidance documents in support of emergency management. This can in turn be provided to other stakeholders to aid their decision making process.

Policymakers and ministers also can benefit from information that the RTFS provides. The RTFS information can:

- Assist with contingency planning by providing a preview of what might happen if a given storm continues along a projected path, and activate appropriate contingency plans based on this insight
- Assist with shelter management by identifying impact areas and shelter locations to support shelter allocation decisions
- Identify potential damage to shelters, thereby aiding decision makers to plan for alternatives
- Assist with determining emergency interventions by identifying areas where populations are at risk so that decision makers can issue warnings and plan for assistance.

Although registered RTFS users can access the CCRIF website directly for the outputs of the forecast, the Caribbean Institute for Meteorology and Hydrology (CIMH) also plays a key role in supporting and training users in the appropriate use of the tool. The CIMH uses outputs from the CCRIF RTFS as input into the Caribbean Dewetra Platform. Data from this platform is used to brief the CDEMA country preparedness team(s) when a storm is approaching one or more of the CDEMA member states. This involves individual briefings with countries and the provision of briefs on approaching events which incorporate information from the RTFS

The role of the National Met Office is to observe and understand the weather and climate of the region and provide meteorological, hydrological and marine services in support of the national needs and international obligations.

APPENDICES

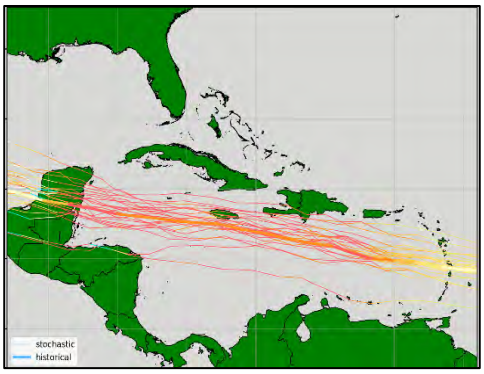

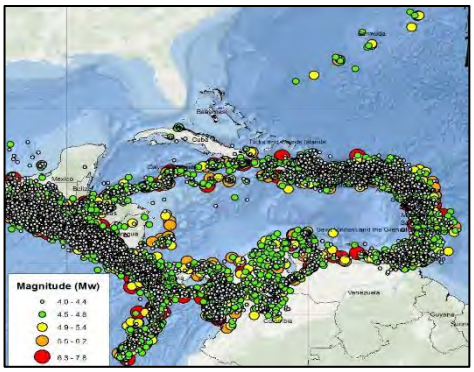

Appendix 1: SPHERA Tropical Cyclone Model

Appendix 2: SPHERA Earthquake Model

APPENDIX 1

SPHERA

SYSTEM FOR PROBABILISTIC HAZARD EVALUATION AND RISK ASSESSMENT

TROPICAL CYCLONE MODEL

Release 1
November 2018

INDEX

1 INTRODUCTION

1.1 Aim and scope

This report describes the methodology implemented by ERN/RED for CCRIF SPC in the SPHERA (System for Probabilistic Hazard Evaluation and Risk Assessment) model for the assessment of extreme wind and storm surge losses triggered by tropical cyclones. In particular, this report outlines *a)* the approach used to compute tropical cyclone-induced losses in the countries covered by the model for both pricing and portfolio loss estimation; and *b)* the methodology adopted for estimating losses to buildings and infrastructures in near-real time due to the occurrence of a tropical cyclone.

This document is intended to be an overview of the loss computation process, and as such the level of detail of every section is limited. Other reports with detailed information on every step of the methodology are available and the interested reader is referred to them for further information.

2 HAZARD

The SPHERA tropical cyclone loss model accounts for two damaging phenomena, wind and storm surge. The effects of precipitation are accounted for in a different excess rainfall model. For the purposes of the SPHERA model, wind and storm surge are quantified by two intensity measures: maximum wind speed and maximum storm surge. "Maximum wind speed" is the maximum velocity reached by the wind at any specific location for any given position of the tropical cyclone. The measure of wind speed used by the SPHERA model is the maximum averaged 1-minutes wind speed (in km/h). "Maximum storm surge" is the maximum level of water (in metres) caused at any specific location by the combined effect of a tropical cyclone (pressure drop and wind friction) and the astronomical tide for any given position of the tropical cyclone[4]. For any location of the storm both intensity measures are computed via mathematical models at all sites where one or more assets are located according to the exposure database. Due to the relatively short historical record of events, a stochastic catalogue of simulated events is employed to achieve an accurate representation of the hazard in the study area for return periods longer than the historical record.

In this section, the methodology adopted to create the stochastic catalogue of events is described, and then the wind model and storm surge model components of the hazard module are briefly illustrated.

2.1 Stochastic catalogue simulation

Reliable historical data on cyclone tracks are only available for a relatively short period of time and are not sufficient to assess risk especially for longer return periods (Rumpf et al., 2007). To overcome this limitation, large sets of synthetic cyclones, or stochastic cyclones, can be generated. The theoretical cyclones, also called stochastic cyclones, have characteristics (e.g., central pressure, radius of maximum wind and translational speed) that are statistically consistent to those of the real, or observed, cyclones, but their large number can help estimate more precisely and robustly the tropical cyclone risk in a specific area. This approach has been widely used in the past decade (Emanuel et al., 2006; Hall and Jewson, 2007; James and Mason, 2005; Rumpf et al., 2007; Vickery et al., 2009, 2000). In this model, a probabilistic approach was used to generate a catalogue of possible storms from the analysis of the historical tracks included in the HURDAT2[5] database by the US National Oceanic and Atmospheric Agency (NOAA). The approach is based on the following steps:

[4] Note: in general, the term "storm surge" usually indicates the sea level rise due exclusively to a storm, not including the astronomical tide effect. However, in this report, to avoid excessive repetitions, the term "storm surge" is referred to the sum of both effects, unless specifically indicated.

[5] https://www.nhc.noaa.gov/data/

1. Synthetic tracks were generated based on the historical tracks, applying random perturbations to the changes in direction of the observed tracks included in HURDAT2. The genesis of the synthetic cyclones was based on the genesis of the historical cyclones.
2. For every event, the minimum sea level pressure was computed at every time-step (6 hours) based on an autoregressive model (AR2) fitted on observed data, with a random term representing the natural variability of the process. The parameters of the AR2 model were derived from historical data for each cell on a 5x5 degrees grid covering the whole region of interest in order to properly reproduce the spatial variability of the phenomena.
3. For each time-step, the radius of maximum wind was computed as function of the minimum sea level pressure and the latitude according to the relationship proposed by Vickery and Wadhera (2008a) with a random term dependent on the sea level pressure.
4. The maximum wind speed along the track was generated depending on the minimum sea level pressure and the radius of maximum wind based on regression fitted on observed data. The available maximum wind speed, minimum sea level pressure and radius of maximum wind data for the Atlantic and Pacific basins were used to fit a second-degree polynomial relationship with a random term (Vickery and Wadhera, 2008b). Given that the physical processes that drive the relationship between pressure and wind vary in space, the parameters of the regression were calibrated in a spatially-variable manner, i.e. the spatial domain was divided into square zones of 10x10 degrees and for each zone a different regression was calibrated. The random term of the regression was modelled in two parts with inter-event and intra-event errors.
5. The filling effect, i.e. the decay in cyclone intensity when the cyclone eye makes landfall, was modelled with an exponential model (Kaplan and DeMaria, 1995), whose decay was calibrated on observed data, with a random term.

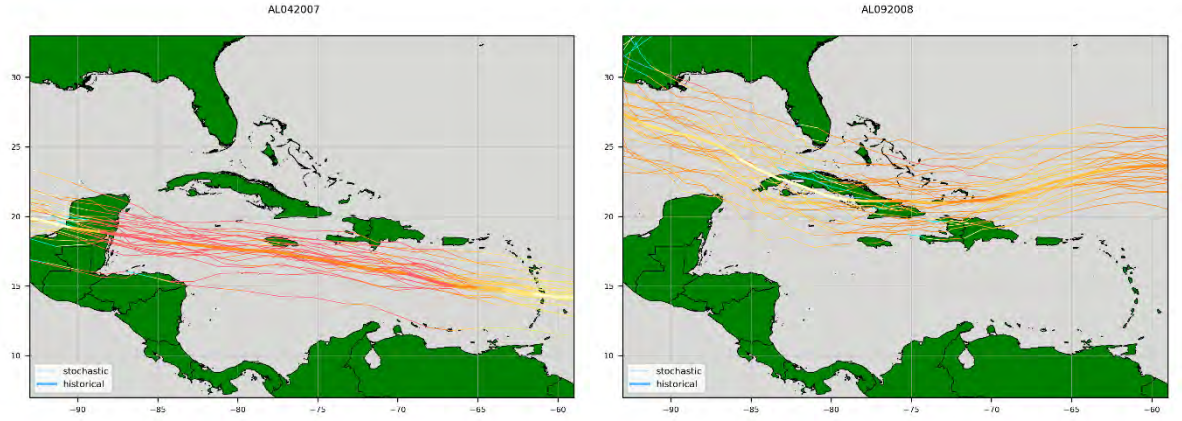

Figure 2-1 – Examples of parent observed hurricane track and derived perturbed tracks. The colour scale indicates hurricane intensity – see following sections for more info on how this was generated. The thickest track represents the historical cyclone that was used to generate the perturbed tracks.

The historical records of tropical cyclones in the Atlantic and Pacific Oceans are known to be partially incomplete (Solow and Moore, 2000). A frequency analysis was carried out on the historical catalogues. The analyses were performed separately for the two main basins, since their periods of records for tropical cyclones are different. With the aim of overcoming the limitation due to the incompleteness of the HURDAT2 historical data, the periods of incompleteness in the historical catalogue (pre-1970 for the Pacific, pre-1930 for the Atlantic) were filled by simulated events, as needed to match the frequency and distribution of events estimated from the complete parts of the historical records. These simulated hurricanes were added to the HURDAT2 historical catalogue that was utilized for the generation of the stochastic catalogue.

The characteristics of the stochastic catalogue were validated by comparing them to those of the historical data. In particular, the following features were compared:

- Number of events per country.
- Spatial density maps.
- Central pressure.
- Maximum wind speed.

Figure 2-2 shows the event frequency validation. These plots were obtained by counting the number of events crossing the perimeter of rectangular boxes enclosing the countries of study, and then dividing the total count by the duration in years of the historical and stochastic catalogues respectively. Some representative countries are shown as examples.

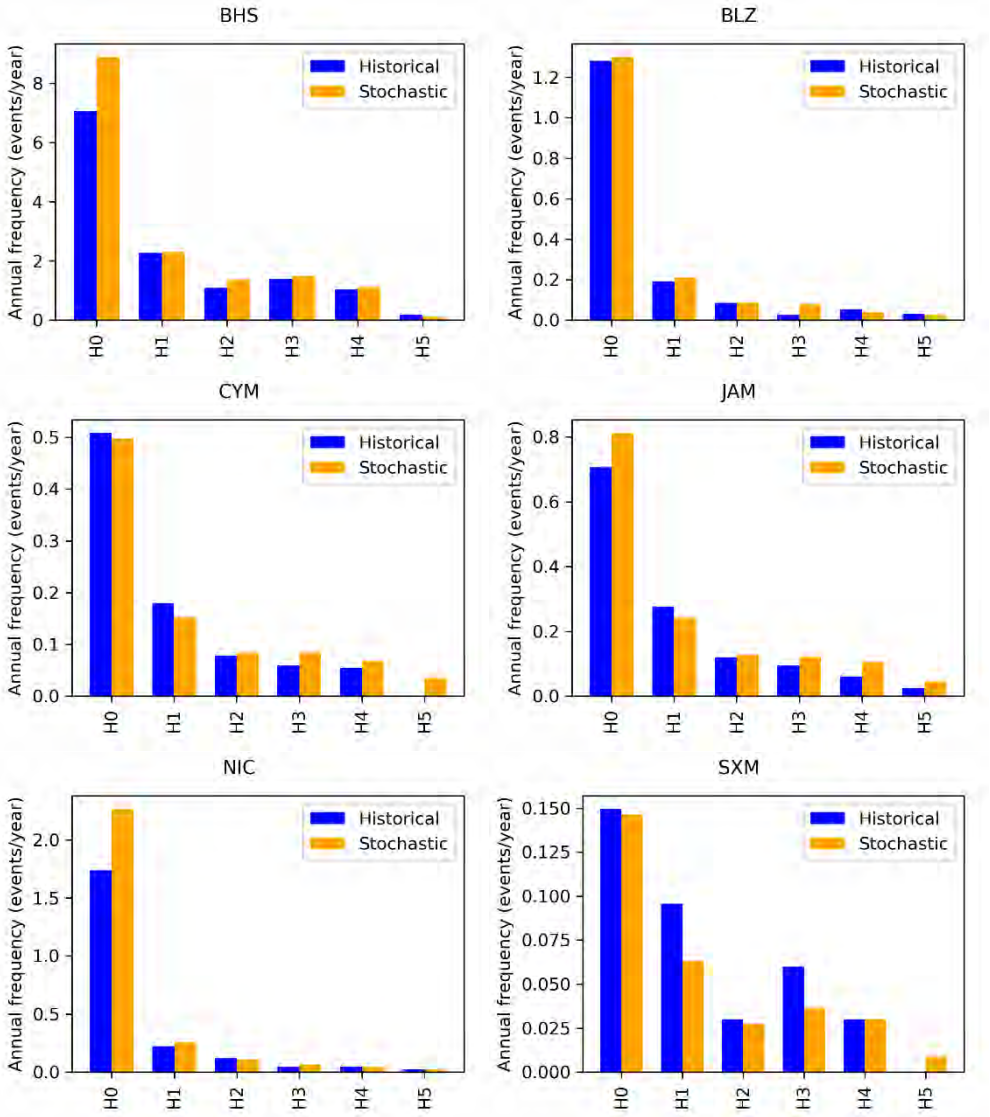

Figure 2-2 – Event frequency (events per year) by hurricane category, obtained by counting the event tracks crossing rectangular boxes enclosing the countries of study (+50 km in all the directions). OBS: from HURDAT2. SIM: from SPHERA stochastic catalogue. The country codes can be found in Annex A.

Figure 2-3 and Figure 2-4 show event density maps obtained from the historical (HURDAT2) and stochastic catalogues respectively. These density maps represent the annual event frequency over 10,000 km^2.

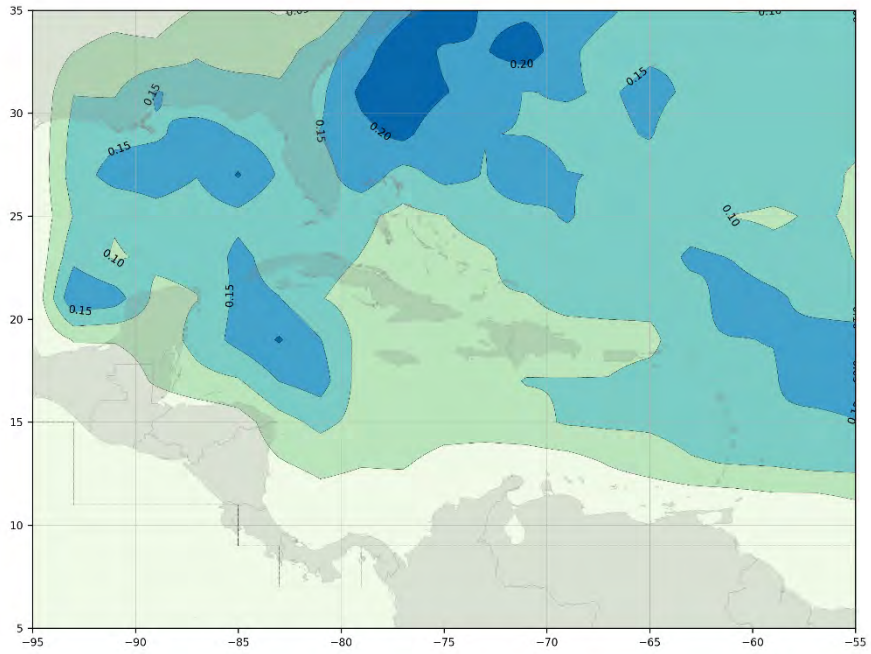

Figure 2-3 – Tropical cyclone density map, from the HURDAT2 catalogue, in event per year per 10,000 km^2.

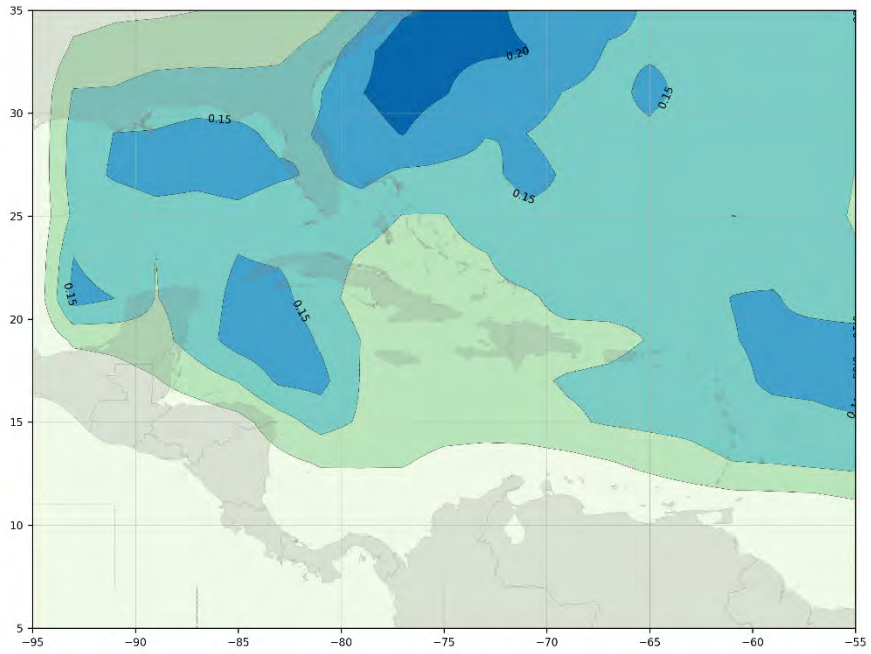

Figure 2-4 – Tropical cyclone density map, from the SPHERA stochastic catalogue, in event per year per 10,000 km^2.

Figure 2-5 shows the comparison between observed (from HURDAT2) and simulated (from SPHERA stochastic catalogue) minimum sea level pressure, obtained by selecting the event tracks crossing rectangular boxes enclosing the countries of study.

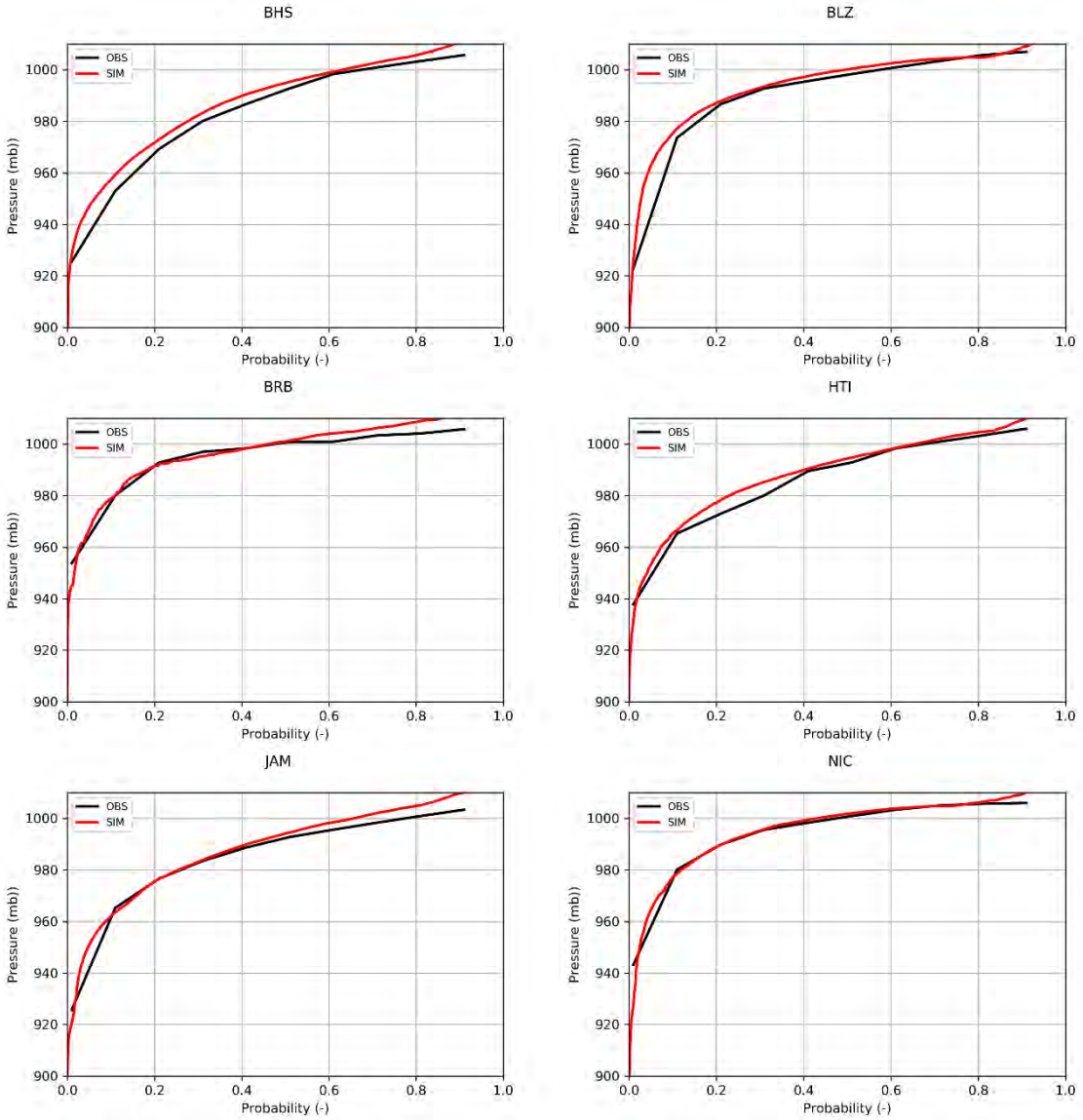

Figure 2-5 – Exceedance probability of observed (from HURDAT2) and simulated (from SPHERA stochastic catalogue) minimum sea level pressure, obtained by selecting the event tracks crossing rectangular boxes enclosing the countries of study. The country codes can be found in Annex A.

Figure 2-6 shows the comparison between observed (from HURDAT2) and simulated (from SPHERA stochastic catalogue) maximum wind speed, in terms of return period, obtained by selecting the event tracks crossing rectangular boxes enclosing the countries of study.

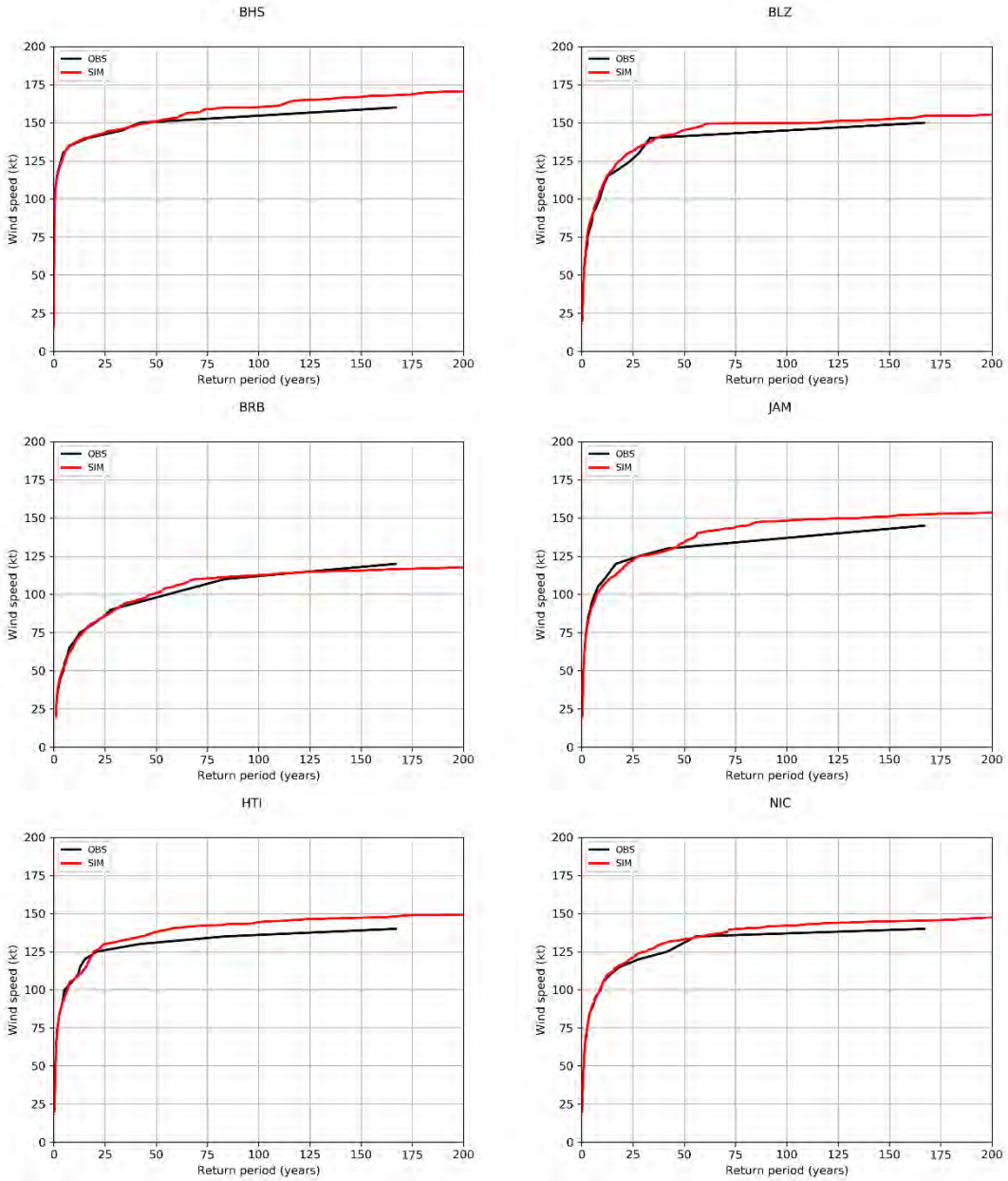

Figure 2-6 – Return period of observed (from HURDAT2) and simulated (from SPHERA stochastic catalogue) maximum wind speed, obtained by selecting the event tracks crossing rectangular boxes enclosing the countries of study. The country codes can be found in Annex A.

2.2 Wind hazard model

A tropical cyclone is a rotating storm system characterized by a low-pressure centre and strong winds. Several types of mathematical models are available to reproduce this complex phenomenon and compute wind speed values over a large geographical domain, ranging from complex numerical weather model to simpler and faster parametric models.

The wind component of the SPHERA model is based on a modified version of a parametric wind model published by Silva et al. (2002). This model is a modification of the Holland (1980) model, widely used in the field of tropical cyclone risk modelling. The model computes 1-minute sustained wind speed at 10m height (and pressure) over a large domain, on the basis of input parameter values that can be usually found in the tropical cyclone best track database provided by all major national oceanographic agencies. These data include cyclone position, minimum sea level pressure, maximum wind speed and radius of maximum wind. The wind is computed as a function of the distance from the eye, the

maximum wind speed and the Coriolis force parameter (dependent upon the latitude), and it is computed at every location of the domain. Then, the forward speed of the cyclone is also taken into account, as well as the rotational component of the cyclone movement. This operation is repeated at every time step of the cyclone, and at the end the maximum wind speed at every location over the domain is retained and used for loss computation purposes. The wind model time-step is variable, inversely proportional to the forward speed of the cyclone. This was done to ensure that if the cyclone is moving fast, a realistic footprint can still be obtained. The maximum time step is one hour.

This wind estimation model was chosen because of the following reasons:

- Its computational times are much shorter than those of numerical weather models, thus allowing fast real-time calculations and the simulation of a large dataset of events.
- It is a rather recent development (Silva et al., 2002) of a very well established parametric model (Holland, 1980).
- It was developed specifically for the study area (while most of the parametric models available in the literature were developed for the US coasts).

To validate the quality of the wind speed hazard results, a comparison with a dataset of reconstructed tropical cyclone wind fields was carried out. The National Oceanic and Atmospheric Administration's (NOAA) Hurricane Research Division (HRD) produced real time analyses of tropical cyclone surface wind observations on an experimental basis since 1993. The HRD Real-time Hurricane Wind Analysis System (H*WIND) is a distributed system that ingests real-time tropical cyclone observations measured by land-, sea-, space-, and air-borne platforms into an object relational database and adjusts them to a common framework. It also graphically displays the data relative to the storm with interactive tools, so that scientists can quality control, objectively analyze and visualize the information. Some validation results are shown as follows. For each historical hurricane (see following figures for Dean, Ike and Katrina), the plots show the wind field estimated with SPHERA (wind field in colour scale) and the contour levels of wind speed available from HWIND data.

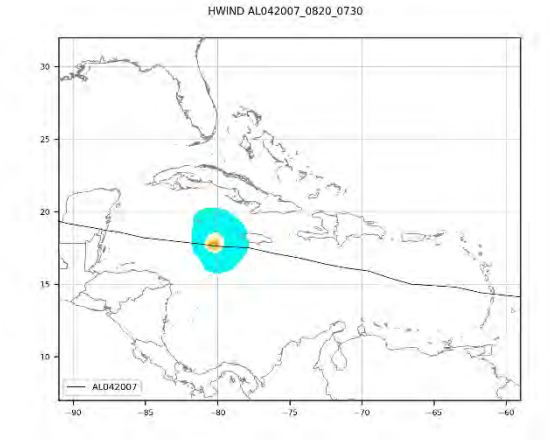

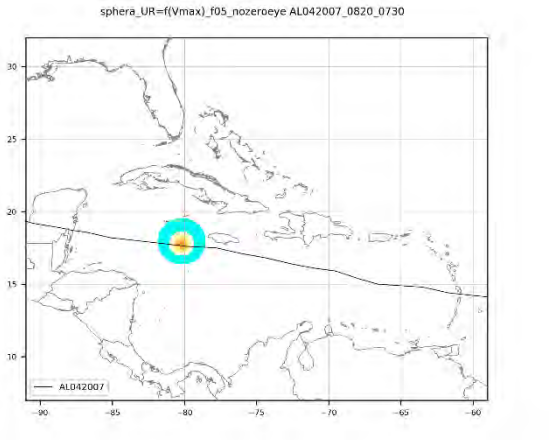

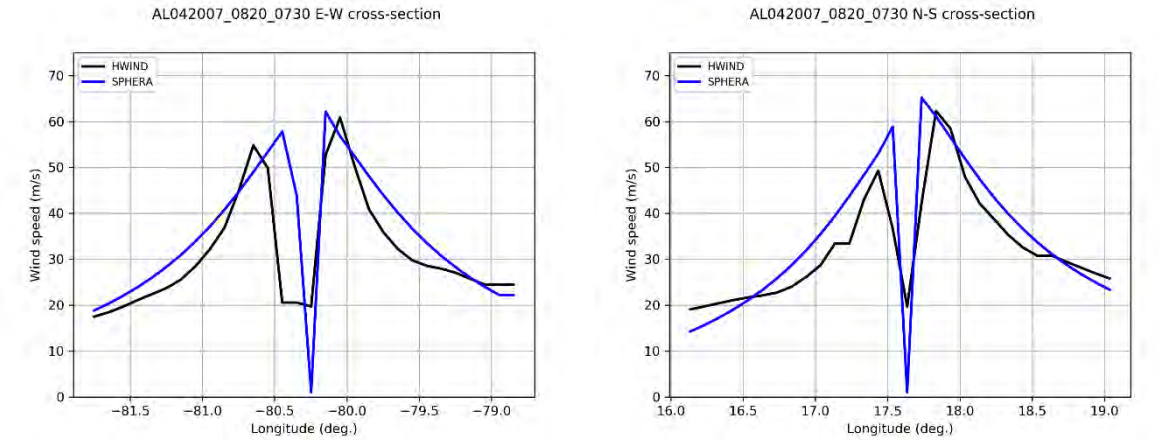

FIGURE 2-7 – EVENT AL042007 (DEAN), 20/08/2007 07:30. TOP LEFT: HWIND WIND MAP. TOP RIGHT: SPHERA WIND MAP. BOTTOM LEFT: E-W WIND PROFILES. BOTTOM RIGHT: N-S WIND PROFILES.

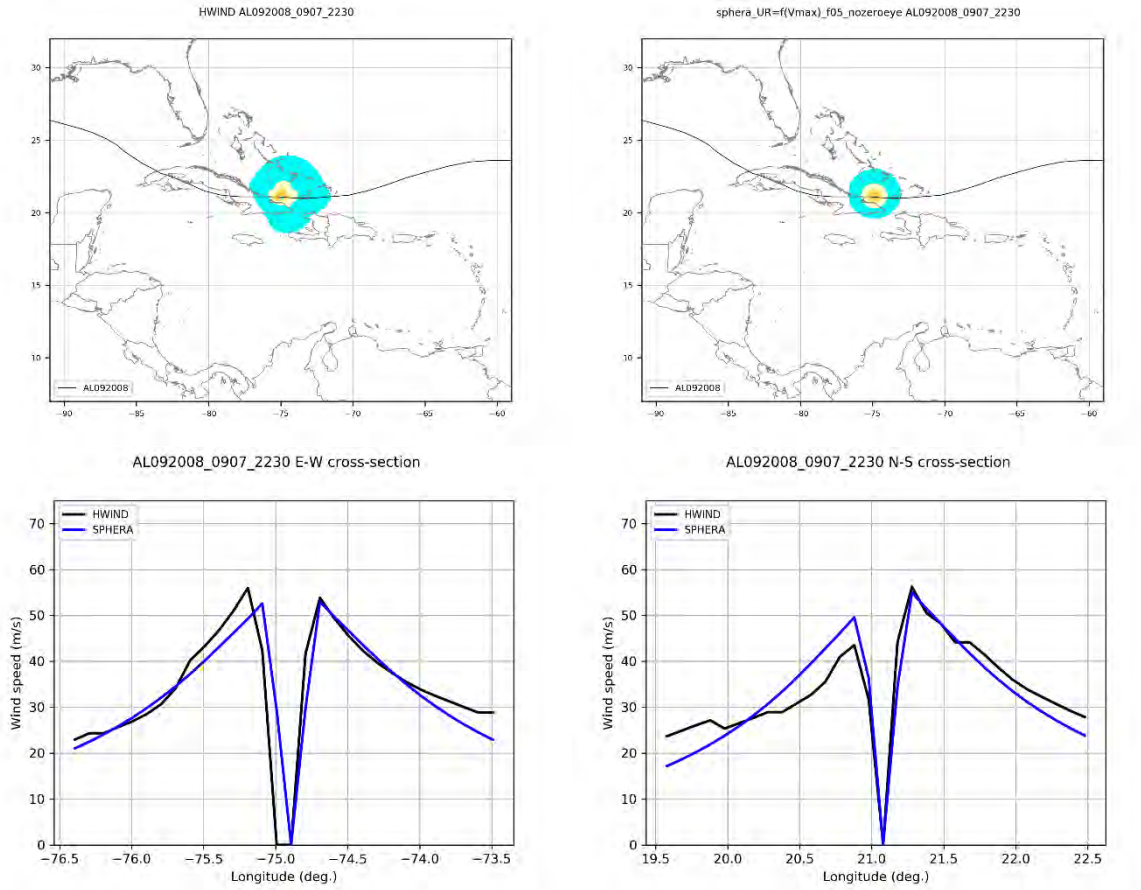

FIGURE 2-8 – EVENT AL092008 (IKE), 07/09/2008 22:30. TOP LEFT: HWIND WIND MAP. TOP RIGHT: SPHERA WIND MAP. BOTTOM LEFT: E-W WIND PROFILES. BOTTOM RIGHT: N-S WIND PROFILES.

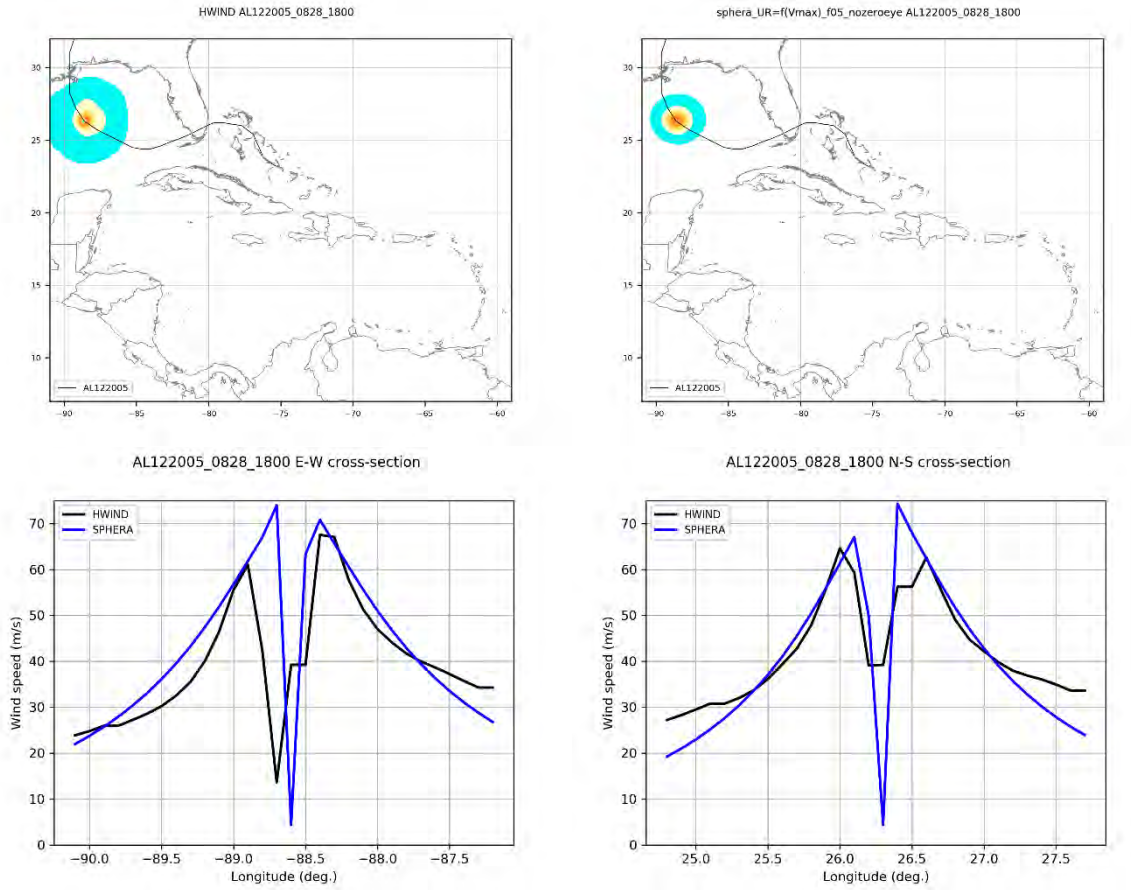

FIGURE 2-9 – AL122005 (KATRINA), 28/08/2005 18:00. TOP LEFT: HWIND WIND MAP. TOP RIGHT: SPHERA WIND MAP. BOTTOM LEFT: E-W WIND PROFILES. BOTTOM RIGHT: N-S WIND PROFILES.

The above formulation for the computation of a wind field due to a tropical cyclone is valid on open sea. However, due to the effect of topography and surface roughness, the wind speed on land by tropical cyclones can have variations.

The topographic factor accounts for the increase or decrease in wind speed due to the topographic characteristics around the site where an asset is located, for example at the top of promontories, slopes, islands or closed valleys. To take into account changes in wind speed due to the effect of topography surrounding the asset site, the wind speed is increased by factor applied to the wind speed computed for flat terrain. The topography factors are assigned from the area classification according to the type of relief, using the Topographic Position Index (TPI). The TPI compares the elevation of a central cell in a DEM with the mean elevation of the neighbouring area (Weiss, 2001; Wilson and Gallant, 2000).

Additionally, the movement of the air masses is restricted by the friction with the surface of the terrain, which causes the velocity to be practically zero in contact with it and increases with the height until reaching the velocity of the undisturbed flow, called gradient velocity. For a very smooth terrain, as is the case of open field with very low vegetation, the wind maintains a very high speed even very close to the surface, while for instance in the centre of large cities, with tall buildings, the speed at the surface of the land is much lower than that at a height of several tens of meters. For the estimation of the surface roughness effect in SPHERA, we utilized the formulation suggested in ESDU (1993, 1983, 1982), which is based on 3 main factors: (*i*) a factor that relates the velocity at 10 metres with the roughness of the site, with the same velocity but with a reference roughness; (*ii*) a factor that relates

the speed with the height variation; and (*iii*) a factor that relates a time measurement of one hour with shorter gusts.

2.3 Storm surge hazard model

Storm surge is a natural phenomenon that occurs on the coasts when the atmospheric conditions cause water level oscillations in the time range of a few minutes to a few days (excluding wind-generated waves) (WMO, 2011), as shown in Figure .

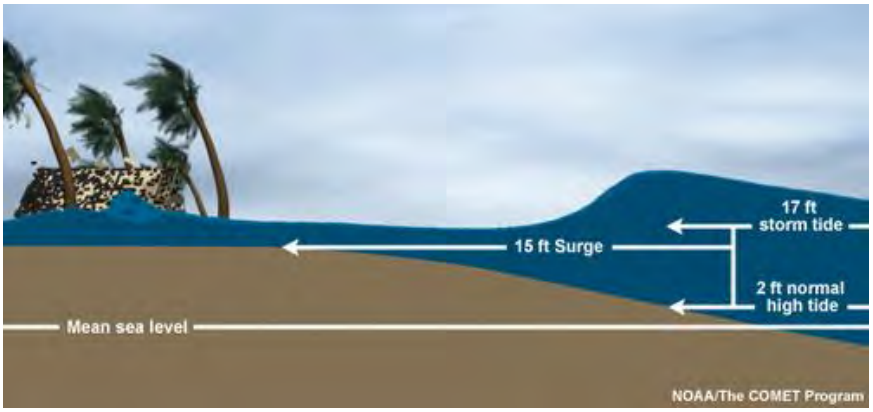

Figure 2-10 – Scheme of the storm surge phenomenon (The source of this material is the COMET® Website at http://meted.ucar.edu/ of the University Corporation for Atmospheric Research (UCAR), sponsored in part through cooperative agreement(s) with the National Oceanic and Atmospheric Administration (NOAA), U.S. Department of Commerce (DOC). ©1997-2017 University Corporation for Atmospheric Research. All Rights Reserved).

The generation of a storm surge arises from the interaction between air and sea. The atmospheric forcing is due to the atmospheric pressure gradient normal to the water body surface and to the tangential wind stress over the water surface. The pressure forcing is also called “inverse barometric effect”. The wind field associated with the storm pushes the water towards the coast, thereby causing a pile-up of water at the coast and it is the main driving force of the storm surge.

The model used for storm surge modelling in this project is GeoClaw, which belongs to the ClawPack 5.4.1 software suite (Clawpack Development Team, 2017), developed by the University of Washington and available under the 3-clause Berkeley Software Distribution (BSD) license (http://www.clawpack.org/license.html). ClawPack (“Conservation Laws Package”) is a collection of finite volume methods for linear and nonlinear hyperbolic systems of conservation laws. It is composed of different subsets, with different characteristics. The subset used in this study is, as mentioned above, GeoClaw, which includes an AMR (Adaptive Mesh Refinement) algorithm that allows using a grid with different spatial resolution that changes in time: small grid cells are used only for regions where high accuracy is required. It also includes algorithms for handling geophysical problems and routines specialized to depth-averaged geophysical flows as shallow water solvers and storm surge forcing.

This model was chosen for the following reasons:

- It is a well-established model (by UniWashington/Columbia) with a large user community for storm surge , tsunami, dam break and other geophysical flows (Berger et al., 2011; Mandli et al., 2016; Mandli and Dawson, 2014, and others).
- It is part of the well-known ClawPack package, a collection of state-of-the-art finite volume methods for resolving conservation laws.
- It is free and open source (thus it can be easily modified, customized and adapted to every context).
- It has no licence limitations for commercial purposes.
- It is very fast, and thus especially suitable for large domains, due to:

  - Parallel computation: It uses openMP parallelization;
  - Adaptive Mesh Refinement algorithm: the space and time resolution is automatically changed during the simulation to minimize the computational times while maximizing the accuracy. This also avoids the need for running the model on several nested domains, thus reducing the complexity of implementation.
- It runs on Linux Operative System and thus it can be run on High Performance Computing facilities, in case many simulations need to be run (as is the case for running a large stochastic catalogue like the one developed in this study).

Several datasets were used to set-up and calibrate/validate the storm surge model. The data considered to set-up the model includes a sea bathymetry, a DEM and the wind field computed with the SPHERA wind hazard model. The source of sea bathymetry used to implement the storm surge model is the General Bathymetric Chart of the Oceans (GEBCO) (Fisher et al., 1982). GEBCO aims to provide the most authoritative, publicly available bathymetry data sets for the world's oceans. In this model, the 1x1 km gridded bathymetric dataset was used, on a domain covering the Caribbean and Central America. For emerged areas, information with better resolution than GEBCO is available. For example, NASA's Shuttle Radar Topography Mission (SRTM) (Jarvis et al., 2008) provides a digital elevation model (DEM) covering the whole globe at different resolutions: 250m, 90m and 30m. In the SPHERA storm surge model, the SRTM DEM was combined with GEBCO information resampled at 250 m to obtain a new digital elevation model with the same resolution as GEBCO for sea-covered areas and 250 m resolution for emerged areas. Furthermore, the 90 m SRTM DEM was used to identify the elevation of all the assets included in the exposure database and then used to post-process the results of the storm surge model.

The storm surge model provides sea level variations responding to a tropical cyclone forcing (pressure and wind) but does not include any tidal forcing or tidal boundary conditions. Therefore, the astronomical tide needs to be accounted for externally. For this reason, the FES2014 tidal model (Carrere et al., 2015) was employed. FES2014 is the last version of the FES (Finite Element Solution) tide model developed in 2014-2016. It is an improved version of the FES2012 model. FES uses hydrodynamics computing to provide tide waves on a global scale dedicated to scientists or defence and industry communities. The methodology is based on finite elements modelling combined with in-situ and altimetry data assimilation. The accuracy is a few centimetres in the open ocean and a few decimetres near coastal areas.

The storm surge model was validated by comparing its results with sea level observation from the UHSLC (University of Hawaii Sea Level Center) network. A set of historical events were selected to perform the model validation. Some validation results are shown as follows. For each event and station, the plot shows the observed level (rescaled to reference level = 0 m), the simulated level (storm surge model results plus astronomical tide levels from FES2014) and the astronomical tide level (from FES2014). The legend is shown in Figure 2-11. The fit of the model results on the historical data is in general very good.

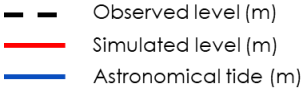

FIGURE 2-11 – LEGEND OF THE PLOTS BELOW.

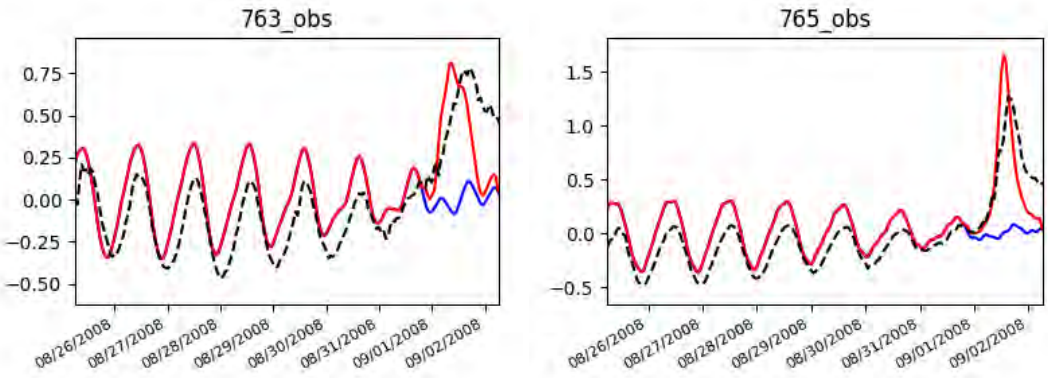

FIGURE 2-12 – STORM SURGE MODEL VALIDATION AT DAUPHIN IS., US (LEFT) AND GRAND ISLE, US (RIGHT) FOR EVENT 07-2008 (GUSTAV).

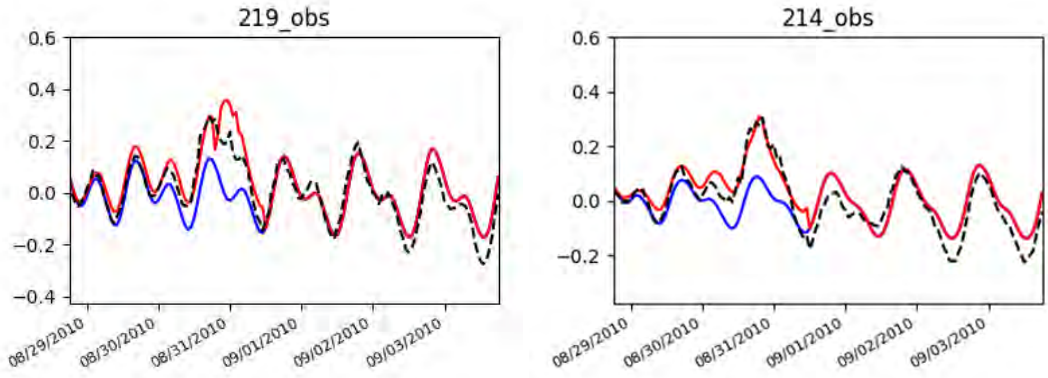

FIGURE 2-13 – STORM SURGE MODEL VALIDATION AT CULEBRA, PUERTO RICO (LEFT) AND LAMESHUR BAY, US VIRGIN ISLANDS (RIGHT) FOR EVENT 07-2010 (EARL).

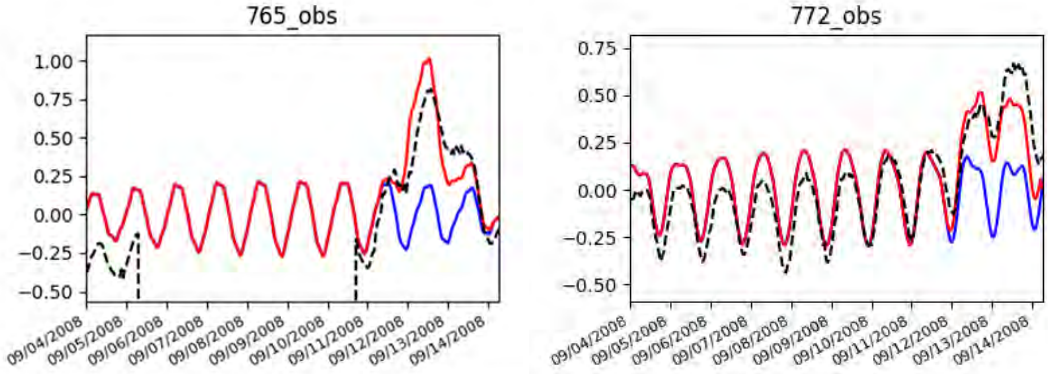

FIGURE 2-14 – STORM SURGE MODEL VALIDATION AT GRAND ISLE, US (LEFT) AND SABINE PASS, US (RIGHT) FOR EVENT 09-2008 (IKE).

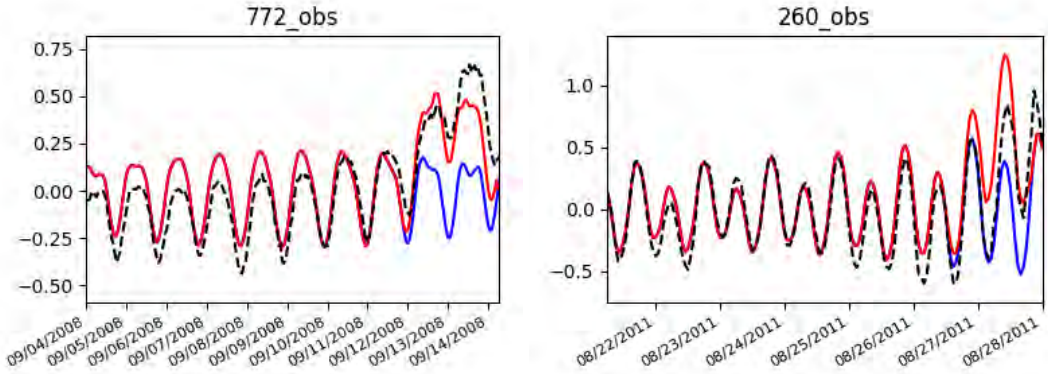

FIGURE 2-15 – STORM SURGE MODEL VALIDATION AT PORT ISABEL, US (LEFT) AND DUCK PIER, US(RIGHT) FOR EVENT 09-2008 (IKE).

Below a comparison of observed and simulated maximum surge levels for all the calibration event is shown.

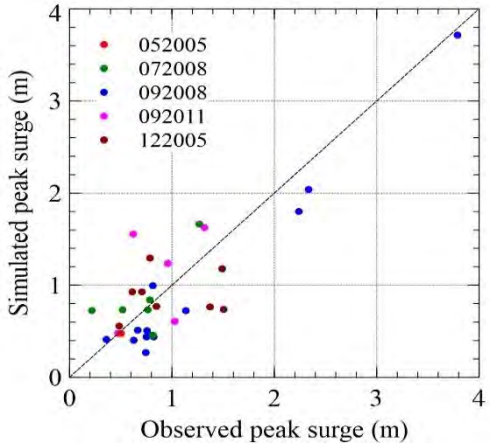

FIGURE 2-16 – OBSERVED VS SIMULATED PEAK SURGE VALUES FOR FIVE HISTORICAL EVENTS (052005: EMILY 2005, 072008: GUSTAV 2008, 092008: IKE 2008, 092011: IRENE 2011, 122005: KATRINA 2005).

2.4 Hazard assessment

In this section, some of the results of the hazard assessment carried out within the SPHERA model are shown. Figure 2-17 shows the map of the 1 in 100 years 1'-sustained wind speed, i.e. the wind speed value that is expected to be exceeded, on average, once in 100 years.

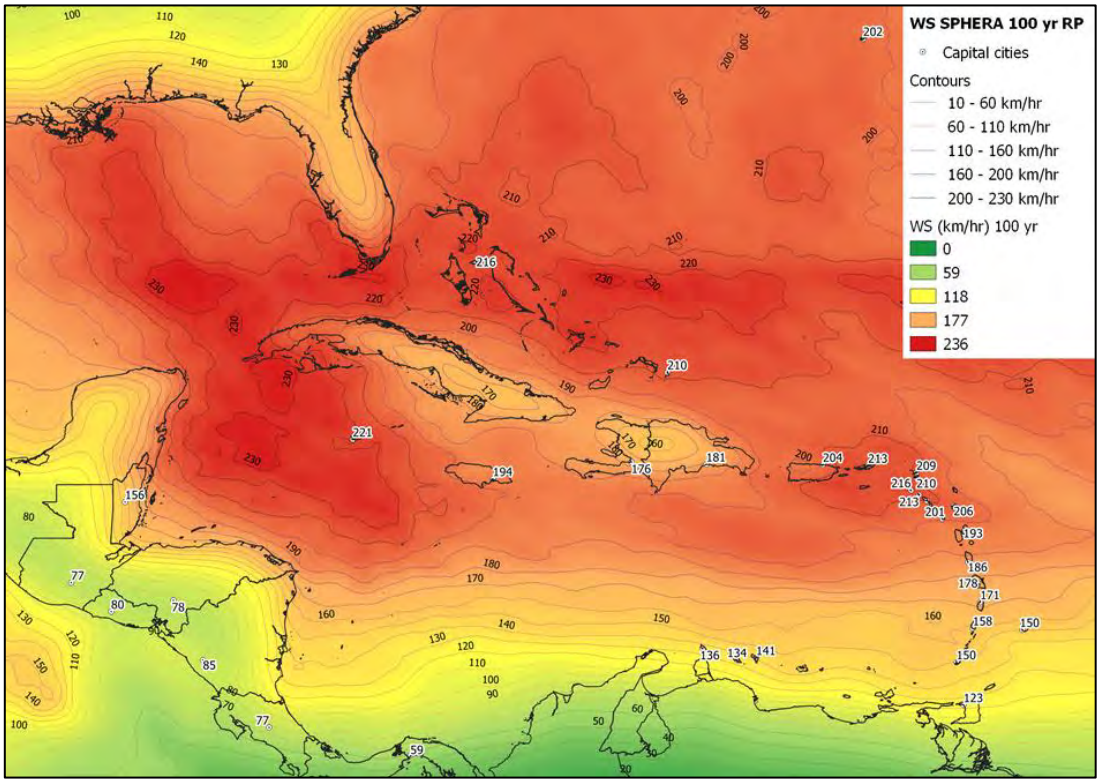

FIGURE 2-17 – 100-YEAR WIND SPEED MAP.

Table 2-1 shows the 100, 250 and 500 years wind speed values for several capital cities in the study area.

Country	Capital City	WS100yr	WS250yr	WS500yr
Anguilla	The Valley	209	236	246
Antigua and Barbuda	Saint John	206	236	250
Aruba	Oranjestad	136	166	184
Bahamas	Nassau	216	240	250
Barbados	Bridgetown	150	172	187
Belize	Belmopan	156	179	196
Bermuda	Hamilton	202	226	239
Bonaire	Bonaire	141	170	185
British Virgin Islands	Road Town	213	238	250
Cayman Islands	George Town	221	245	259
Costa Rica	San Jose	77	98	117
Curacao	Willemstad	134	165	182
Dominica	Roseau	186	213	234
Dominican Republic	Santo Domingo	181	204	224
El Salvador	San Salvador	80	91	101
Grenada	Saint George's	150	170	182
Guadeloupe	Pinte a Pitre	193	219	237
Guatemala	Guatemala City	77	87	94
Guyana	Georgetown	20	29	35
Haiti	Port au Prince	176	200	220
Honduras	Tegucigalpa	78	91	102
Jamaica	Kingston	194	224	240
Martinique	Fort de France	178	199	216
Montserrat	Plymouth	201	231	244
Nicaragua	Managua	85	100	113
Panama	Panama City	59	77	85
Puerto Rico	San Juan	204	233	245
Saba	Saba	216	241	253
Sint Marteen	Philipsburg	210	237	247
St. Eustatius	St. Eustatius	213	240	252
St. Kitts and Nevis	Basseterre	210	238	250
St. Lucia	Castries City	171	192	209
St. Vincent and the Grenadines	Kingstown	158	178	194
Suriname	Paranaribo	12	18	22
Trinidad and Tobago	Port of Spain	123	149	167
Turks and Caicos Islands	Cockburn Town	210	237	249

TABLE 2-1 – SPHERA TROPICAL CYCLONE WIND SPEED (1-MINUTE AVERAGE WIND SPEED) FOR RETURN PERIODS OF 100 YEARS, 250 YEARS AND 500 YEARS AT THE LOCATION OF MAIN CITIES.

Figure 2-18 shows the map of the 1 in 100 years sea level (storm surge + astronomical tide), i.e. the sea level value that is likely to be exceeded once in 100 years.

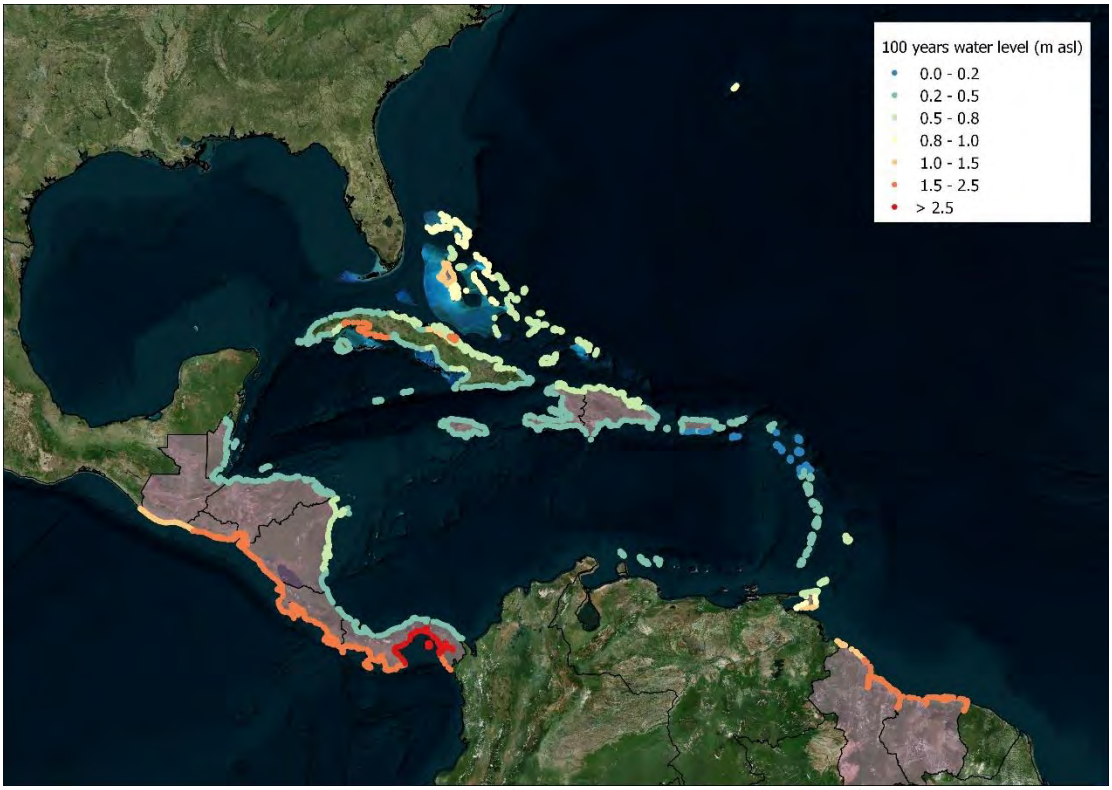

FIGURE 2-18 – 100-YEAR SEA LEVEL (STORM SURGE + ASTRONOMICAL TIDE) MAP.

3 EXPOSURE DATABASE

Any risk model developed for parametric insurance purposes requires as a fundamental component an Industry Exposure Database (IED), which allows estimating the economic losses caused by natural hazards in a credible way. The purpose of this paragraph is to describe the methodology adopted to develop the IED for the SPHERA model version 1.3, covering Central American and Caribbean countries. The SPHERA exposure dataset leverages several data sources related to the built-up environment and surrounding topography. These datasets include national building census surveys, land use/land cover maps, night-time lights imagery, population censuses, Digital Elevation Models (DEMs), and satellite images, among others. The final SPHERA exposure database includes information pertaining to the number of assets of varying lines of business, their spatial location, area, replacement value and physical characteristics, such as construction type and material, and height classification. The SPHERA exposure also includes information pertaining crops in terms of harvested area and total production per year. Table 3-1 summarizes the Lines of Business developed for the final SPHERA exposure.

TABLE 3-1 LINES OF BUSINESS INCLUDED IN SPHERA EXPOSURE DATABASE

Lines of Business	
Building Stock	Residential building stock
	Commercial and industrial building stock
	Hotels, education and healthcare building stock
	Public building stock
Infrastructures	Airports
	Ports
	Power facilities
	Road Network
Crops	6 categories of cash crops

The distribution of the exposed assets within each administrative division was performed considering a wide range of datasets, in order to obtain a high accuracy and up-to-date exposure for earthquake and tropical cyclone loss evaluation. The SPHERA database was aggregated at the same level of granularity used in the computation of the effects of earthquakes and tropical cyclones. The granularity was selected as a trade-off between speed of execution of loss assessment and desired precision of the model and it is not identical in every area of a country and across different countries.

The exposed systems are georeferenced and represented in GIS in shapefile and raster formats. They provide estimates of the asset count and replacement cost (or production value for crops) for each structure class (or crop class) at a 30 arc second resolution (approximately 1 km) for inland areas and at a higher resolution (approximately between 120m and 250m) at coastal areas, in order to achieve a higher precision for storm-surge loss evaluation.

3.1 Methodology and datasets used

3.1.1 Identification of types of construction

The first phase of the IED development consists in the identification of the most common types of construction in each country. The type of construction plays an important role in determining the expected vulnerability of the building stock when subjected to different types of natural disasters. This information was used to assign replacement costs to each building within a class, or to infer where such type of construction can be found (e.g., natural fibre huts are more likely to be located in rural areas, while reinforced concrete buildings are more likely to be found in urban ones). For this purpose, census data, technical documentation, peer-reviewed literature and reports from the World Housing Encyclopaedia were used to define the building classes present in each country. In addition, a Google image search was performed to identify the common types of construction. An example of this search is illustrated in Figure 3-1 for the building stock in Jamaica.

FIGURE 3-1 – BUILDING STOCK IN JAMAICA.

3.1.2 Data sources and estimation of asset count and value

The information regarding the residential building stock was collected from the most recent national census survey data. The census data provide the number of dwellings and their distribution in terms of material of the walls and type of dwelling (e.g., house, apartment). The information on dwelling type and wall material was used to classify the census data into the building classes previously identified, and to assign to each asset an appropriate replacement cost. The number of assets was estimated from the number of dwellings reported in the census. Finally, building classes were categorized as either urban or rural.

Commercial, industrial and public building stocks were estimated using a different approach, as no useful national dataset (such as national census survey data) currently exists. The first step was to collect statistics regarding the work force in the commercial, industrial and public sectors. The required area per employee for these sectors was consulted when available. With this information, it was possible to calculate the total area for each sector as well as each administrative division. Information about area requirements per employee was unavailable for some countries, and thus proxy data of other countries were used, by applying reduction factors for countries where working conditions are

significantly different. Depending on the country, different categories of buildings, related to the size of the assets and their class, were used to distribute the area for each kind of building. A weight was then assigned to each category, based on how common they are in the region and finally the total area for each type of building was divided by the weighted average of the building size assigned to each category in order to calculate the number of assets in each country.

The distribution of educational and healthcare infrastructure was extracted from public datasets (e.g., data from local governments) when these were available. Alternatively, the area for each of these occupancies was calculated following the approach adopted for the other non-residential building stock.

For airports, a global dataset with airport locations is available from OpenFlights. This dataset contains location attributes such as country, ISO code and region. These data were used to assess the relative size of each airport, from large hub to domestic airport.

A global dataset with port locations is available from worldportsource.com. This dataset includes location attributes such as country, longitude and latitude, and also information about port type and size (see Figure 3-2). These data were used to assess the relative size of the ports, from large to small.

FIGURE 3-2 – DISTRIBUTION OF PORTS IN THE CARIBBEAN.

The definition of the number of power facilities, source of energy, geographic location and energy generation capacity was performed considering several sources of information, including the Shift Project Data Portal, OpenStreetMap data, World Bank Development Indicators Database, and local literature concerning the evolution of energy generation in each country. In particular, the location was mostly identified using an algorithm that detects elements (e.g., dams, electrical towers, large transformers, wind fields, solar panels) related with the generation of electricity from OpenStreetMap data. Then, each location was crossed with the latest available data concerning energy generation, or statistically attributed based on the most common source of energy in each country. The final dataset was ultimately verified using Google Earth Imagery.

The development of the exposure database for the road network was performed using data from the Digital Chart of the World, OpenStreetMap Data and the Global Roads Open Access Dataset.

The replacement cost for each type of asset was estimated at country basis by using information from national census and local data. In case of unavailability of local information data from international sources were used. Projects or papers such as Pacific Catastrophe Risk Assessment and Financing

Initiative (PCRAFI) Risk Assessment Summary Report, U.S. Energy Information Administration website, the Cost of Road Infrastructure in Developing Countries paper by Collier et al., Hurricane Mitch Preliminary Damage Assessment Report, developed by the US Army Corps of Engineers among others.

3.1.3 SPATIAL DISTRIBUTION OF EXPOSED ASSETS

With the exception of airports, ports and power facilities for which the exact location was known, it was necessary to spatially distribute all other exposed assets within each administrative division. This distribution was performed considering a wide range of datasets that can be grouped in *Earth observation-based* and *Non-Earth observation-based*. In Earth observation-based databases are included *Night time lights layer* (i.e. data representative of light intensity during the night at a 30 arc-second resolution), particularly useful in distributing commercial and industrial stock, as there is a strong correlation between electrification and industrialization, *Digital Elevation Models (DEM)* were used as a proxy for human activity, as urban settlements tend to exist in relatively flat areas (e.g., valleys and coastlines) as opposed to regions with a steep slope (e.g., mountainsides), *satellite imagery* which plays a fundamental role in the mapping of urban density. The remote sensing imagery leveraged for this module was acquired from the optical 'Landsat-8' satellite. Figure 3-3 shows an example of these data for Belize.

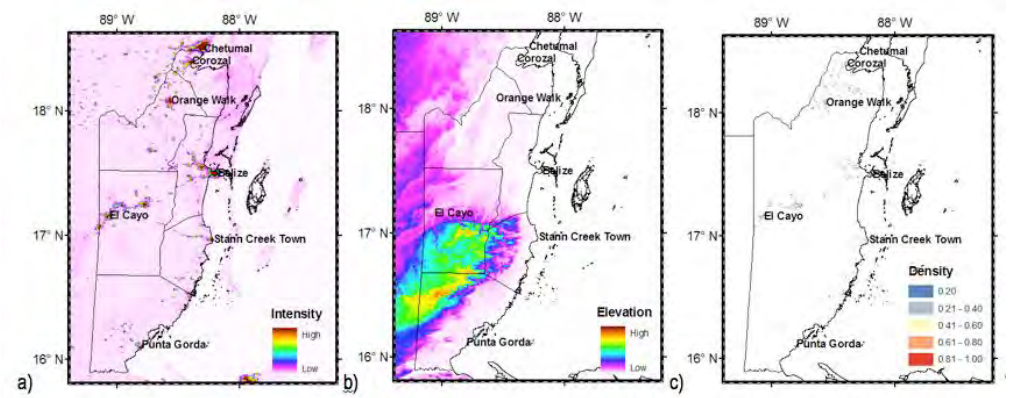

FIGURE 3-3 – A) NIGHT-TIME LIGHTS; B) ELEVATION; AND C) BUILDING DENSITY ACCORDING TO REMOTELY SENSED DATA BELIZE.

Non-earth observation-based datasets include *land use (LU) maps* which classify the territory of each country according to its use and were used to better estimate the spatial distribution of the SPHERA model's building stock, and to identify areas dedicated to specific types of economic activity; *Roads Datasets* containing the transportation network for each country and used to detect the presence of buildings; *OpenStreetMap (OSM)* which contains a plethora of spatial data such as roads, buildings, land use areas or points of interest; *Rivers and inland water* for detecting areas where no buildings should exist due to the presence of rivers or other inland water bodies (e.g., lakes, lagoons). Figure 3-4 shows an example of the non-earth observation data for Belize.

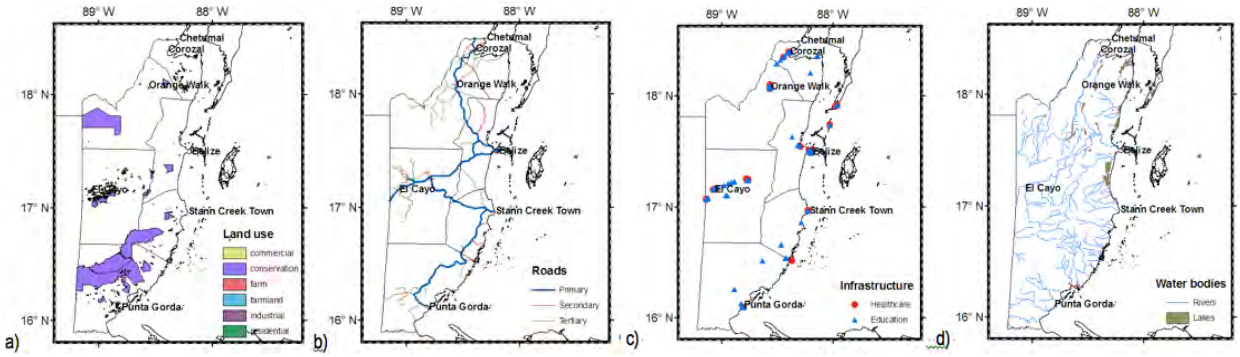

FIGURE 3-4 – A) LAND USE MAPPING; B) TRANSPORTATION NETWORK (ROADS); C) HEALTHCARE AND EDUCATIONAL INFRASTRUCTURE (FROM OSM) IN THE COUNTRY OF BELIZE; D) RIVERS AND INLAND WATER BODIES.

3.1.4 ASSESSMENT OF CROP EXPOSURE

The SPHERA model exposure database also includes cash crops, which are crops grown with the intended purpose of selling them for profit. Since cash crops are destined for future sale, they hold a relevant financial potential during their growth season, which is constantly in danger due to various types of threats, including weather-related threats.

Within this framework, the SPHERA model aims at computing the losses caused by a tropical cyclone to the crop production of a country. In particular, SPHERA computes the direct losses in terms of lack or reduction of annual harvest, i.e. the difference between the expected annual crop production and the actual annual production, given that a tropical cyclone occurred and had an impact on agricultural areas. The SPHERA model does not compute indirect losses to crops and losses to livestock.

The implementation of a crop exposure database required three basic steps; Identification and geolocalization of cultivated areas, Estimation of the expected crop yield and Estimation of the crop value. The methodology followed in the identification of the spatial distribution of crops in the area is detailed in (Dell'Acqua et al., 2018) and it is based on spaceborne remote sensing (MODIS product (Lobell and Asner, 2004; Wardlow and Egbert, 2008), able to cluster the territory into homogeneous areas by analysing the satellite images over a relatively long time interval, combined with agro-climatic mapping, able to identify the crop kinds that potentially could grow in the territory given the agro-climatic conditions.
The "expected" production, which refers to the production that is reasonable to expect from a unit area, was estimated as the average production, from historical records of crop yield. The only dataset available over a long time period and over all the countries of study is FAOSTAT, provided by FAO.

The final crop exposed value, i.e. the expected annual income from the harvest of a specific crop type, for each point of the grid was obtained as the product of harvest area (ha), crop yield (ton/ha) and crop price (USD/ton) derived from FAO databases. Figure 3-5 shows the distribution of the annual production of crop in the different classes considered for each country.

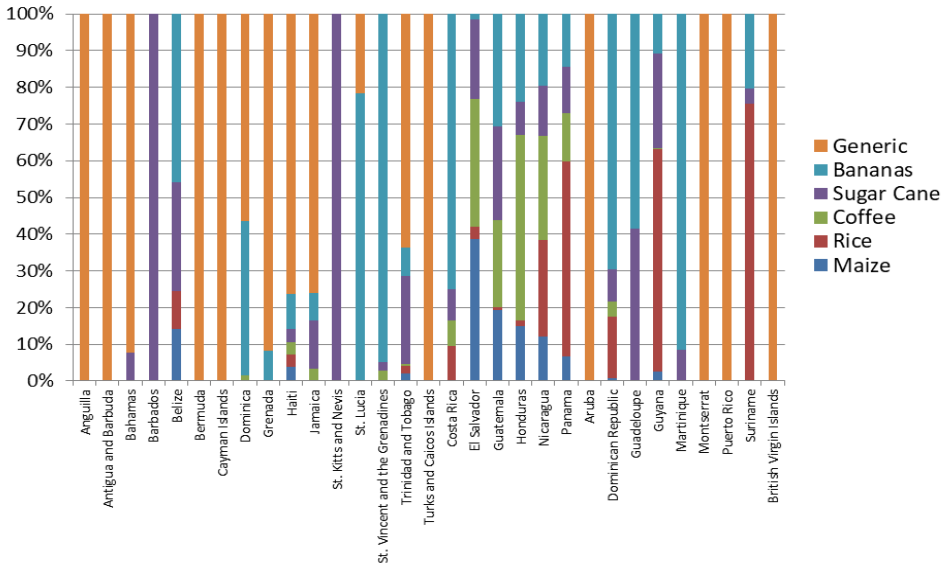

Figure 3-5 –Annual production by of crop type as a Percentage of total production.

3.2 Outputs and validation

This section presents the outcomes of the SPHERA exposure database. It compares the total capital stock of SPHERA countries, and presents examples of how they are distributed among the lines of business. A comparison of key data from SPHERA exposure database is made against MPRES model (developed by KAC), and UNISDR's GAR15. Finally, some examples are provided to show how the estimated distribution of assets compares with the existing building stock, as observed through satellite imagery. Figure 3-6 shows the total exposure value (without crops) for Caribbean countries.

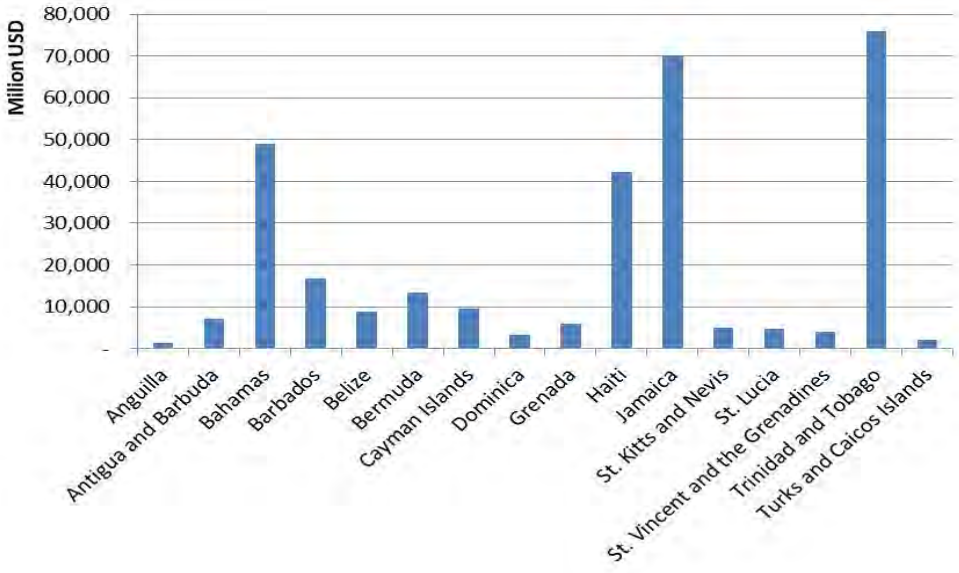

FIGURE 3-6 – COMPARISON OF TOTAL EXPOSURE VALUES FOR SOME CARIBBEAN COUNTRIES.

As explained above, the total number of assets and capital stock (for each building class) are spatially disaggregated leveraging several datasets. An example of the results for Haiti is presented in this section. Figure 3-7 (a) shows the distribution of the total exposed value, whereas Figure 3-7 (b) shows the distribution of the exposed value for residential sector and Figure 3-7 (c) shows the distribution of exposed values for roads in Haiti.

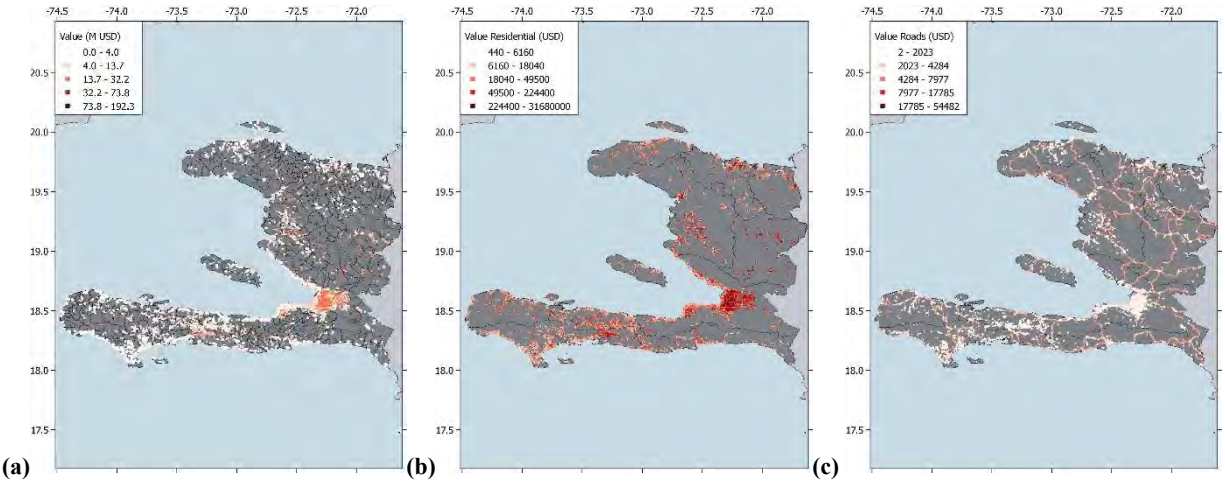

FIGURE 3-7 – (A) DISTRIBUTION OF TOTAL EXPOSURE VALUE, (B) RESIDENTIAL VALUE AND (C) ROAD VALUE OF HAITI.

The IED module of SPHERA model was validated against reputable third-party data sources, among which the 2015 Global Assessment Report on Disaster Risk Reduction (GAR15) developed by UNISDR. Figure 3-8 compares the overall exposed value by country derived for the new SPHERA model with the

capital stock value reported in GAR15 and that in the MPRES (KAC) model. It appears that the new SPHERA exposure is in line with the GAR 2015 values nearly in all the countries.

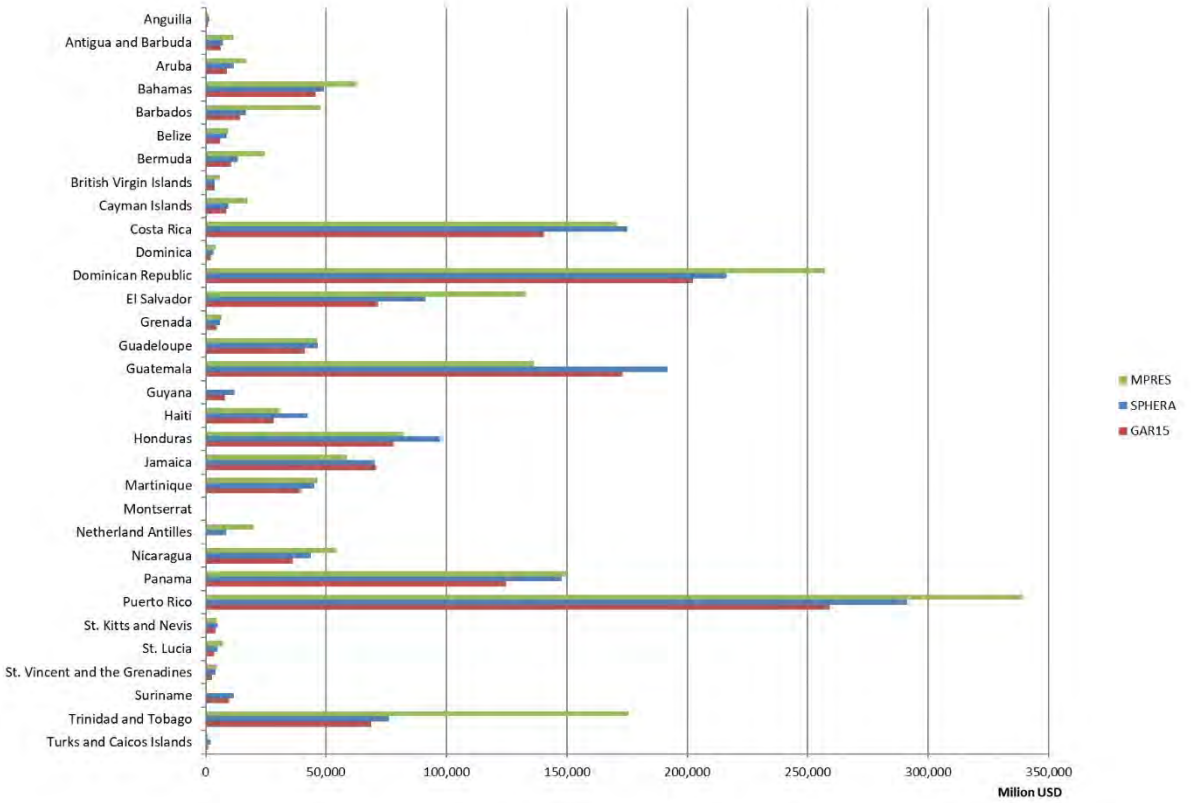

FIGURE 3-8 – COMPARISON OF THE SPHERA EXPOSURE (NO CROPS) WITH MPRES (NO AGRICULTURE STOCK), GAR AND XSR2.0 EXPOSURE DATABASES.

Some other verification tests were done to assure the reliability and validity of the obtained SPHERA IED results. Table 3-2 shows the cost per dwelling on GDP per capita, and the number of people per dwelling. Such indicators were used to cross-check the consistency of the results in the region and to verify if the residential exposure depicts a realistic socio-economic condition in the different countries. The results obtained are generally reasonable and the indicators do not show any outlier among the different countries.

Country	Population (M)	GDP per capita	Ratio (Cost per dwl/Gdp per capita)	Pop per dwl
Anguilla	0.015	21,493	7	3
Antigua and Barbuda	0.105	13,715	13	3
Bahamas	0.391	22,817	11	3
Barbados	0.285	15,429	7	3
Belize	0.367	4,879	6	5
Bermuda	0.065	85,748	4	2
Cayman Islands	0.061	64,105	4	3
Dominica	0.074	7,116	8	2
Grenada	0.107	9,212	10	4
Haiti	10.847	818	11	5
Jamaica	2.881	5,106	11	5
St. Kitts and Nevis	0.055	15,772	10	4

Country	Population (M)	GDP per capita	Ratio (Cost per dwl/Gdp per capita)	Pop per dwl
St. Lucia	0.178	7,736	5	4
St. Vincent and the Grenadines	0.11	6,739	7	4
Trinidad and Tobago	1.365	17,322	10	4
Turks and Caicos Islands	0.035	23,615	5	5

TABLE 3-2 – INDICATORS OF SOCIO-ECONOMIC CONDITIONS USED FOR EXPOSURE VALIDATION.

Finally, the SPHERA exposure database was validated also in terms of geographic distribution, by comparing it with satellite imagery. Figure 3-10 shows the consistency between the exposure developed for the SPHERA model and satellite images.

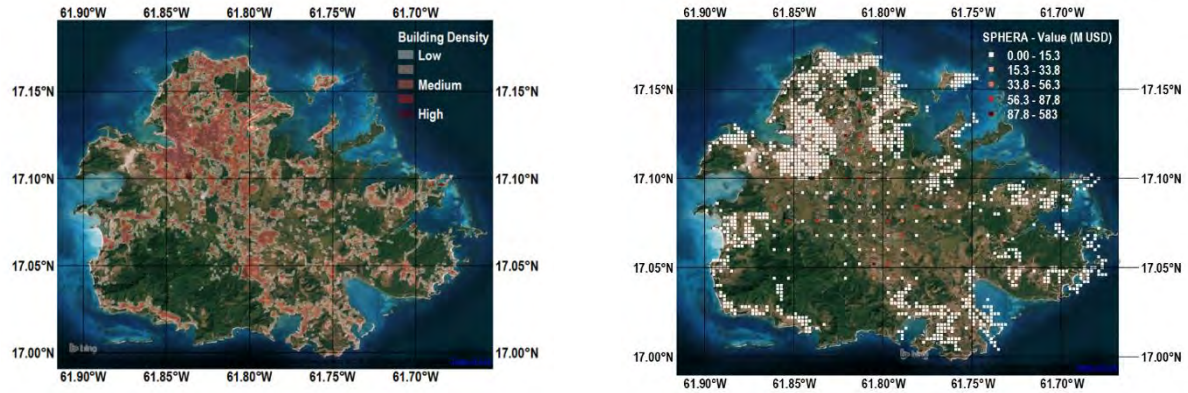

FIGURE 3-9 – (A) ANTIGUA BUILDING DENSITY SATELLITE IMAGE AND (B) SPHERA EXPOSURE DISTRIBUTION IN THE SAME AREA

4 VULNERABILITY

A vulnerability function is a curve that relates a given level of intensity caused by an event (here a tropical cyclone) at a given location with the economic cost of repairing the physical damage to an asset at risk (building or infrastructure), expressed in terms of relative damage between 0 and 1, where 1 indicates a damage equal to the total replacement cost of the asset (Figure).

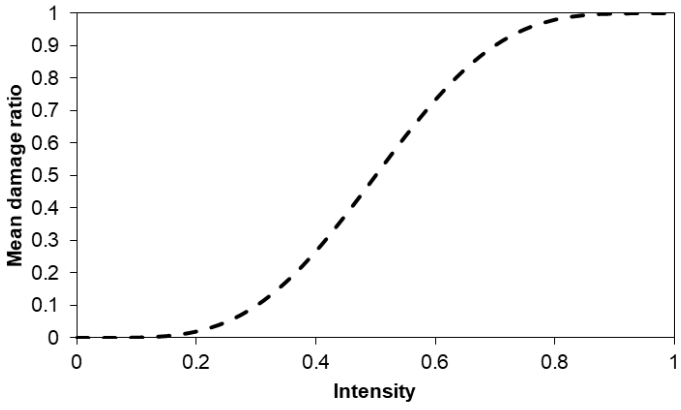

Figure 4-1 – Conceptual example of vulnerability curve.

Two different sets of vulnerability functions were developed, one for wind losses and another for storm surge losses.

4.1 Wind vulnerability

The wind vulnerability module provides a probabilistic relationship between the wind speed at a site and the loss ratio expected by a specific building at that site. The model reflects the large size of the structure inventory and the lack of data to fully characterize each building individually by considering classes of structures rather than individual buildings. These classes cover all the structures of the building exposure database.

Construction typologies, occupancy classes, building code requirements, construction practices and other parameters affecting the wind vulnerability of the physical assets present in the exposure model of the Central American and Caribbean countries were evaluated. The vulnerability model includes up-to-date empirical, expert opinion-based, analytical and hybrid fragility and vulnerability functions collected during an exhaustive search of peer-reviewed publications, public and private reports, conference proceeding, among other sources.

The vulnerability functions are specific for the different classes of assets located in the different countries and are defined as function of structural system, height and occupancy. Other building characteristics such as roof shape and roof material that are not explicitly considered in the exposure database, are accounted for with the use of country-specific modifiers that generate a country-specific function for every class of structure. Given the uncertainty associated with the estimation of losses for classes of assets, the vulnerability functions provide the mean loss ratio and its associated uncertainty for varying levels of wind speed.

4.1.1 BUILDING TAXONOMY

This vulnerability model is defined for different structural classes based on the characteristics of the buildings found in the SPHERA exposure model. Some simplifications were made for characteristics that do not make any difference from the point of view of the structure response to strong winds, like ductility, which is not considered on most structural codes and offers a small benefit for rigid structures such as low or midrise buildings (Gani and Légeron, 2012).

The different structural configurations considered for wind vulnerability are based on:

i) Structural system or construction material.
ii) Building height or number of stories.
iii) Occupancy of the building.

The structural system is the most important parameter of the vulnerability model, as different structural systems have different failure mechanisms. For example, wood structures are inherently more vulnerable to wind due to their light-weight and dependence on connection performance. The structural systems are defined based on the dominant material of the main wind force resisting system, without including the roof. Occupancy, on the other hand, allows representing better the detailed characteristics of a structural system, such as glazing or building internal spaces. Based on the exposure database, seven different occupancies were defined.

Some relevant building characteristics that affect the behaviour and resistance of a building under wind load, such as the roof material and the roof shape, are not explicitly considered in the exposure database. However, they are needed to characterize the vulnerability of a building to wind forces. Country-specific data about roof material and roof shape were collected and used as secondary modifiers for the present vulnerability analysis at country level, where thirty-nine building classes were identified in the exposure model.

4.1.2 FUNCTIONAL FORM

In this project, the use of regression analysis was not possible due to the lack of reliable information of building damage/losses in the Caribbean. Hence, we decided to modify existing vulnerability functions for other regions based on multiple criteria, as explained in this document. The general procedure employed to develop the current vulnerability functions was based on the following steps:

- Identify the existing models available in the literature for all the building typologies in the exposure database.
- Fit a vulnerability curve using a parametric form.
- Homogenize the available information (e.g., making all the curves dependent on the same wind intensity measure).
- Aggregate the country-specific functions for every building class based on their secondary modifiers.
- Calibrate and validate the country-specific functions using damage/loss data.

To keep the form of the original vulnerability function, the expected loss ratio β, was represented as:

$$E(\beta) = \left[1 - 0.5^{\theta}\right]\varphi \qquad \text{EQUATION 4-1}$$

$$\theta = \left[\frac{V - \alpha V_0}{\alpha V_{50} - \alpha V_0}\right]^{\rho} \quad V > V_0 \qquad \text{EQUATION 4-2}$$

V = Wind speed (1 minute sustained)
V_0 = Wind speed below which damage is zero.
V_{50} = Wind speed inducing an expected 50% damage level.
φ = Modifier that accounts for the structural system.
ρ = Damage evolution parameter.
α = Calibration and country specific modifier

Three parameters need to be calibrated to fit the above function: V_0, V_{50} and ρ. The values of V_0 and V_{50} depend on several parameters, including occupancy, structural system, number of stories, roof shape, deck material, among others. The damage evolution parameter, ρ, sets the relationship between damage and intensity. It represents how fast does damage increase with wind speed. It sets the shape and slope of the curve and varies depending on building class. The parameter φ limits the maximum expected damage ratio for structural systems, where full destruction is not expected, such as reinforced concrete frames. The V_{50} variable is based on a similar expression developed for seismic vulnerability by Ordaz et al. (2000) and represents the intensity that produce the 50% of the mean damage ratio of the fitted curve. The point could be obtained either analytically, where the full expression of the vulnerability curve was available, or in an approximate way, where only the shape of the curve was known. In this project, the V_{50} parameter was obtained from the available HAZUS information and other sources (e.g., Konthesingha et al., 2015; Wehner et al., 2010). Finally, the parameter α is country-specific a calibration factor that accounts for the variability in the quality of the building stock, code compliance and hurricane preparedness of each country in the region.

4.1.3 SECONDARY MODIFIERS

Secondary modifiers are building characteristics that affects their behaviour and resistance to wind loads but are not explicitly considered in the exposure database. These characteristics need to be taken into account for a better prediction of the expected losses after the occurrence of an intense wind event.

The secondary modifiers used in the current vulnerability model are the roof shape and the roof material. The roof shape has important effects on the wind pressure distribution of the roof and on the peak pressures that occur most significantly on the roof ridge and eaves. Country-specific data is available for the following roof shapes: Arch, Gable, Hip, Complex, Flat, Mono-pitch.

Gable, hip and flat roofs are the most dominant typologies present in the exposure database; hence, for simplicity, arch and complex roofs were assigned the same modifiers as gable roofs, a practice that is consistent with pressure coefficient data, while mono-pitch roofs were assigned the same modifiers as flat roofs. The effects of roof shape are more evident for lower wind speeds where the loss ratio is dominated by roof damage. Regarding roof material, light supporting systems, such as metal or wood truss system, were contemplated for sheet metal/eternit and shingle/tiles, while for concrete roofing material we assumed heavy supporting systems, such as a concrete slab or composite steel/concrete deck. The adopted roof materials are: Sheet Metal/ Eternit, Shingle/Tiles, Concrete, Makeshift/Thatched.

For mid- and high-rise buildings, makeshift roof covers are not considered. The proportions of roof shape were obtained through a survey of satellite images (e.g., Google Earth) on a random sample of points in urban and rural areas. The proportions of roof material were obtained from national building censuses.

4.1.4 INFRASTRUCTURE AND FACILITIES

The infrastructure vulnerability functions were based on previous information developed by ERN for some Central American countries. Most of these curves represent a group of several buildings or systems in close proximity that form a certain infrastructure system such as a power plant. The infrastructure classes considered here are: Airports, Ports, Power plants and Roads.
In the case of power plants, this model assumes that all thermoelectric plants have the same vulnerability function. Hydro, solar and wind power plants, however, have a different response to wind speed and were analyzed independently.

4.1.5 DURATION OF THE STORM

It has been observed that the damages caused by wind are related to the number of hours that sustained winds persists. The greater the event length, the greater the damage to the infrastructure of the affected areas. Done et al. (2017) found that hurricane wind durations longer than 1.5 hours can increase loss by up to 50 percent compared to durations below 1.5 hours. This is similar to the results found by Powell et al. (1995) who observed a significant relationship of increased damage with duration of sustained wind speeds (Figure 4-2).

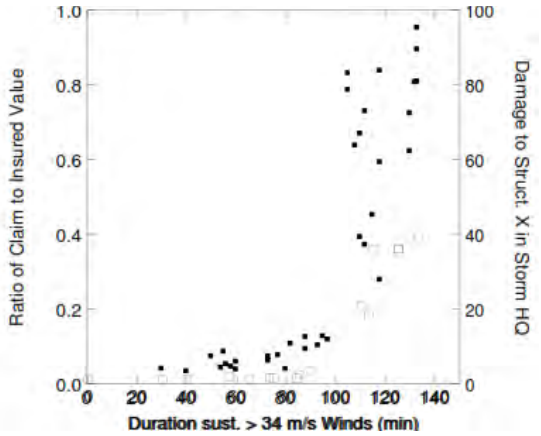

FIGURE 4-2 SCATTER PLOT OF DURATION OF SUSTAINED WINDS VERSUS CLAIM RATIO AND EXPECTED DAMAGE (POWELL AND ARES, 1995)

As can be seen in Figure 4-2, sustained wind speed duration has a positive relationship with an increment in expected losses when comparing model calculated with claim data losses. This is true also for the Caribbean region, where historical data shows a positive correlation between hurricane wind speed duration and the reported historical losses (Figure 4-3).

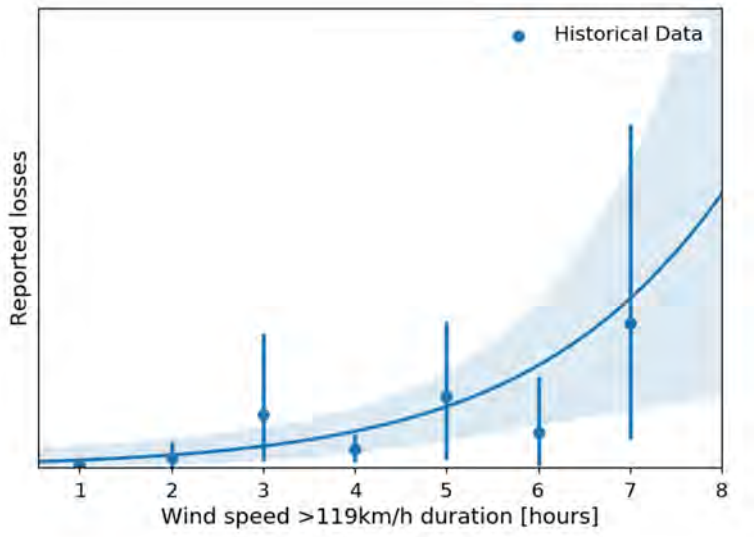

FIGURE 4-3 REGRESSION LINE OF AVAILABLE HISTORICAL DATA AND HISTORICAL LOSSES.

There are several reasons for damage increases associated to larger wind durations. An example of this is the low cycle fatigue effect, i.e., a decrease in the resistance of an element due to the cyclic nature of wind loads. This has been observed in fasteners and connections, where the probability of failure of the element for a given wind speed increases. Another reason is the debris-generated damage: the longer an event lasts the higher the chance that a missile impacts a certain window or other opening.

To take into account this effect, SPHERA includes in the loss estimation the effect of the number of hours in which the exposed infrastructure is affected by wind speeds greater than or equal to hurricane category 1 in the Saffir-Simpson scale, which is represented as:

$$\beta_n = 1 - (1 - \beta)^{n^\alpha} \qquad \text{EQUATION 4-3}$$

where: β_n is the expected damage for a given duration period "*n*" in hours, experiencing wind speed equal or higher than 119 km/hr (H1). β is the expected loss for a given wind speed in a specific construction typology (obtained from the vulnerability function, equation 4-1). α is a parameter used to fit the modelled losses to the observed losses based on the duration of the hurricane wind speed.
The loss increment can be computed as a function of the number of hours experiencing hurricane wind speed: $F_D = \beta/\beta_n$; where F_D can be called: duration factor.

4.2 Storm surge vulnerability

The storm surge vulnerability functions were developed using RED's in-house building damage model (Dottori et al., 2016). The model is based on a synthetic approach, which takes into account hazard properties at the building locations (e.g., water depth), the characteristics of the exposed buildings (e.g., structural type) and the replacement costs of its components, in order to compute damage values. The damage mechanisms of each building component were described through a what-if analysis, which depends on hazard and exposure variables.

4.2.1 RESIDENTIAL BUILDINGS

The impact of different exposure characteristics on the storm surge flood vulnerability of residential buildings was taken into account in the development of the vulnerability module. More specifically: material, presence of basement, number of stories in the building, and ground level height (i.e. whether the ground floor is more elevated than the street or the surrounding environment) were adopted as the main characteristics that define the storm surge vulnerability of buildings.

The curves obtained with the above methodology were then aggregated to obtain curves for the categories of building used in the exposure database. In particular, the categories of residential buildings shown in Table 4-1 were adopted.

Category	Description
M_LR	Masonry, low rise
RC_HR	Steel and reinforced concrete, high rise
RC_LR	Steel and reinforced concrete, low rise
RC_MR	Steel and reinforced concrete, mid rise
W-LR	Wood, low rise

TABLE 4-1 – STORM SURGE VULNERABILITY RESIDENTIAL CLASSES BY CONSTRUCTION MATERIAL.

4.2.2 INFRASTRUCTURE AND FACILITIES

Vulnerability curves for infrastructure were also developed, based on literature information (Huizinga et al., 2017; Kok et al., 2004; Scawthorn et al., 2006) for: Ports; Airports; Power plants and Roads.

The vulnerability curves for roads were taken from the available literature. In particular, two sources of information were employed:

- Standard Method 2004 Damage and Casualties Caused by Flooding report (Kok et al., 2004), which is widely used in the Netherlands to assess damages to roads caused by flooding.
- The Global flood depth-damage functions: Methodology and database with guidelines report (Huizinga et al., 2017), which is a collection of internationally-used vulnerability curves from several areas around the world.

No specific vulnerability functions were found in literature for ports and airports. However, the HAZUS report (Scawthorn et al., 2006), a natural hazard analysis tool developed and freely distributed by the Federal Emergency Management Agency (FEMA) in the US, provides average replacement costs for all the components of a port. These replacement costs were used to assign a relative weight to each component, and then a vulnerability curve for ports was computed by calculating the weighted average of the curves of every single component.
For the power plants, the vulnerability curves provided by HAZUS (Scawthorn et al., 2006) were employed.

4.2.3 TIDAL DEFENCE

The vulnerability to coastal flooding of an asset is strongly influenced by the presence of flood defences. While it is out of the purposes of the current risk model to compile an exhaustive inventory of coastal flood defences in the area of study, it is essential to identify stretches of coasts that could be less vulnerable to high water levels than others. A simple way to quantify this factor is to analyze the variation of the astronomical tide. If a country usually experiences small astronomical tides (e.g., 10-20 cm), its vulnerability to sea level rises will be larger than the vulnerability of a country that normally experiences a large astronomical tide variation (e.g., 1.5 m). This is because countries with

large astronomical tide oscillations are prepared to receive such high levels of tide, since they receive them almost on a daily basis.

Therefore, hourly time series of the astronomical tides were obtained at every point of the coast within the area of study and over a large time period (20 years), using the FES2014 tidal software (Carrere et al., 2015). Then, several statistics of the tide distribution were obtained for every stretch of the coast, such as the 95th percentile, the 99th percentile, the 99.5th percentile, the 5-year return period high tide and the maximum tide. The 5-year return period high tide was chosen as a measure for a very high but non-damaging tide. The coasts of the domain were categorized in five classes (Category 5 being the least vulnerable to storm surge given the high natural tides) depending on their 5-year tide. The results are shown in Figure 4-4 and Table 4-2.

FIGURE 4-4 – SPATIAL DISTRIBUTION OF THE 5 YEAR RETURN PERIOD TIDE.

Category	5y tide range (m)
1	0-0.3
2	0.3-0.6
3	0.6-1.0
4	1.0-1.5
5	>1.5

TABLE 4-2 – TIDE DEFENCE CATEGORIES.

The vulnerability curves described above were customized for every stretch of coast to reproduce the effect of tidal defence. This means that the damage ratio was set to zero up to the median level of the tide range of the corresponding category, depending on the location of the asset.

4.3 Vulnerability function calibration

In every risk model, the vulnerability functions need to be adapted to the results of the hazard model. This is because hazard model results, although supported by the best available science, are always affected by uncertainty. Calibration was therefore applied also to the vulnerability functions described in this document. To achieve the best performance of the whole risk model, we calibrated (within reasonable limits) the parameters of the vulnerability functions with the aim of producing estimates of the economic losses caused by historical tropical cyclones that are as close as possible to those reported (see consequence database report for more information). This is a fundamental step for all mathematical models, including hazard and risk models.

For the Tropical Cyclone SPHERA model, as mentioned above the calibration was carried out by adjusting the vulnerability functions to provide robust estimates of the reported losses of historical events at the country scale. In particular, for every country, the following procedure was used:

1. Large loss events with available and reliable values of reported losses were chosen for calibration.
2. All the vulnerability curves of the countries were adjusted by the same amount until the value of the modelled losses was as close as possible to the value of the reported direct losses (indirect losses were removed, when possible, given that they are not considered in SPHERA). A conceptual example of the adjustment is shown in Figure 4-5. In particular:
   a. All the curves were shifted by the same amount, i.e. the relative difference among the different curves was maintained.
   b. The functional shape of the curves was maintained.
3. Once the modelled losses reached a satisfactory result, the model was validated by comparing modelled and reported losses on the events that were not used for calibration (and for which reported loss values were available).

The procedure was repeated for all countries.

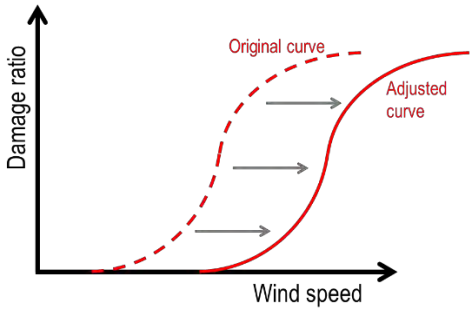

FIGURE 4-5 – SCHEME OF THE ADJUSTMENT APPLIED ON THE VULNERABILITY CURVES.

The events used for the calibration of the vulnerability curves are shown in Table 4-3. The rest of available events were used for validation. If a country is not included in Table 4-3, no calibration was carried out due to the lack of information on historical events.

Country	Calibration event
Anguilla	Lenny 1999
Antigua and Barbuda	Georges 1998
Bahamas	Floyd 1999
Barbados	Ivan 2004
Belize	Iris 2001
Bermuda	Fabian 2003
Cayman Islands	Paloma 2008
Dominica	Hugo 1989
Dominican Republic	Georges 1998
Grenada	Ivan2004
Guadeloupe	Hugo 1989
Haiti	Gilbert 1988
Honduras	Mitch 1998
Jamaica	Ivan 2004
St Kitts and Nevis	Hugo 1989
Martinique	Dean 2007
Montserrat	Luis 1995
Nicaragua	Felix 2007
Puerto Rico	Georges 1998
St . Lucia	Dean 2007
Trinidad and Tobago	Ivan 2004

Country	Calibration event
Turks and Caicos	Ike 2008
St Vincent and the Grenadines	Ivan 2004

TABLE 4-3 – EVENTS USED FOR VALIDATION.

5 LOSS ASSESSMENT

5.1 Loss computation

Once the effects (wind and surge) caused by a tropical cyclone have been computed an estimate of the economic losses is computed by the SPHERA using the classical approach shown below. For a single asset *i*:

$$L_i = V_i(H_i) \times E_i$$

Where:
L: losses (USD).
H: hazard (maximum wind – km/h, maximum storm surge – m).
V(H): vulnerability as a function of the hazard [0-1].
E: exposure, or asset value (USD).

The economic losses caused by a tropical cyclone on the asset *i* are computed as a fraction of the total value of the asset E_i, defined by a specific vulnerability function V_i given a level of the intensity of the storm effects, H_i. In the case of tropical cyclone hazard, H_i is bi-dimensional, i.e., it is defined by two variables, wind speed and storm surge. In this model, two separate sets of vulnerability curves were developed, for wind and storm surge. Therefore:

$$L_{w,i} = V_{w,i}\left(H_{w,i}\right) \times E_i$$
$$L_{s,i} = V_{s,i}\left(H_{s,i}\right) \times E_i$$

Where the subscript *w* refers to wind losses, hazard and vulnerability and the subscript *s* refers to storm surge losses, hazard and vulnerability. The losses are then computed using a combined approach detailed in Ordaz (2015) and also used in Niño et al. (2015), Bernal et al. (2017), Salgado-Gálvez et al. (2017b), Salgado-Gálvez et al. (2016) and Salgado-Gálvez et al. (2017a). The following equation, defined for a number of different perils *n*, induced by tropical cyclones was used (Ordaz, 2015):

$$\frac{L_i}{E_i} = 1 - \prod_{k=1}^{n}\left(1 - \frac{L_{k,i}}{E_i}\right)$$

Where the subscript *k* defines the type of effects associated with tropical cyclones. In this case, *k* = 1 indicates wind and *k* = 2 indicates storm surge (thus, *n* = 2).
Therefore, for a given area formed by several assets *i* (for example a country):

$$L = \sum_{i=1}^{A} L_i$$

Where *A* is the number of assets.
The vulnerability and exposure components of the model are detailed in the following sections.

5.2 Model validation

This section shows the validation results of the SPHERA loss model. The validation was carried out by comparing the results of the SPHERA model event-by-event in terms of economic losses (million USD) with observed losses from available reports. Scatterplots of observed versus simulated losses are shown. These plots are particularly useful to compare directly observed and simulated losses and assess eventual systematic biases. The reported losses are affected by a large uncertainty. However,

they are the only available data that can be used for validation purposes. Here are some of the limitations:

- No reports are available for many events, especially pre-1990 events and especially in small countries.
- The accuracy of the reported losses is variable, since different methodologies were employed at different times and in different countries. Different methodologies often lead to different values of reported losses for the same event.
- For some events, multiple reports are available from different sources, such as insurance companies, governments, NGOs, international institutions, etc. The losses reported in different reports rarely agree with each other. In these cases, the range of losses is shown in the scatterplots.
- The reported losses were trended to current money to account for many aspects, such as the effect of inflation and population growth, so that they can be compared to modelled losses. This trending process is unavoidable but introduces a large uncertainty especially for the oldest events.
- The reported losses usually account for the sum of the losses, thus including losses by wind, storm surge, rainfall, flooding, landslides, waves, etc. The SPHERA model only computes losses due to wind and storm surge. To account for this factor for historical events, a necessarily approximate method was used to separate wind and storm surge losses from losses caused by rainfall and landslides. This method assigns a large percentage of precipitation- and landside-induced losses to storms of lower category. It goes without saying that this method carries a large uncertainty.
- For some countries, especially those particularly prone to flood and landslides (for example, Central American countries), the method utilized to separate wind and surge losses from those caused by precipitation and landslides is more problematic because floods and landslides often produce here much larger losses. Hence, for these countries, the comparison between losses estimated by SPHERA and those reported should be considered with even more caution.
- The reported losses usually account for the sum of the losses, thus including direct and indirect losses from different economic sectors, such as agriculture, industry, etc. The SPHERA model only computes direct losses on buildings, infrastructure and crops. Unfortunately, the details of what losses are accounted for in the reports are most often unspecified. Therefore, for those events where such information is missing estimates of unmodelled losses cannot be removed from the observed figures.

Given the discussed caveats regarding the lack of reliability of the observed values, the results show, in general, a good agreement between the reported losses and the results of the SPHERA model (The country codes can be found in Annex A.).

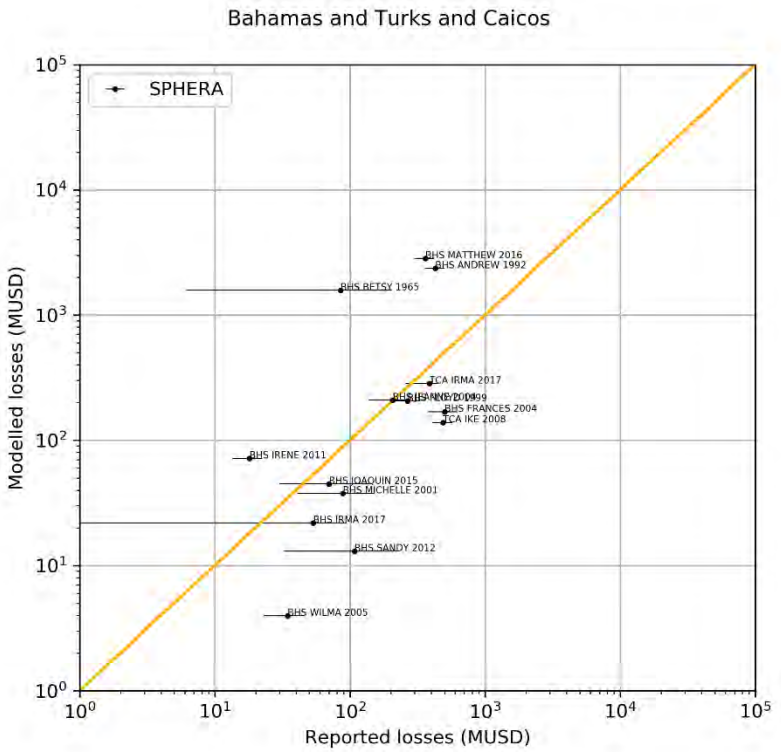

FIGURE 5-1 – SCATTERPLOT OF REPORTED VERSUS MODELLED LOSSES (BAHAMAS AND TURKS AND CAICOS).

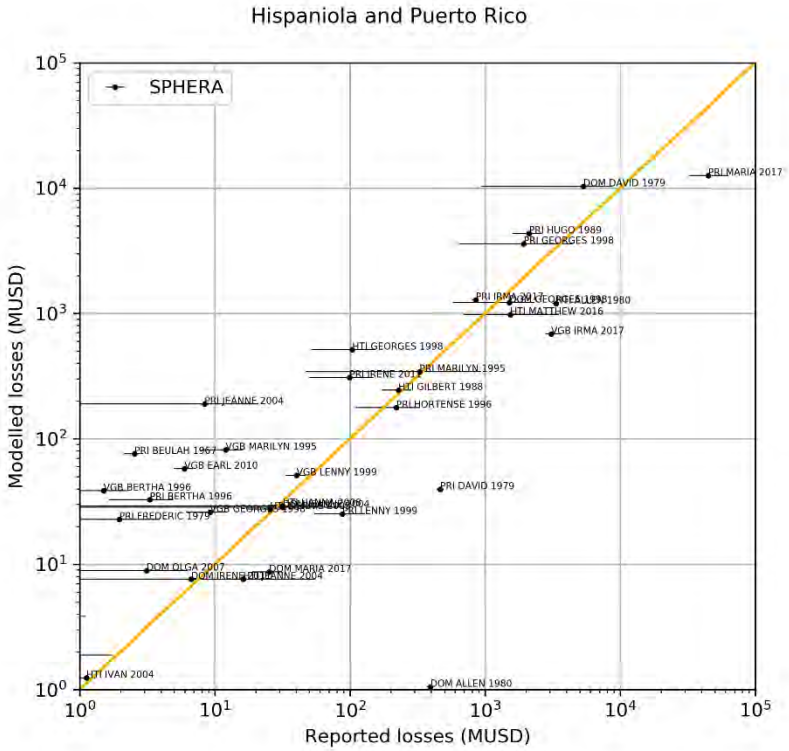

FIGURE 5-2 – SCATTERPLOT OF REPORTED VERSUS MODELLED LOSSES (HISPANIOLA AND PUERTO RICO).

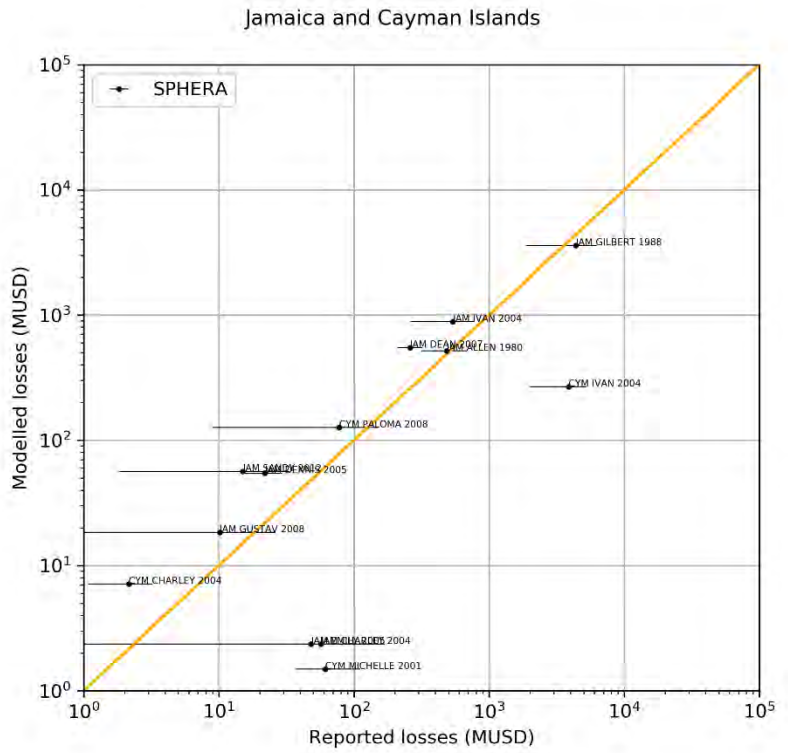

FIGURE 5-3 – SCATTERPLOT OF REPORTED VERSUS MODELLED LOSSES (JAMAICA AND CAYMAN ISLANDS).

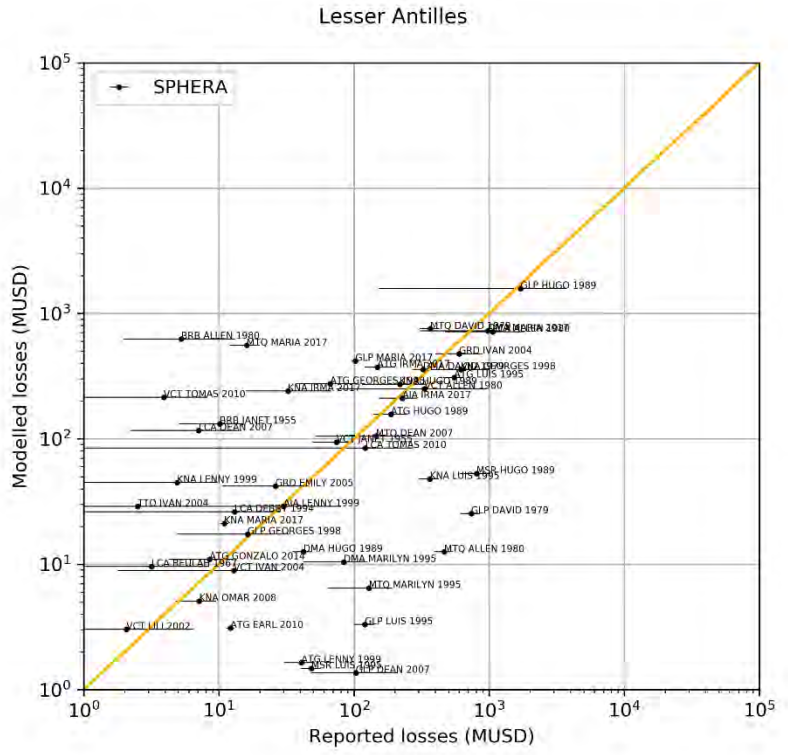

FIGURE 5-4 – SCATTERPLOT OF REPORTED VERSUS MODELLED LOSSES (LESSER ANTILLES).

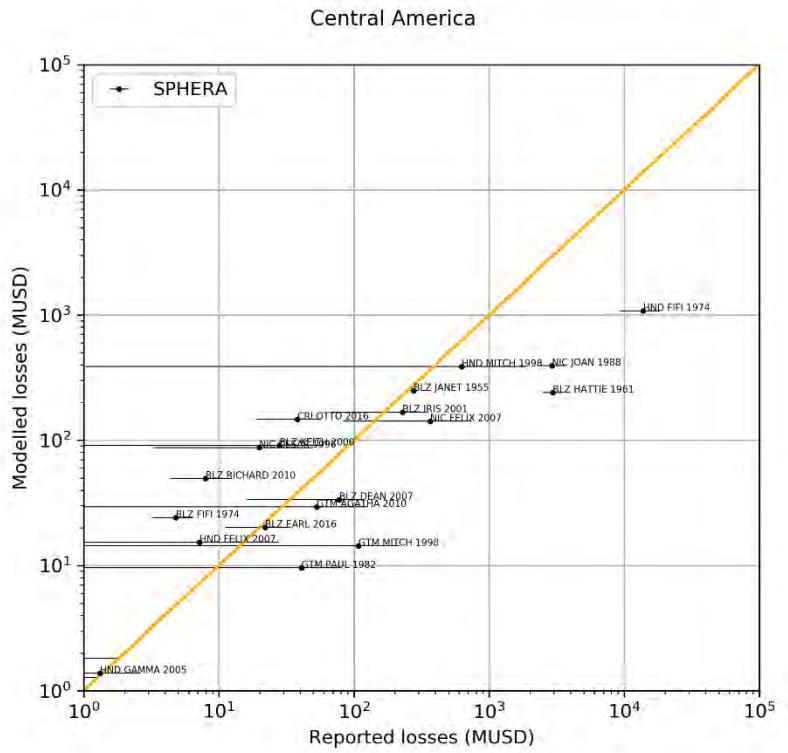

FIGURE 5-5 – SCATTERPLOT OF REPORTED VERSUS MODELLED LOSSES (CENTRAL AMERICA).

Table 5-1 reports the percentage of events that have been either overestimated, or underestimated or well reproduced by SPHERA, aggregated by country. The losses of an event are said to be *overestimated* if the model result is larger than the upper bound of the reported loss range while the losses of an event are considered to be *underestimated* if the model result is smaller than the lower bound. Finally, the losses of an event are considered to be *well reproduced* if the model result is within the range. The colours indicate the goodness of the model performance for all countries: green is desirable, red is undesirable.

Country	Underest.	OK	Overest.
AIA	0	100	0
ATG	0	50	50
BHS	0	67	33
BLZ	0	67	33
BMU	0	0	100
CRI	100	0	0
CYM	50	0	50
DMA	50	50	0
DOM	0	100	0
GLP	0	50	50
GRD	0	100	0
GTM	0	100	0
HND	0	100	0
HTI	50	50	0
JAM	0	40	60
KNA	0	100	0
LCA	0	100	0
MTQ	0	100	0
NIC	50	50	0
PRI	0	50	50

Country	Underest.	OK	Overest.
SXM	100	0	0
TCA	50	50	0
TTO	0	0	100
VCT	0	100	0
VGB	50	0	50

TABLE 5-1 – PERCENTAGES OF UNDER/OVERESTIMATED MODEL RESULTS PER COUNTRY. THE COUNTRY CODES CAN BE FOUND IN ANNEX A

It should be stressed that overestimating or underestimating losses does not necessarily have negative implications in the operation of the parametric insurance underpinned by this model. In summary, if the losses for all the events are systematically overestimated by the same factor, the frequency of the payout events will still be estimated correctly. From a modelling perspective, a 1-in-50 years event will still be a 1-in-50 years event even if all the event losses are overestimated, say, by a factor of 3.

In quantitative terms, according to the definition given above, the losses caused by the events underestimated by SPHERA, are underestimated on average by 55%, with a standard deviation of 25%, and the losses caused by events overestimated by SPHERA are overestimated on average by 147%, with a standard deviation of 178%.

The root mean square error of the SPHERA model results, computed against the mean reported losses is 6,710 M USD. If the worst two events per countries are removed (i.e., two events that would generate a payout, given that their losses have a return time around 15-20 years, longer than the typical attachment points of CCRIF's policies, which is 5 to 20 years), the root mean square error of SPHERA is 6,296 M USD.

6 POST-EVENT LOSS ASSESSMENT

The SPHERA model will also be run in real-time, or near real-time, to compute losses caused by future events. For this reason, the hazard module and the loss module are run every time a cyclone develops in the North Atlantic and Eastern Pacific and threatens any of the countries of study.

The aim of the real-time hazard calculation is to compute the maximum wind speed field and maximum storm surge field caused by a developing cyclone. The calculation is carried out whenever the US National Oceanic and Atmospheric Administration (NOAA) communicates the development of a tropical cyclone on its web page[6].

The same methodology described in the previous sections is employed. The input data for real-time tropical cyclone loss estimation is the a-deck format best track file provided by NOAA[7] (Figure 6-1). This file contains data regarding the ongoing cyclone, including:

- position of the eye.
- minimum sea level pressure.
- maximum wind speed.
- radius of maximum wind.
- radii at different wind speeds and in different quadrants.

[6] https://www.nhc.noaa.gov/

[7] http://ftp.nhc.noaa.gov/atcf/aid_public/

```
AL, 15, 2017091412, 03,  CMC,  18,  98N,  369W,  29, 1010, XX,  34, NEQ,    0,    0,    0,    0,
AL, 15, 2017091412, 03,  CMC,  24, 116N,  371W,  28, 1011, XX,  34, NEQ,    0,    0,    0,    0,
AL, 15, 2017091412, 03,  CMC,  30, 116N,  390W,  32, 1008, XX,  34, NEQ,    0,    0,    0,    0,
AL, 15, 2017091412, 03,  CMC,  36, 125N,  405W,  33, 1008, XX,  34, NEQ,    0,    0,    0,    0,
AL, 15, 2017091412, 03,  CMC,  42, 129N,  421W,  32, 1004, XX,  34, NEQ,    0,    0,    0,    0,
AL, 15, 2017091412, 03,  CMC,  48, 130N,  440W,  36, 1003, XX,  34, NEQ,   66,    0,    0,    0,
AL, 15, 2017091412, 03,  CMC,  54, 130N,  450W,  41, 1001, XX,  34, NEQ,   87,   59,    0,    0,
AL, 15, 2017091412, 03,  CMC,  60, 138N,  458W,  41, 1002, XX,  34, NEQ,   88,  111,    0,   76,
AL, 15, 2017091412, 03,  CMC,  66, 140N,  460W,  41,  998, XX,  34, NEQ,   78,   80,    0,   88,
AL, 15, 2017091412, 03,  CMC,  72, 142N,  467W,  43,  999, XX,  34, NEQ,  101,   95,   23,   81,
AL, 15, 2017091412, 03,  CMC,  78, 149N,  470W,  46,  995, XX,  34, NEQ,   97,  128,   72,   71,
AL, 15, 2017091412, 03,  CMC,  84, 150N,  470W,  48,  995, XX,  34, NEQ,  117,  106,    0,   87,
AL, 15, 2017091412, 03,  CMC,  90, 156N,  471W,  49,  994, XX,  34, NEQ,   88,  122,   89,   93,
AL, 15, 2017091412, 03,  CMC,  96, 160N,  471W,  49,  993, XX,  34, NEQ,  122,  134,   89,  116,
AL, 15, 2017091412, 03,  CMC, 102, 164N,  474W,  52,  991, XX,  34, NEQ,  121,  132,   79,  102,
AL, 15, 2017091412, 03,  CMC, 102, 164N,  474W,  52,  991, XX,  50, NEQ,    0,    0,    0,   58,
AL, 15, 2017091412, 03,  CMC, 108, 170N,  476W,  48,  993, XX,  34, NEQ,  133,  131,   98,  115,
AL, 15, 2017091412, 03,  CMC, 114, 176N,  478W,  51,  994, XX,  34, NEQ,  128,  140,   92,  108,
AL, 15, 2017091412, 03,  CMC, 114, 176N,  478W,  51,  994, XX,  50, NEQ,   54,    0,    0,   31,
AL, 15, 2017091412, 03,  CMC, 120, 180N,  480W,  49,  992, XX,  34, NEQ,  166,  150,   82,  108,
AL, 15, 2017091412, 03,  CMC, 126, 184N,  481W,  53,  990, XX,  34, NEQ,  170,  159,  114,  162,
AL, 15, 2017091412, 03,  CMC, 126, 184N,  481W,  53,  990, XX,  50, NEQ,   56,    0,    0,    0,
AL, 15, 2017091412, 03,  CMC, 132, 189N,  481W,  50,  991, XX,  34, NEQ,  174,  131,  132,  143,
AL, 15, 2017091412, 03,  CMC, 138, 190N,  480W,  52,  988, XX,  34, NEQ,  210,  161,  115,  150,
AL, 15, 2017091412, 03,  CMC, 138, 190N,  480W,  52,  988, XX,  50, NEQ,   68,    0,    0,   83,
AL, 15, 2017091412, 03,  CMC, 144, 193N,  479W,  54,  990, XX,  34, NEQ,  243,  176,  109,  174,
AL, 15, 2017091412, 03,  CMC, 144, 193N,  479W,  54,  990, XX,  50, NEQ,    0,    0,    0,   84,
AL, 15, 2017091412, 03,  CMC, 150, 199N,  472W,  57,  988, XX,  34, NEQ,  157,  137,   99,  116,
AL, 15, 2017091412, 03,  CMC, 150, 199N,  472W,  57,  988, XX,  50, NEQ,    0,   92,    0,   63,
AL, 15, 2017091412, 03,  CMC, 156, 211N,  466W,  50,  991, XX,  34, NEQ,  155,  154,  114,  129,
```

FIGURE 6-1 – EXAMPLE OF A-DECK BEST TRACK FILE (HURRICANE MARIA, 2017).

The wind speed and storm surge fields resulting from the occurring events are computed using the SPHERA hazard module. Two recent examples are reported below:

- Hurricane Irma, 2017.
- Hurricane Maria, 2017

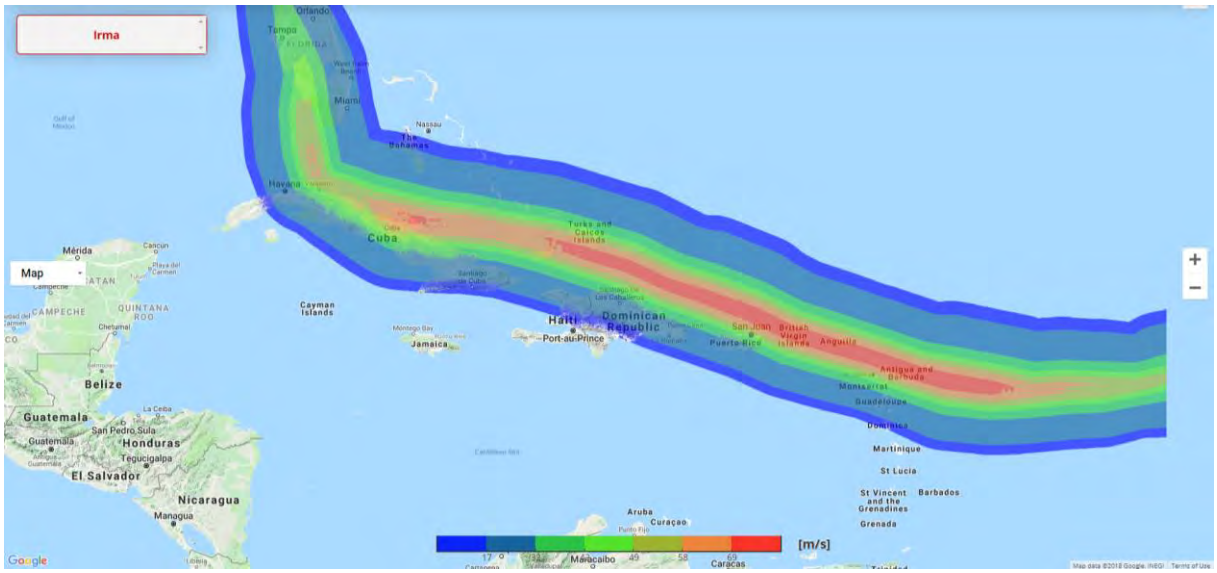

FIGURE 6-2 – HURRICANE IRMA MAXIMUM WIND SPEED FIELD ESTIMATED BY SPHERA.

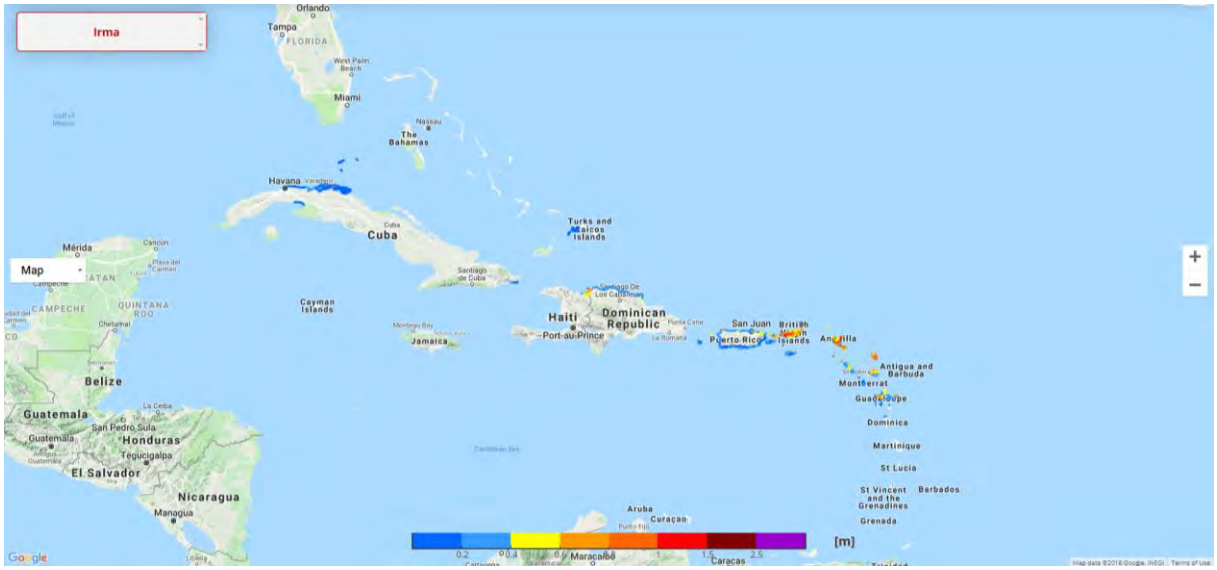

FIGURE 6-3 – HURRICANE IRMA STORM SURGE MAXIMUM HEIGHT ESTIMATED BY SPHERA.

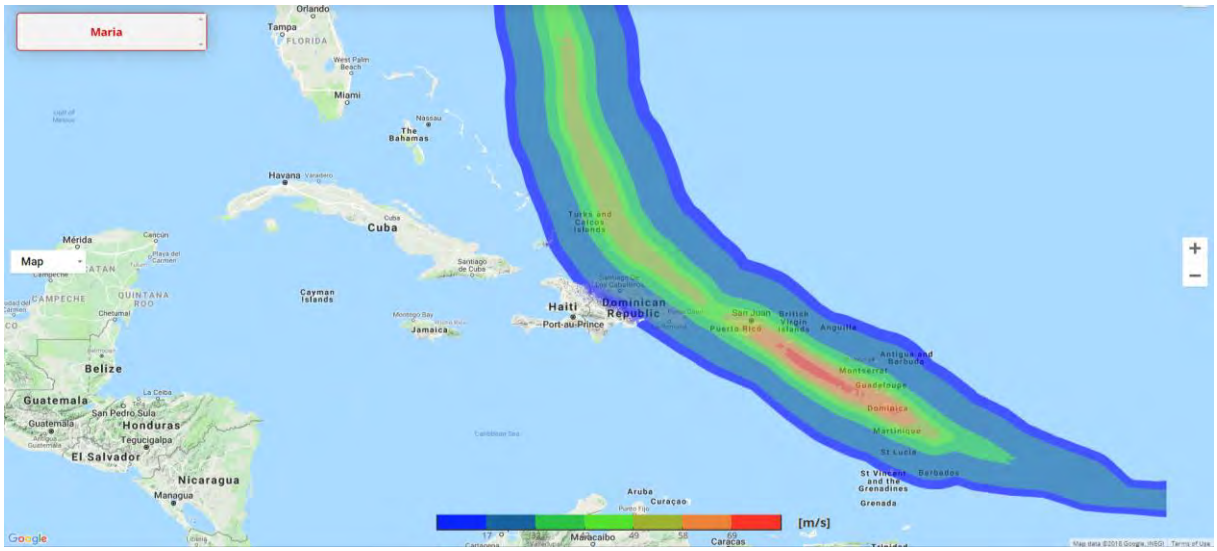

FIGURE 6-4 – HURRICANE MARIA MAXIMUM WIND SPEED FIELD ESTIMATED BY SPHERA.

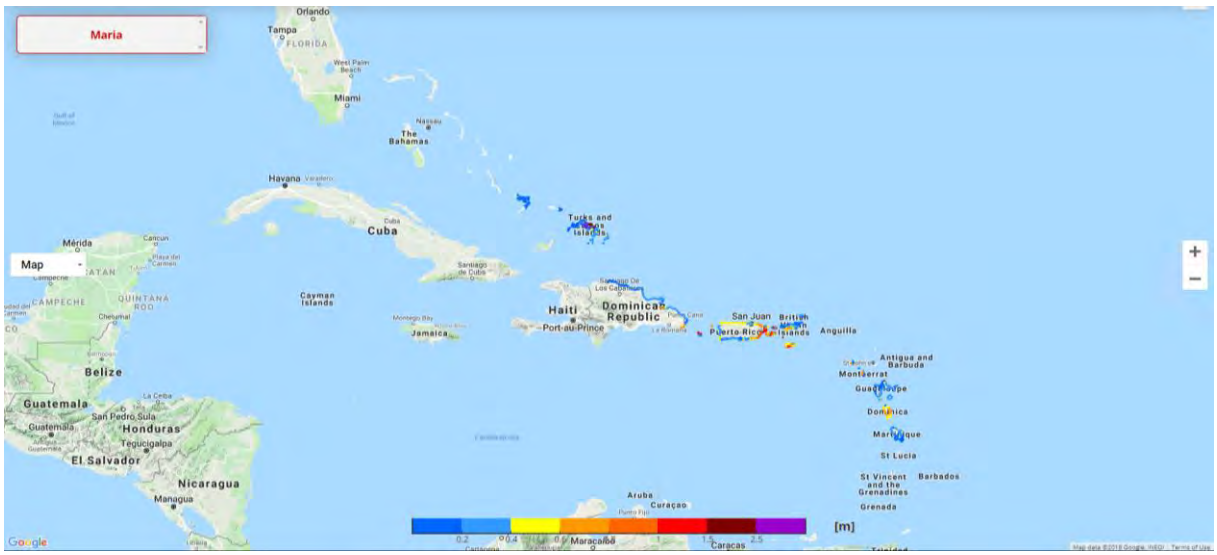

FIGURE 6-5 – HURRICANE MARIA STORM SURGE MAXIMUM HEIGHT ESTIMATED BY SPHERA.

Losses are also computed for all countries in real time, as the cyclone develops, following a pre-established protocol. Once the cyclone eye is in a position such that it cannot cause further damage to a country, the value of computed losses is considered as final. If the country has subscribed an insurance policy, the loss estimate is used to compute a potential payout, based on the policy parameters. The loss assessment in SPHERA includes the damage accumulation caused by slow moving hurricanes. This is an important component in the model given the damage observed after the impact of hurricanes with a low translational speed, as described in Section xxx.

The methodology implemented for the real-time loss assessment is the same already described for the long-term assessment, since a complete consistency is needed between the two configurations of the SPHERA model. The main difference between the two cases is that in the near real-time configuration, the loss assessment module computes the economic losses caused by a single event while in the stochastic catalogue case the module computes losses for a large collection of scenarios rather than by one only.

In the near real time, the loss assessment is carried out by gathering the input data to characterize the event by NOAA and computing the wind and storm surge fields associated with it (as described in Section 2.2 and 2.3). The economic losses computed in each of the countries affected by the event and covered by the model are then computed by the loss module (see the first part of this section) using as input the wind and storm surge fields, the database of exposed assets and the tropical cyclone vulnerability models. The model in real-time configuration estimates the economic losses considering the same uncertainties taken into account for long-term loss assessment. The final output of the real-time loss assessment is the expected loss experienced by each country affected by the event under analysis and corresponding uncertainty.

7 REFERENCES

Berger, M.J., George, D.L., LeVeque, R.J., Mandli, K.T., 2011. The GeoClaw software for depth-averaged flows with adaptive refinement. Adv. Water Resour. 34, 1195–1206. doi:10.1016/j.advwatres.2011.02.016

Bernal, G.A., Salgado-Gálvez, M.A., Zuloaga, D., Tristancho, J., González, D., Cardona, O.-D., 2017. Integration of Probabilistic and Multi-Hazard Risk Assessment Within Urban Development Planning and Emergency Preparedness and Response: Application to Manizales, Colombia. Int. J. Disaster Risk Sci. 8, 270–283. doi:10.1007/s13753-017-0135-8

Carrere, L., Lyard, F., Cancet, M., Guillot, A., 2015. FES 2014, a new tidal model on the global ocean with enhanced accuracy in shallow seas and in the Arctic region, in: Copernicus (Ed.), EGU General Assembly. Vienna.

Clawpack Development Team, 2017. Clawpack Version 5.4.1, http://www.clawpack.org. doi:10.5281/zenodo.820731

Dell'Acqua, F., Iannelli, G., Torres, M., Martina, M., 2018. A Novel Strategy for Very-Large-Scale Cash-Crop Mapping in the Context of Weather-Related Risk Assessment, Combining Global Satellite Multispectral Datasets, Environmental Constraints, and In Situ Acquisition of Geospatial Data. Sensors 18, 591. doi:10.3390/s18020591

Done, J.M., Simmons, K., Czajkowski, J., 2017. Effectiveness of the Florida Building Code to Hurricane Wind Field Parameters.

Dottori, F., Figueiredo, R., Martina, M.L.V., Molinari, D., Scorzini, A.R., 2016. INSYDE: a synthetic, probabilistic flood damage model based on explicit cost analysis. Nat. Hazards Earth Syst. Sci. 16, 2577–2591. doi:10.5194/nhess-16-2577-2016

Emanuel, K., Ravela, S., Vivant, E., Risi, C., 2006. A Statistical Deterministic Approach to Hurricane Risk Assessment. Bull. Am. Meteorol. Soc. 87, 299–314. doi:10.1175/BAMS-87-3-299

ESDU, 1993. ESDU 84011- Wind Speed Profiles over Terrain with Roughness Changes (No. 84011). Engineering Science Data Unit.

ESDU, 1983. ESDU 83045 - Strong Winds in the Atmospheric Boundary Layer. Part 2 Discrete Gust Speeds. Engineering Science Data Unit.

ESDU, 1982. ESDU 82026 - Strong Winds in the Atmospheric Boundary Layer. Part 1 mean-hourly wind speeds. Engineering Science Data Unit.

Fisher, R., Jantsch, M., Comer, R., 1982. General bathymetric chart of the oceans (GEBCO). Can. Hydrogr. Serv. Ottawa, Canada.

Gani, F., Légeron, F., 2012. Relationship between specified ductility and strength demand reduction for single degree-of-freedom systems under extreme wind events. J. Wind Eng. Ind. Aerodyn. 109, 31–45. doi:10.1016/j.jweia.2012.06.006

Hall, T.M., Jewson, S., 2007. Statistical modelling of North Atlantic tropical cyclone tracks. Tellus A Dyn. Meteorol. Oceanogr. 59, 486–498. doi:10.1111/j.1600-0870.2007.00240.x

Holland, G.J., 1980. An Analytic Model of the Wind and Pressure Profiles in Hurricanes. Mon. Weather Rev. 108, 1212–1218. doi:10.1175/1520-0493(1980)108<1212:AAMOTW>2.0.CO;2

Huizinga, J., de Moel, H., Szewczyk, W., 2017. Global flood depth-damage functions: Methodology and the database with guidelines. No. JRC105688. Joint Research Centre.

James, M.K., Mason, L.B., 2005. Synthetic Tropical Cyclone Database. J. Waterw. Port, Coastal, Ocean Eng. 131, 181–192. doi:10.1061/(ASCE)0733-950X(2005)131:4(181)

Jarvis, A., Reuter, H.I., Nelson, A., Guevara, E., 2008. Hole-filled SRTM for the globe Version 4. available from CGIAR-CSI SRTM 90m Database (http//srtm. csi. cgiar. org) 15.

Kaplan, J., DeMaria, M., 1995. A Simple Empirical Model for Predicting the Decay of Tropical Cyclone Winds after Landfall. J. Appl. Meteorol. 34, 2499–2512. doi:10.1175/1520-0450(1995)034<2499:ASEMFP>2.0.CO;2

Kok, M., Huizinga, H., Vrouwenfelder, A., Barendregt, A., 2004. Standard method 2004. Damage and casualties caused by flooding, Highway and Hydraulic Engineering Department.

Konthesingha, K.M.C., Stewart, M.G., Ryan, P., Ginger, J., Henderson, D., 2015. Reliability based vulnerability modelling of metal-clad industrial buildings to extreme wind loading for cyclonic regions. J. Wind Eng. Ind. Aerodyn. 147, 176–185. doi:10.1016/j.jweia.2015.10.002

Lobell, D.B., Asner, G.P., 2004. Cropland distributions from temporal unmixing of MODIS data. Remote Sens. Environ. 93, 412–422. doi:10.1016/j.rse.2004.08.002

Mandli, K.T., Ahmadia, A.J., Berger, M., Calhoun, D., George, D.L., Hadjimichael, Y., Ketcheson, D.I., Lemoine, G.., LeVeque, R.J., 2016. Clawpack: building an open source ecosystem for solving hyperbolic PDEs. PeerJ Comput. Sci. 2, e68. doi:10.7717/peerj-cs.68

Mandli, K.T., Dawson, C.N., 2014. Adaptive mesh refinement for storm surge. Ocean Model. 75, 36–50. doi:10.1016/j.ocemod.2014.01.002

Niño, M., Jaimes, M.A., Reinoso, E., 2015. A risk index due to natural hazards based on the expected annual loss. Nat. Hazards 79, 215–236. doi:10.1007/s11069-015-1837-0

Ordaz, M., 2015. A simple probabilistic model to combine losses arising from the simultaneous occurrence of several hazards. Nat. Hazards 76, 389–396. doi:10.1007/s11069-014-1495-7

Ordaz, M., Miranda, E., Reinoso, E., Cruz, S.S., 2000. Modelo de estimación de pérdidas por sismo en México con fines de seguros 33.

Powell, M.D., Houston, S.H., Fl, M., Ares, I., 1995. Real-time Damage Assessment in Hurricanes. Miami Florida, p. 3.

Rumpf, J., Weindl, H., Höppe, P., Rauch, E., Schmidt, V., 2007. Stochastic modelling of tropical cyclone tracks. Math. Methods Oper. Res. 66, 475–490. doi:10.1007/s00186-007-0168-7

Salgado-Gálvez, M.A., Bernal, G.A., Barbat, A.H., Carreño, M.L., Cardona, O.-D., 2016. Probabilistic estimation of annual lost economic production due to premature deaths because of earthquakes. Hum. Ecol. Risk Assess. An Int. J. 22, 543–557. doi:10.1080/10807039.2015.1095072

Salgado-Gálvez, M.A., Bernal, G.A., Zuloaga, D., Marulanda, M.C., Cardona, O.-D., Henao, S., 2017a. Probabilistic Seismic Risk Assessment in Manizales, Colombia: Quantifying Losses for Insurance Purposes. Int. J. Disaster Risk Sci. 8, 296–307. doi:10.1007/s13753-017-0137-6

Salgado-Gálvez, M.A., Zuloaga, D., Henao, S., Bernal, G.A., Cardona, O.-D., 2017b. Probabilistic assessment of annual repair rates in pipelines and of direct economic losses in water and sewage networks: application to Manizales, Colombia. Nat. Hazards. doi:10.1007/s11069-017-2987-z

Scawthorn, C., Flores, P., Blais, N., Seligson, H., Tate, E., Chang, S., Mifflin, E., Thomas, W., Murphy, J., Jones, C., Lawrence, M., 2006. HAZUS-MH Flood Loss Estimation Methodology. II. Damage and Loss Assessment. Nat. Hazards Rev. 7, 72–81. doi:10.1061/(ASCE)1527-6988(2006)7:2(72)

Silva, R., Govaere, G., Salles, P., Bautista, G., Díaz, G., 2002. Oceanographic vulnerability to hurricanes on the Mexican coast, in: Coastal Engineering 2002: Solving Coastal Conundrums. pp. 39–51.

Solow, A.R., Moore, L., 2000. Testing for a Trend in a Partially Incomplete Hurricane Record. J. Clim. 13, 3696–3699. doi:10.1175/1520-0442(2000)013<3696:TFATIA>2.0.CO;2

Vickery, P.J., Masters, F.J., Powell, M.D., Wadhera, D., 2009. Hurricane hazard modeling: The past, present, and future. J. Wind Eng. Ind. Aerodyn. 97, 392–405. doi:10.1016/j.jweia.2009.05.005

Vickery, P.J., Skerlj, P.F., Twisdale, L.A., 2000. Simulation of Hurricane Risk in the U.S. Using Empirical Track Model. J. Struct. Eng. 126, 1222–1237. doi:10.1061/(ASCE)0733-9445(2000)126:10(1222)

Vickery, P.J., Wadhera, D., 2008a. Statistical Models of Holland Pressure Profile Parameter and Radius to Maximum Winds of Hurricanes from Flight-Level Pressure and H*Wind Data. J. Appl. Meteorol. Climatol. 47, 2497–2517. doi:10.1175/2008JAMC1837.1

Vickery, P.J., Wadhera, D., 2008b. Statistical Models of Holland Pressure Profile Parameter and Radius to Maximum Winds of Hurricanes from Flight-Level Pressure and H*Wind Data. J. Appl. Meteorol. Climatol. 47, 2497–2517. doi:10.1175/2008JAMC1837.1

Wardlow, B.D., Egbert, S.L., 2008. Large-area crop mapping using time-series MODIS 250 m NDVI data: An assessment for the U.S. Central Great Plains. Remote Sens. Environ. 112, 1096–1116. doi:10.1016/j.rse.2007.07.019

Wehner, M., Ginger, J., Holmes, J., Sandland, C., Edwards, M., 2010. Development of methods for assessing the vulnerability of Australian residential building stock to severe wind. IOP Conf. Ser. Earth Environ. Sci. 11, 012017. doi:10.1088/1755-1315/11/1/012017

Weiss, A., 2001. Topographic position and landforms analysis, in: Poster Presentation, ESRI User Conference, San Diego, CA (Vol. 200).

Wilson, J.P., Gallant, J.C., 2000. Terrain analysis: principles and applications. John Wiley & Sons.

WMO, 2011. Guide to Storm surge Forecasting, World Meteorological Organisation. WMO-No. 1076.

ANNEX A: COUNTRY ISO CODES

Code	Country	Code	Country
ABW	Aruba	**HND**	Honduras
AIA	Anguilla	**HTI**	Haiti
ATG	Antigua and Barbuda	**JAM**	Jamaica
BES	Bonaire, Sint Eustatius, Saba	**KNA**	Saint Kitts and Nevis
BHS	The Bahamas	**LCA**	Saint Lucia
BLZ	Belize	**MSR**	Montserrat
BMU	Bermuda	**MTQ**	Martinique
BRB	Barbados	**NIC**	Nicaragua
CRI	Costa Rica	**PAN**	Panama
CUW	Curacao	**PRI**	Puerto Rico
CYM	Cayman Islands	**SLV**	El Salvador
DMA	Dominica	**SUR**	Suriname
DOM	Dominican Republic	**SXM**	Sint Maarten
GLP	Guadeloupe	**TCA**	Turks and Caicos Islands
GRD	Grenada	**TTO**	Trinidad and Tobago
GTM	Guatemala	**VCT**	Saint Vincent and the Grenadines
GUY	Guyana	**VGB**	British Virgin Islands

APPENDIX 2

SPHERA

System for Probabilistic Hazard Evaluation and Risk Assessment

SUMMARY OF THE EARTHQUAKE LOSS ASSESSMENT METHODOLOGY

Version 1.3
November 2018

INDEX

1 INTRODUCTION

1.1 Aim and scope

This report summarizes the methodology implemented by ERN/RED for CCRIF SPC in the SPHERA (System for Probabilistic Hazard Evaluation and Risk Assessment) v1.3 model for earthquake loss assessment. The report outlines the approach used for the probabilistic seismic hazard analysis, the development of the exposure database, the approach followed for the derivation of the vulnerability functions and the methodological framework for the long-term earthquake loss assessment. Finally, it describes the methodology adopted to estimate in near-real time the modelled losses to buildings and infrastructures due to the occurrence of an earthquake and the consequent payout to the insured countries according to the event parameters provided by a reputable third party, here the USGS.

1.2 Organization of the report

Section 2 of this report describes the methodology adopted for the probabilistic seismic hazard analysis, or PSHA (methodology and results), developed for the Caribbean, Central America and the Northern Andes regions, together with the datasets and sources of information used for it. All the details and the references about the development of the seismic hazard model and the PSHA are available in the SPHERA earthquake hazard module report. The PSHA was developed with the aim of generating a set of possible future earthquakes for the area under study (i.e. stochastic event set) to be later used in a fully probabilistic estimation of the losses induced by them on the exposed assets of the different countries. Each of these events has a rate of occurrence attached to it, which is compatible with the seismicity parameters observed historically for the different seismic sources, and a set of rules that account for the probabilistic representation of the ground motion intensity it may generate.

Section 3 of this report describes the methodology adopted for the development of the exposure database, the types of assets included, the lines of business that are considered in the SPHERA model and the classification of countries into different vulnerability types to account for local construction practices and the enforcement of earthquake building codes. This section includes the sources of information that were used for its derivation and comparisons against other openly available databases for the domain under study.

Section 4 summarizes the analytical approach followed for deriving the vulnerability functions for all types of assets included in the exposure database, and how a probabilistic representation is made available for the subsequent loss assessment. A description about the selection of the hazard intensity measures is provided together with some examples of vulnerability functions for different types of assets and vulnerability classifications.

Section 5 presents the methodological framework for probabilistic seismic loss assessment and what the outcomes of this process are, together with a summary of the results obtained at country level in terms of average annual losses (AAL) and probable maximum losses (PML) for different return periods. In addition, this section includes a summary of the loss validation process followed during the development of SPHERA and the comparison of modelled and observed losses for 25 events in the region for which country scale direct losses reports were available and also for the stochastic event set.

Finally, Section 6 summarizes the procedure that is implemented in SPHERA to evaluate in near-real time the economic losses induced by the occurrence of an earthquake in the Caribbean and Central America regions. First, the approach followed for the generation of the seismic hazard intensities (i.e. ground motion fields) to be used in the rapid estimation of losses caused by earthquakes (near real-time seismic hazard estimation) is described. This estimation is to be made within hours after the occurrence of the event using information such as location of the epicentre (or of the rupture), depth of the hypocentre and magnitude, made available by well-known international institutions such as the

United States Geological Survey (USGS). Finally, the report describes how the ground motion fields computed with such third party data are then used to obtain a reliable estimation of the cost of repairing the physical damage inflicted by the earthquake to the exposed assets, using the same exposure and vulnerability modules considered for the long-term assessment.

1.3 Geographical coverage

The SPHERA model covers 34 countries for both near-real time and long-term earthquake loss assessment. Such countries are divided in three groups:

- Group 1: Anguilla, Antigua and Barbuda, The Bahamas, Barbados, Belize, Bermuda, Cayman Islands, Dominica, Grenada, Haiti, Jamaica, Saint Kitts and Nevis, Saint Lucia, Saint Vincent and the Grenadines, Trinidad and Tobago and Turks and Caicos Islands.
- Group 2: Dominican Republic, Costa Rica, El Salvador, Guatemala, Honduras, Nicaragua and Panama.
- Group 3: Aruba, British Virgin Islands, Curaçao, Guadeloupe, Guyana, Martinique, Montserrat, Bonaire-Saba-Saint Eustatius, Sint Maarten, Puerto Rico and Suriname.

Figure 1-1 shows the location of these countries.

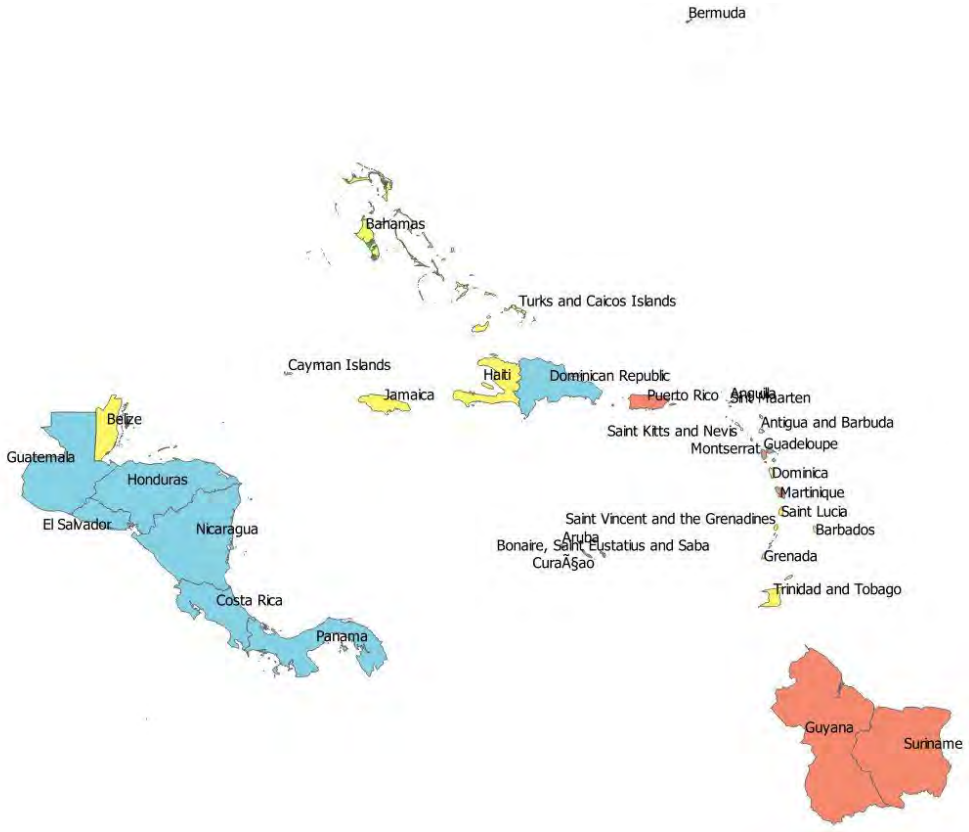

FIGURE 1-1 – LOCATION OF THE THREE GROUPS OF COUNTRIES BEING COVERED IN THE EXPOSURE DATABASE: GROUP 1 COUNTRIES IN YELLOW, GROUP 2 IN BLUE AND GROUP 3 IN RED

2 PROBABILISTIC SEISMIC HAZARD ANALYSIS

The long-term seismic hazard module was designed to model the occurrence of future earthquakes to be statistically consistent in time and space with the historical seismicity in the region covered by the SPHERA model. It allows characterizing the occurrence of future earthquakes and determining the relationship between seismic hazard intensities (e.g. spectral accelerations) and their exceedance rates in all the sites covered by the model, by means of probabilistic seismic hazard analyses (PSHAs). The methodological framework to build a seismic hazard model, even using the state-of-the-art tools, in its essence is still based on the approaches first proposed by Cornell (1968) and Esteva (1970).

As a first step, an updated and complete historical earthquake catalogue must be compiled. Then, the region of study must be divided in sub-regions in which the occurrence of earthquakes can be assumed to be uniform in time and space and to present similar characteristics (e.g. crustal or subduction seismicity). The future earthquake occurrence process for each of these regions is statistically modelled using the information collected about the historical seismicity (earthquake catalogues). In each sub-region it is then possible to simulate possible future earthquakes compatible with the historical seismicity. Finally, for each of these simulated events ground motion prediction equations (GMPEs) allow obtaining quantitative measures of ground motion intensities such as peak ground accelerations at the sites of interest. The following sections summarize the methodology followed for each of the above steps; the full details can be found in the Seismic Hazard Model Technical Report.
The seismic hazard module can provide several results through the development of PSHA, such as ground motion intensity exceedance curves (also known as hazard curves), uniform hazard spectra, hazard maps and stochastic event sets. In this report the emphasis will be made on the latter the since the stochastic event set is the output of the hazard module that is used in the fully probabilistic seismic loss assessment framework implemented in SPHERA. The following sections present the most relevant details of each of the components needed when developing the PSHA.

2.1 Earthquake catalogue

The historical earthquake catalogue adopted in this study made use of data from several international sources such as the latest version (v5.1) of the ISC-GEM global instrumental catalogue (Storchak et al., 2013) and the USGS-NEIC (Wald et al., 2006), as well as from other sources (e.g. Engdahl and Villasenor, 2002) for verification. In summary, the instrumental catalogue covers the 1900-2017 period and has a minimum threshold magnitude equal to M_W4.0. In addition, a review of historical seismicity was made for the domain under study, comprehensively reviewing events dating back to 1520. Among these events are included the 1770 Port au Prince earthquake, the 1867 Virgin Islands earthquake and the 1690 Saint Kitts and Nevis earthquake, among others.

A de-clustering process, following a magnitude and time dependent procedure similar to that proposed by Gardner and Knopoff, (1974) was employed in order to include in the working catalogue only those events classified as mainshocks. Additionally, particular events were validated (mostly in Central America and Mexico) leading in some cases to relocations. Magnitudes were homogenized in moment magnitude (M_w), using global relationships. The final working catalogue includes a total of 15,438 events.

Also, a completeness verification process was performed for different magnitudes, following the procedure proposed by Tinti and Mulargia, (1985) and using a regional approach given the large geographical extent of the area under analysis.

Figure 2-1 shows the magnitude distribution of all the events and Figure 2-2 shows their depth distribution. In addition, Table 2-1 shows the accumulated number of events by magnitude.

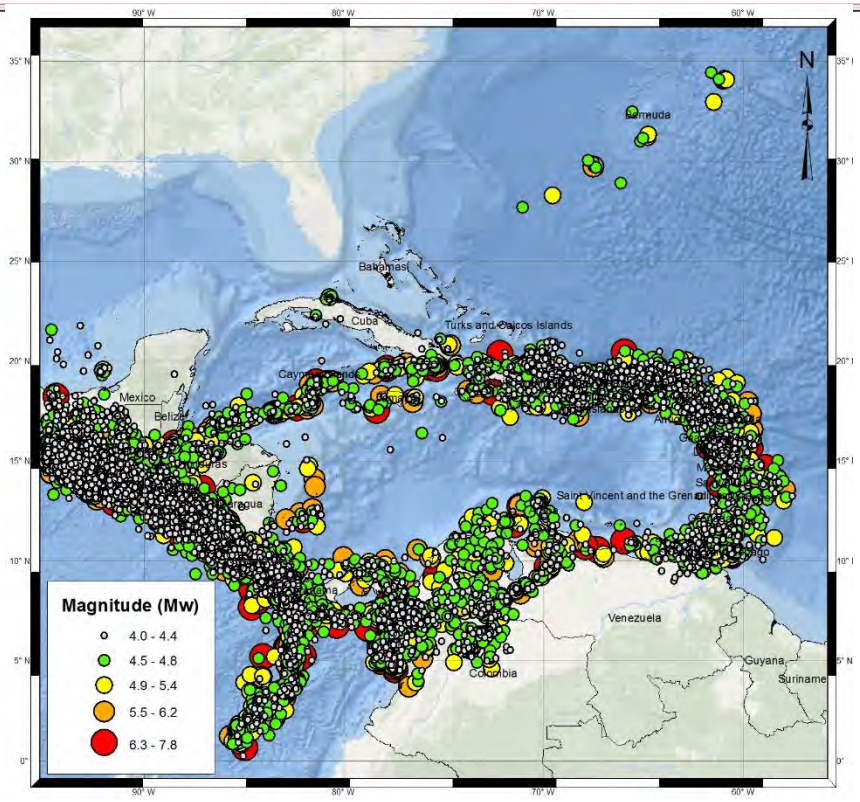

FIGURE 2-1 – MAGNITUDE OF THE EVENTS INCLUDED IN THE WORKING CATALOGUE (M_W)

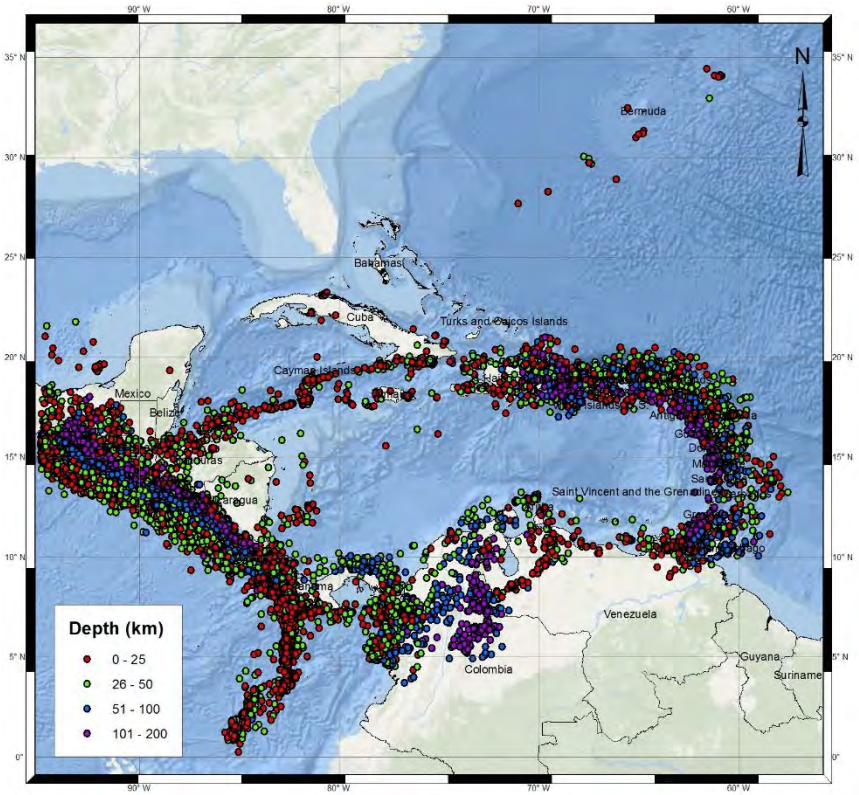

FIGURE 2-2 – DEPTH DISTRIBUTION (KM) OF THE EVENTS INCLUDED IN THE WORKING CATALOGUE

TABLE 2-1 – MAGNITUDE DISTRIBUTION OF THE WORKING CATALOGUE

Magnitude	Number of events
>=4.0	15,438
>=4.5	10,450
>=5.0	3,713
>=5.5	1,441
>=6.0	695
>=6.5	269
>=7.0	116
>=7.5	40
>=7.8	9

2.2 Tectonic zonation

Based on different tectonic and geological studies previously performed in the region, a tectonic zonation was carried out for the area of study, with the aim of identifying regions on which the seismic activity can be considered as uniform in time and space. Depending on the characteristic of the sources and the faulting mechanisms, different geometrical models were employed. This is because, for example, earthquakes occurring in subduction zones have very different characteristics than those that occur with strike-slip mechanisms in intraplate areas.

During the development of a PSHA it is critical to choose the appropriate geometrical representation and modeling approaches for the different seismic sources that were identified as relevant. Depending on the characteristics of these sources, such as variations in depth and shapes of the ruptures, among others, some of the geometric models are known to be more suitable than others. In the model developed for this study, different geometrical models were used to describe the seismic sources, depending on the characteristics of the tectonic processes occurring at each location. For instance, interface sources in the Caribbean were modeled as *rectangular faults*, which allow to explicitly control the dip and depth of the source and to guarantee that the rupture does not extend beyond the limits of the fault (strict boundary condition). On the other hand, all intraslab sources were modeled with the slab-geometry feature included in R-CRISIS in which the seismicity along the fault is concentrated in a set of vertical slices (treated as rectangular faults with dip=90° and variable width) where ruptures are assumed to occur.

For the case of most intraplate sources, area sources and area-plane geometry sources were used. They are defined as 3D polygons in which the seismicity is assumed to be uniform. Strikes and dips were assigned to each source to define the orientation of the ruptures, together with their shape (either elliptical or rectangular, with different aspect ratios). For example, for all sources where strike-slip mechanisms were identified as predominant, vertical ruptures with rectangular shapes (with aspect ratios between 2 and 5) were used. Figure 2-3 summarizes the geometry of all the sources considered in this PSHA together with the description of the geometrical model employed for the representation of each of them.

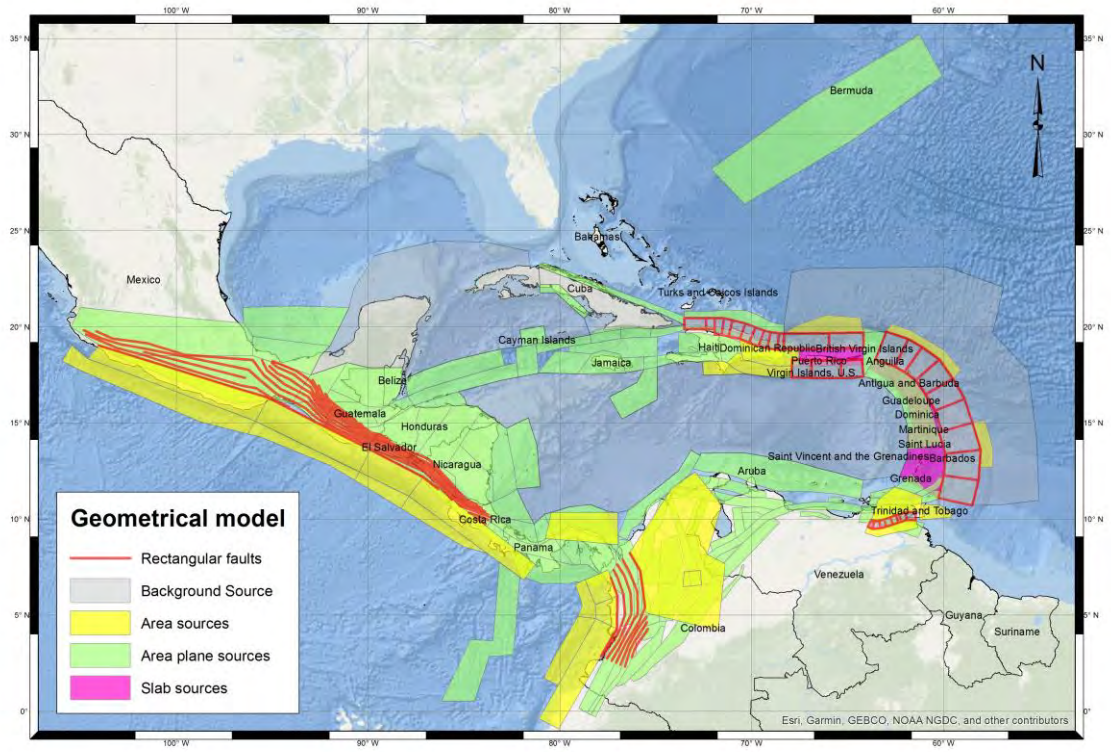

FIGURE 2-3 – SEISMIC SOURCES AND ASSIGNED GEOMETRICAL MODEL

2.3 Earthquake occurrence models

For the estimation of the seismicity parameters that characterize the future earthquake occurrence at each seismic source, only those earthquakes from 1900 onwards were considered. This is justified by the lack of completeness for earthquakes before that date, even though instrumental records are known to exist in the region from approximately 1870.

In this model the seismicity of all sources is assumed to follow a Poissonian process, which assumes independency in time and space between events (this is the reason why it was important to perform a declustering in the working catalogue).

Two Poissonian seismicity models are commonly used in the development of PSHA: 1) the modified Gutenberg-Richter model and 2) the characteristic earthquake model.

In the modified G-R seismicity model future earthquake occurrences are defined by the following relationship:

$$\lambda(M) = \lambda_0 \frac{\exp(-\beta M) - \exp(-\beta M_U)}{\exp(-\beta M_0) - \exp(-\beta M_U)} \qquad \text{(Eq. 1)}$$

where λ_0 is the exceedance rate of the minimum threshold magnitude, M_0; β is a parameter equivalent to the "*b*-value" for the source (except that it is given in terms of its natural logarithm) and M_U is the maximum magnitude for the source.

λ_0 and β (a and b) parameters were calculated using a maximum likelihood approach considering that the completeness window varies as a function of M_0, meaning that the complete sub-catalogues were later combined to obtain the final seismicity parameter for each seismic source.

There may be cases, mainly related to the interface and intraslab sources, where the modified G-R seismicity model underestimates the occurrences of large magnitude events. For these cases it is recommended that the modified G-R model is combined with the characteristic earthquake model. Such combination uses the modified G-R model for magnitude range from M_0 to M_U^{GR} and the CE model from that value onwards. The CE model uses the following magnitude recurrence relationship:

$$\lambda(M) = \lambda_{0CH} \frac{\Phi\left[\frac{M_U - EM}{s}\right] - \Phi\left[\frac{M - EM}{s}\right]}{\Phi\left[\frac{M_U - EM}{s}\right] - \Phi\left[\frac{M_{0CH} - EM}{s}\right]} \qquad \text{(Eq. 2)}$$

Here $\Phi[\cdot]$ is the standard normal cumulative function, M_0 and M_U are the minimum and maximum characteristic magnitudes respectively, and EM and s are parameters defining the distribution of M. EM can be interpreted as the expected value of the characteristic earthquake magnitude and s is its standard deviation. λ_{0CH} is the exceedance rate of magnitude M_0.

In summary, 245 sources use the modified G-R seismicity model whereas 10 sources use the characteristic earthquake one.

The definition of the expected value of the maximum magnitudes (Mmax or M_U) was based on different criteria, depending mostly on the tectonic environment and also considering the maximum observed magnitudes at each source (historical and instrumental). For instance, at crustal sources, the M_U values were set by using the values provided in previous PSHA developed in the region, complemented with some verifications to guarantee that said values were in agreement with the observed magnitudes at each source according to the historical seismicity and, especially in the smaller sources, that according to relationships between M_U and rupture lengths the area of the ruptures could be accommodated within the geometrical boundaries of each source.

2.4 Ground motion prediction equations

To quantify the hazard in terms of ground motion intensity measures, in this case spectral accelerations, a GMPE needs to be assigned to each of the seismic sources. GMPEs are relationships between ground motion intensity measures and magnitude, distance, and other parameters of the source and the site. GMPEs have the form of the schematic plot shown in Figure 2-4.

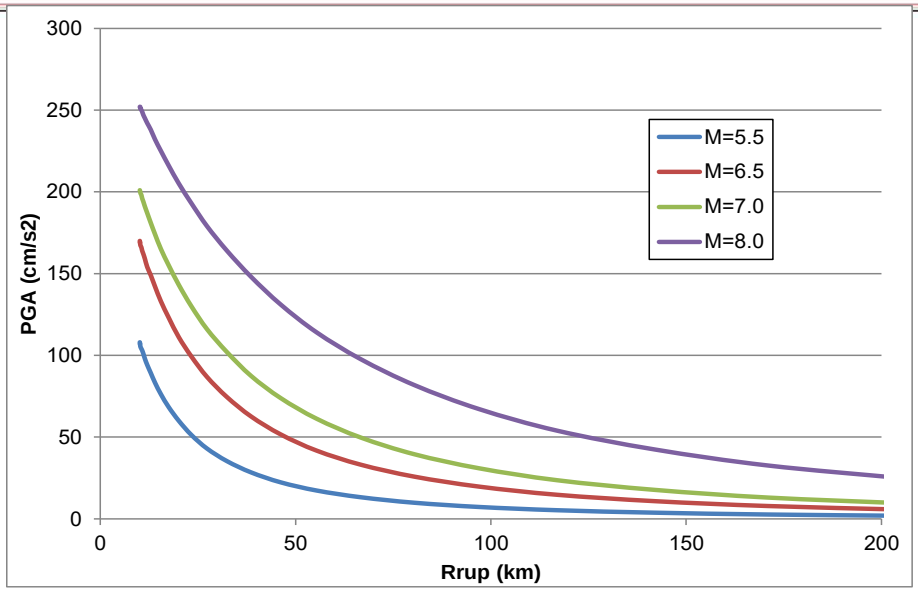

FIGURE 2-4 – SCHEMATIC PLOT FOR PEAK GROUND ACCELERATION AS PREDICTED BY A GENERIC GMPE FOR FOUR DIFFERENT MAGNITUDE EVENTS

A review of previous studies was performed for the region of interest, complemented with the consideration of ground motion attenuation models developed using regional records (for Mexico and the Northern Andes).

Since the number of GMPEs developed for the region is small, a combination of them was assembled for each tectonic environment in the form of a composite (or hybrid) GMPE. These composite GMPEs are a combination of applicable existing ground motion models that use subjective weights in a very similar manner to the logic-tree approach commonly used in PSHA. The hybrid approach, however, is much more efficient than the logic tree approach and, therefore, it is usually preferred in loss estimation models where the computations are very heavy. Table 1 summarizes the GMPEs used for each composite model, classified by region and tectonic environment (Abrahamson et al., 2014; Arroyo et al., 2010; Bernal Granados, 2014; Chiou and Youngs, 2014; Garcia, 2005; Kanno, 2006; Lin and Lee, 2008; Youngs et al., 1997; Zhao, 2006). The soil parameter was set equal to rock conditions for all the GMPEs, since the soil amplification effects were treated in a separate manner, as explained in more detail in the following section.

Table 2-2 **–** GMPEs adopted for each tectonic environment and by region/country

Region/Country	Tectonic environment	Base GMPEs	Weights
Mexico	Crustal	Chiou-Youngs (2014) - Abrahamson et al. (2014) - Zhao et al. (2006)	0.33 - 0.33 - 0.34
	Interface	Zhao et al. (2006) - Youngs et al. (1997) - Lin and Lee (2008) - Arroyo et al. (2010)	0.25 - 0.25 - 0.25 - 0.25
	Intraslab	Zhao et al. (2006) - Youngs et al. (1997) - Kanno et al. (2006) - García et al. (2005)	0.25 - 0.25 - 0.25 - 0.25
Central America and the Caribbean	Interface	Zhao et al. (2006) - Youngs et al. (1997) - Lin and Lee (2008)	0.33 - 0.33 - 0.34
	Intraslab	Zhao et al. (2006) - Youngs et al. (1997) - Kanno et al. (2006)	0.33 - 0.33 - 0.34
	Outer-rise	Chiou-Youngs (2014)	1.0
	Crustal	Chiou-Youngs (2014) - Abrahamson et al. (2014) - Zhao et al. (2006)	0.33 - 0.33 - 0.34
Northern Andes	Interface	Zhao et al. (2006) - Youngs et al. (1997) - Lin and Lee (2008) - Bernal (2014)	0.25 - 0.25 - 0.25 - 0.25
	Intraslab	Zhao et al. (2006) - Youngs et al. (1997) - Kanno et al. (2006) - Bernal (2014)	0.25 - 0.25 - 0.25 - 0.25
	Crustal	Chiou-Youngs (2014) - Abrahamson et al. (2014) - Zhao et al. (2006) - Bernal (2014)	0.25 - 0.25 - 0.25 - 0.25

2.5 Site-effects

Local soil amplification effects were considered in the model by estimating an amplification factor, *AF*, using the methodology proposed by Chiou and Youngs (2014) (CY14). This methodology requires information about the Vs30 parameter (namely the average shear wave velocity in the top 30m of soil),

which was extracted from the USGS site. Vs30 data were available with a 30 arc-seconds resolution level and has coverage of the totality of the area under analysis as shown in Figure 2-5.

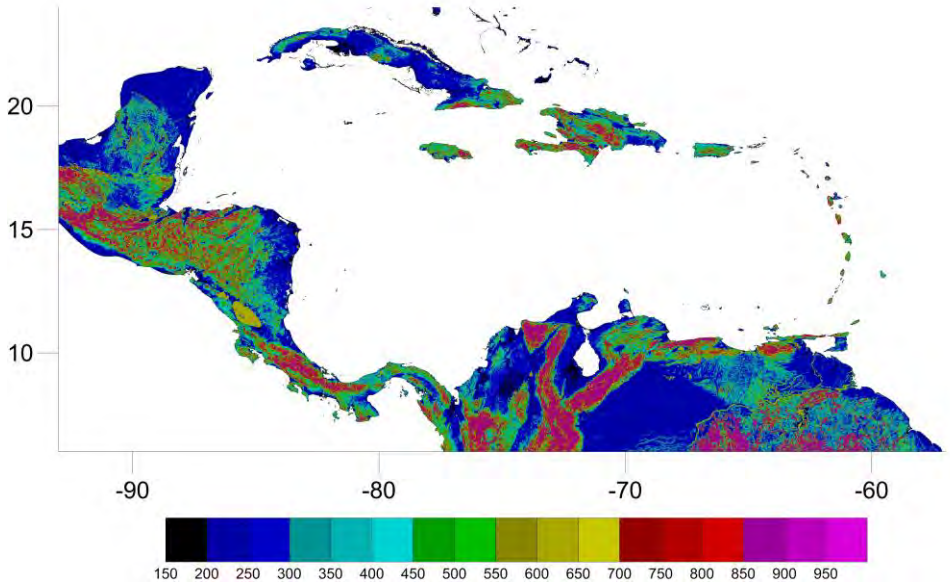

FIGURE 2-5 – VS_{30} VALUES (M/S) FOR THE AREA UNDER STUDY

2.6 Methodology

Once the seismicity parameters were defined for each one of the sources, and appropriate GMPEs were assigned to each source, the seismic hazard at each site of interest can be computed by integrating the contribution of all the earthquakes that may occur in each source. Seismic hazard was computed for uniformly spaced calculation grid of sites with a resolution level compatible with all the PSHA input data. The grid covers the entire domain of study.

More specifically, the seismic hazard can be estimated using the following expression:

$$\nu(a) = \sum_{n=1}^{N} \int_{M_0}^{M_U} -\frac{\partial \lambda}{\partial M} Pr(A > a \mid M, R_i) dM \qquad \text{(Eq. 1)}$$

Where a is the selected seismic intensity, R_i is the distance, N the total number of seismic sources and $Pr(A>a|M,R_i)$ the probability that the selected intensity is exceeded given the magnitude and the distance of the i-th source and the analysis point, R_i.

With equation 1, the hazard intensity exceedance plot (also known as the hazard curve) can be obtained at each computation site and for any given level of probability. For example, Figure 2-6 shows the seismic hazard map for the study area expressed in terms of peak ground acceleration (PGA) on soil for 10% exceedance probability in 50 years (475-year return period, approximately). In addition, Figure 2-7 shows a detail of the Eastern Caribbean zone with the hazard maps in terms of PGA on soil for 40% (left) and 10% (right) exceedance probability in 50 years (100 and 475-year return period, respectively).

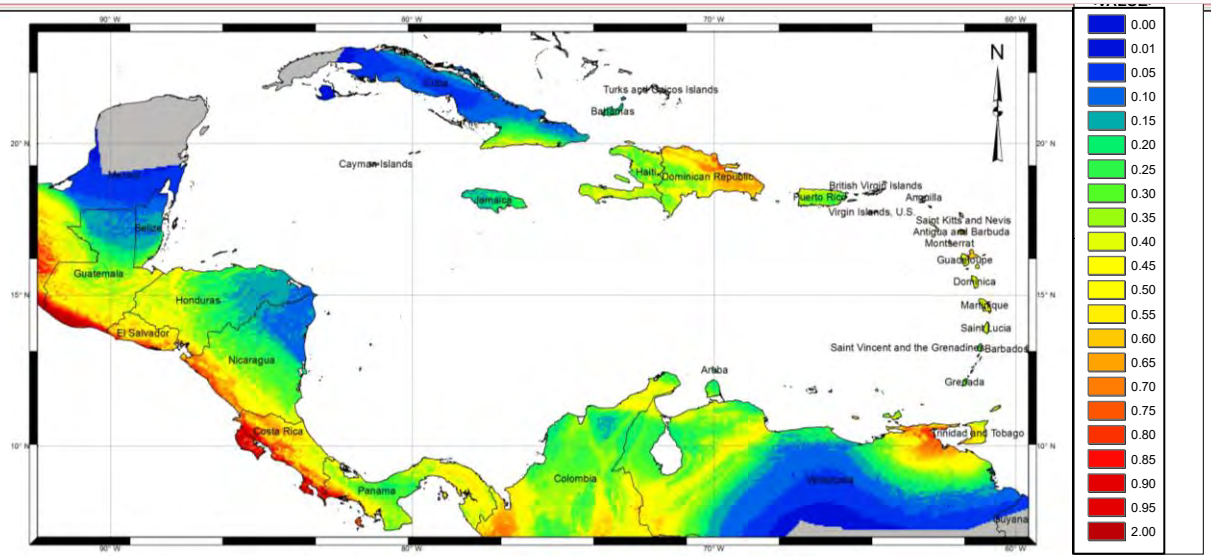

FIGURE 2-6 – SEISMIC HAZARD MAP MAP FOR PGA (IN G) ON SOIL FOR 475-YEAR RETURN PERIOD

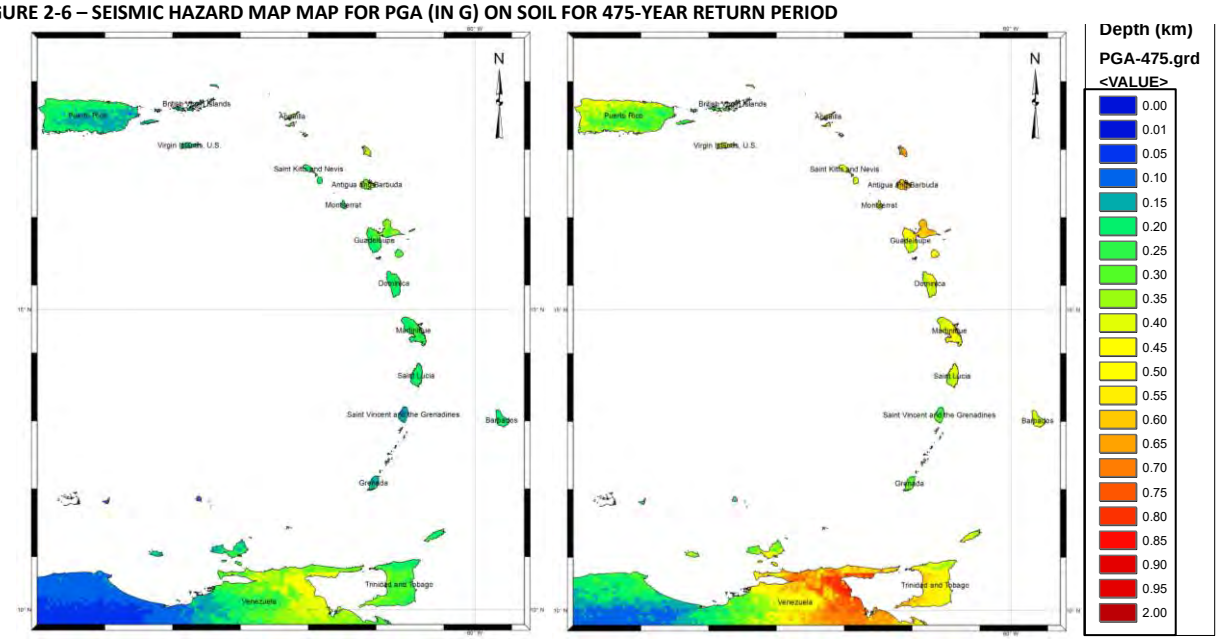

FIGURE 2-7 – SEISMIC HAZARD MAPS FOR PGA (IN G) ON SOIL IN THE CARIBBEAN FOR 100-YEAR (LEFT) FOR 475-YEAR (RIGHT) RETURN PERIOD

In this project, the R-CRISIS software was used to implement the hazard model. R-CRISIS is a worldwide and well-known solution for performing PSHA. The program is the result of more than 30 years of continuous innovations, developments and improvements, providing the most comprehensive, yet easy to use, software suitable for academic and commercial uses. A total of 255 seismic sources are included in the R-CRISIS model. Four correspond to background sources included to consider the occurrence of future events at locations on which no historical earthquake records exist.

2.7 Stochastic event-set

As mentioned in the introduction, the main objective of developing this PSHA is to obtain a stochastic event-set populated by simulated future earthquakes to be used for a fully probabilistic seismic loss assessment study of the assets in these countries. Using all the input data previously described, it is possible to generate a stochastic event-set after the definition of several parameter values.

First of all, a minimum magnitude of 5.0 was selected for the event generation process. Earthquakes with lower magnitudes were deemed to cause losses of negligible amount for the purposes of this model, and are normally excluded by standard CCRIF's policies. After this, 9 magnitude bins between the minimum and the maximum magnitude (which varies from source to source) were sampled. An average spacing of 15km was set in both orthogonal directions for the generation of epicentres of future earthquakes. Events that did not generate a peak ground acceleration exceeding 1 cm/s^2 anywhere in these countries were removed from the event set.

Each event has unique rupture characteristics, an annual occurrence frequency and a probabilistic representation of the footprint associated to the ground motion intensities (spectral accelerations here) caused by that particular event. The footprints are represented by means of the first two statistical moments of the intensity measure at each site, compatible with the assumption of the hazard intensity being a random variable.

Figure 2-8 shows the location of the epicentres of the stochastic events (around 616,000). This figure displays the maximum magnitude of the earthquakes at each location. In order to facilitate the interpretation of the figure, the location of the epicentres associated to the four background sources are not displayed. On the other hand, Figure 2-9 shows an example of a ground motion intensity map (in g) computed for a single scenario using the hazard module of SPHERA.

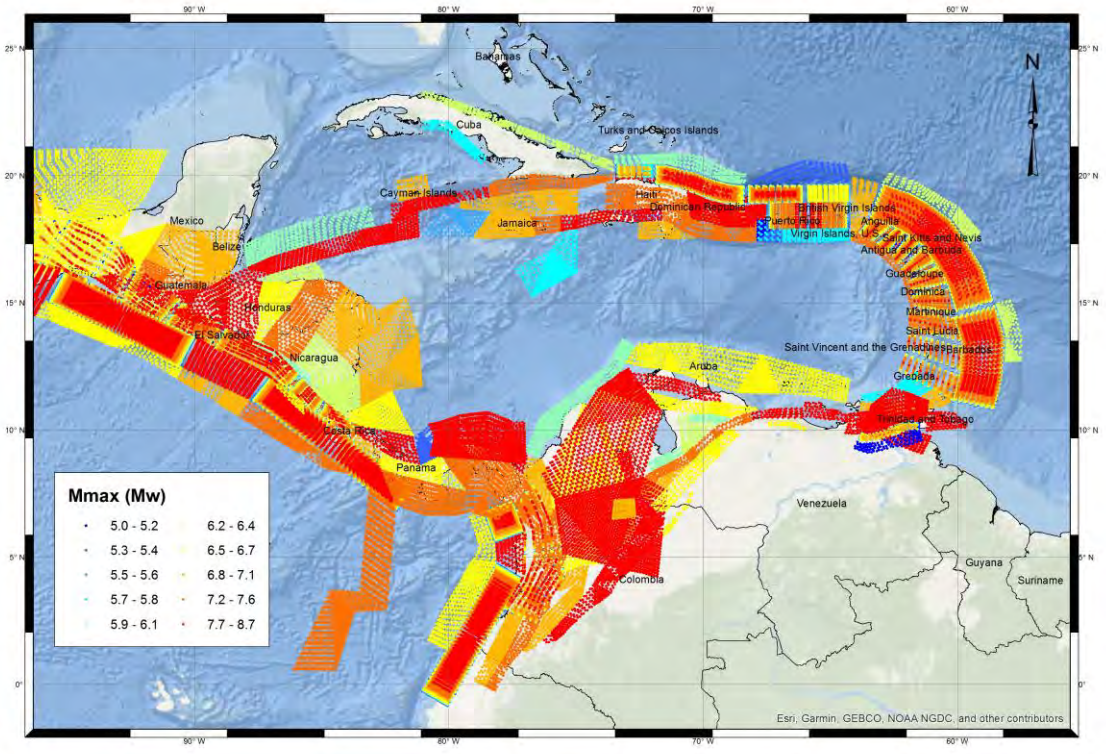

FIGURE 2-8 – EPICENTRES AND MU OF EARTHQUAKES INCLUDED IN THE STOCHASTIC EVENT SET (THOSE ASSOCIATED WITH THE BACKGROUND SOURCES ARE NOT DISPLAYED)

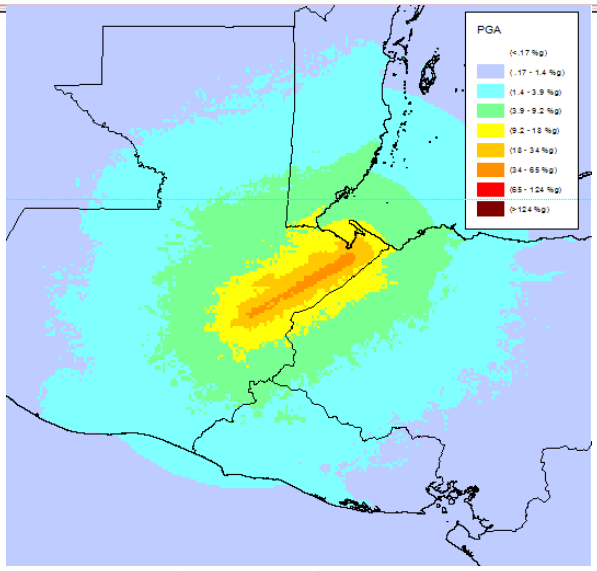

FIGURE 2-9 – EXAMPLE OF GROUND MOTION INTENSITY (HERE PGA IN G) COMPUTED WITH SPHERA FOR ONE SCENARIO

2.8 Validation of hazard results

2.8.1 GROUND MOTION INTENSITY MAP VALIDATION

The results of SPHERA seismic hazard module were compared with the shakemaps developed by the USGS for the following historical earthquakes: Guatemala, 1976 (usp0000ex3); Jamaica, 1993 (usp0005kqb); Tobago, 1997 (usp000810j); El Salvador, 2001 (usp000a9jv), Martinique, 2007 (usp000ftj1) and Haiti, 2010 (usp000h60h). For each of them, the data for PGA were obtained and compared with the PGA values estimated by SPHERA. The SPHERA values were obtained using the strike, dip, rupture shape, rupture aspect ratio and ground motion prediction equation data assigned to each seismic source. For instance, Figure 2-10 shows the comparison between SPHERA and USGS shakemaps for the August 2018 Gulf of Paria earthquake. Details for the other events can be found in the *Earthquake Model Validation Technical Report*.

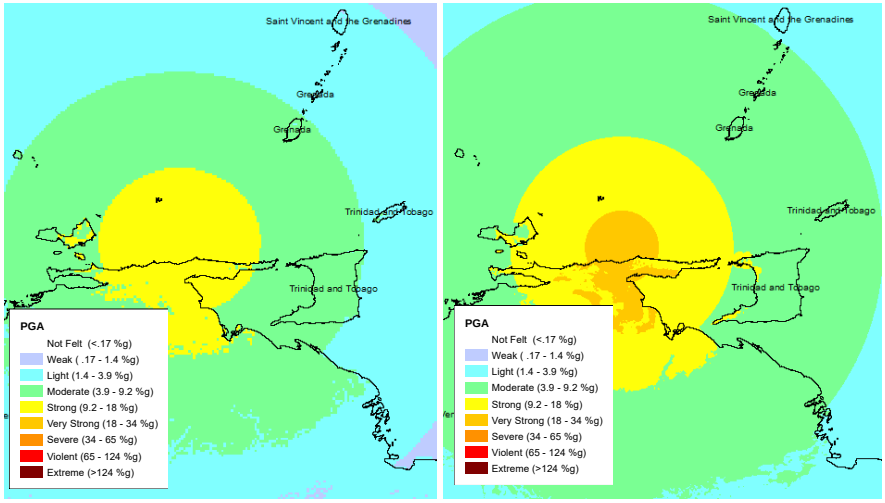

FIGURE 2-10 – COMPARISONS BETWEEN PGA ESTIMATES FOR THE GULF OF PARIA 2018 EARTHQUAKE FROM SPHERA (LEFT) AND FROM USGS (RIGHT)

2.8.2 HAZARD MAP VALIDATION

The SPHERA earthquake model was developed to obtain a large and comprehensive set of hypothetical (stochastic) events that simulate future seismicity in the region. For each event, which has assigned a

frequency of occurrence based on similar events in historical times, the ground motion intensities are then estimated in the affected region. The result of this exercise is a representation of the seismic hazard at each location in the domain of study. The earthquake hazard maps generated with the stochastic catalogue of earthquakes in SPHERA are validated via a comparison with other hazard maps available in the literature.

For facilitating the comparisons, the same colour scales and intensity ranges from the maps available in the literature were also adopted in SPHERA. More specifically, for the Eastern Caribbean Islands, the SPHERA's earthquake hazard maps for rock PGA at 475-year return period were compared against those of the study carried out by Bozzoni et al. (2011) in Figure 2-11.

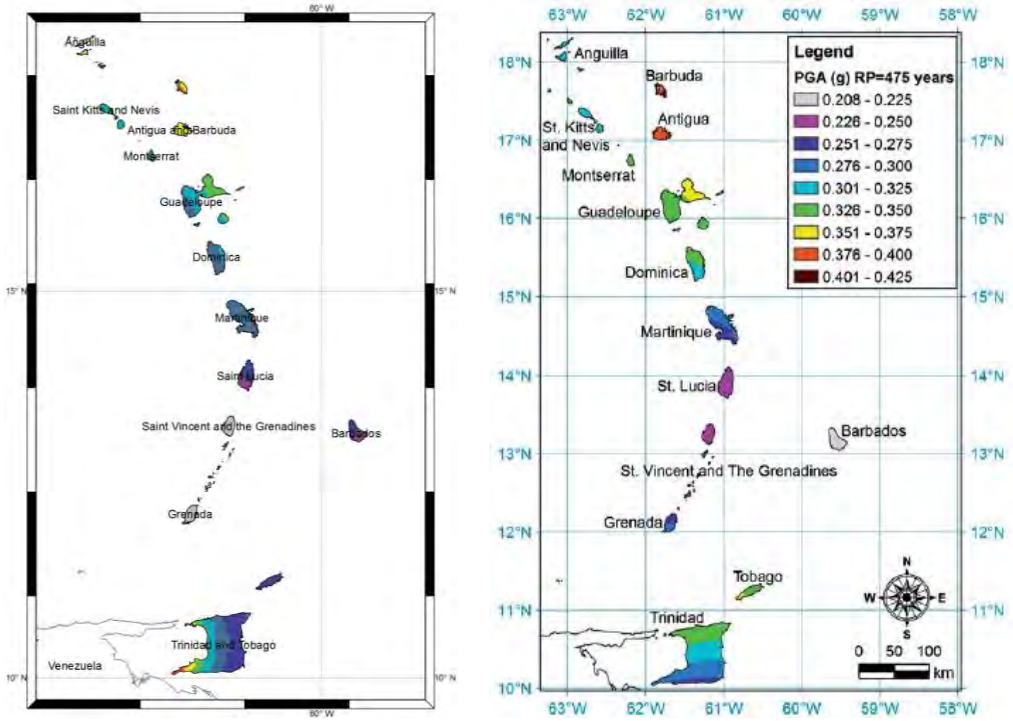

FIGURE 2-11 – COMPARISONS BETWEEN PGA 475-YEAR ESTIMATES FROM SPHERA (LEFT) AND FROM BOZZONI ET AL. (2011) (RIGHT)

For Central America, the SPHERA's earthquake hazard maps were compared against the results of the study carried out by (Benito et al., 2012), in the framework of the RESIS-II project, as shown in Figure 2-12. For Puerto Rico, the U.S. and the U.K. Virgin Islands, the SPHERA's earthquake hazard maps were also compared against the results presented in the study carried out by Mueller et al. (2010). Finally, for the Hispaniola Island, the SPHERA's earthquake hazard maps were compared against the results of the study carried out by Frankel et al. (2011). The comparison shows overall a good agreement between the accelerations estimated by SPHERA and the information in the literature. The complete comparisons can be found in the *Earthquake Model Validation Technical Report*.

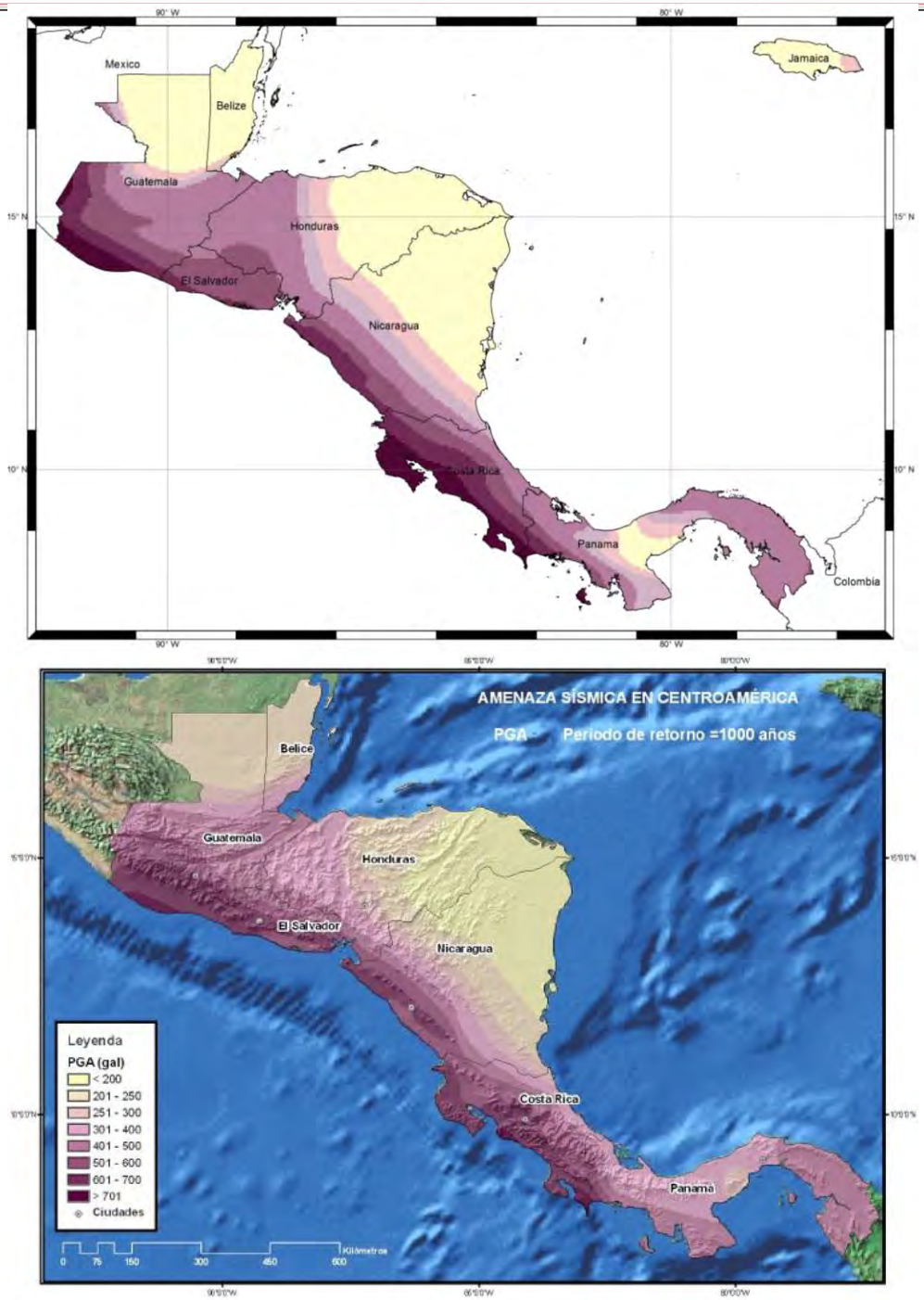

FIGURE 2-12 – COMPARISONS BETWEEN THE 1000-YEAR ROCK PGA ESTIMATES FROM SPHERA (TOP) AND FROM BENITO ET AL. (2012) (BOTTOM)

3 EXPOSURE DATABASE

Any risk model developed for parametric insurance purposes requires as a fundamental component an Industry Exposure Database (IED), which allows estimating the economic losses caused by natural hazards in a credible way. The purpose of this paragraph is to describe the methodology adopted to develop the IED for the SPHERA model version 1.3, covering Central American and Caribbean countries.

The SPHERA exposure dataset leverages several data sources related to the built-up environment and surrounding topography. These datasets include national building census surveys, land use/land cover maps, night time lights imagery, population censuses, Digital Elevation Models (DEMs), and satellite images, among others. The final SPHERA exposure database includes information pertaining to the number of assets of varying lines of business, their spatial location, area, replacement value and physical characteristics, such as construction type and material, and height classification. The SPHERA exposure also includes information pertaining crops in terms of harvested area and total production per year. Table 3-1 summarizes the Lines of Business developed for the final SPHERA exposure database.

Table 3-1 – Lines of Business included in SPHERA exposure database

Lines of Business	
Building Stock	Residential building stock
	Commercial and industrial building stock
	Hotels, education and healthcare building stock
	Public building stock
Infrastructures	Airports
	Ports
	Power facilities
	Road Network
Crops	6 categories of cash crops

The distribution of the exposed assets within each administrative division was performed considering a wide range of datasets, in order to obtain a high accuracy and up-to-date exposure for earthquake and tropical cyclone loss evaluation. The SPHERA database was aggregated at the same level of granularity used in the computation of the effects of earthquakes and tropical cyclones. The granularity was selected as a trade-off between speed of execution of loss assessment and desired precision of the model and it is not identical in every area of a country and across different countries.

The exposed systems are georeferenced and represented in GIS in shapefile and raster formats. They provide estimates of the asset count and replacement cost (or production value for crops) for each structure class (or crop class) at a 30 arc-second resolution (approximately 1 km) for inland areas and at a higher resolution (approximately between 120m and 250m) at coastal areas, in order to achieve a higher precision for storm-surge loss evaluation.

3.1 Methodology and datasets used

3.1.1 IDENTIFICATION OF TYPES OF CONSTRUCTION

The first phase of the IED development consists in the identification of the most common types of construction in each country. The type of construction plays an important role in determining the expected vulnerability of the building stock when subjected to different types of natural disasters. This information was used to assign replacement costs to each building class, or to infer where such type of construction can be found (e.g., natural fibre huts are more likely to be located in rural areas, while reinforced concrete buildings are more likely to be found in urban ones). For this purpose, census data, technical documentation, peer-reviewed literature and reports from the World Housing Encyclopaedia were used to define the building classes present in each country. In addition, a Google image search was performed to identify the common types of construction. An example of this search is illustrated in Figure 3-1 for the building stock in Jamaica.

FIGURE 3-1 – EXAMPLE OF BUILDINGS IN JAMAICA

3.1.2 DATA SOURCES AND ESTIMATION OF ASSET COUNT AND APPRAISAL

The information regarding the residential building stock was collected from the most recent national census survey data. The census data provide the number of dwellings and their distribution in terms of material of the walls and type of dwelling (e.g., house, apartment). The information on dwelling type and wall material was used to classify the census data into the building classes previously identified, and to assign to each asset an appropriate replacement cost. The number of assets was estimated from the number of dwellings reported in the census. Finally, building classes were categorized as either urban or rural.

Commercial, industrial and public building stock were estimated using a different approach, as no useful national dataset (such as national census survey data) currently exists. The first step was to collect statistics regarding the work force in the commercial, industrial and public sectors. The required area per employee for these sectors was consulted when available. With this information, it was possible to calculate the total area for each sector as well as each administrative division. Information about area requirements per employee was unavailable for some countries, and thus proxy data of other countries were used, by applying reduction factors for countries where working conditions are significantly different. Depending on the country, different categories of buildings, related to the size of the assets and their class, were used to distribute the area for each kind of building. A weight was then assigned to each category, based on how common they are in the region and finally the total area for each type of building was divided by the weighted average of the building size assigned to each category in order to calculate the number of assets in each country.

The distribution of educational and healthcare infrastructure was extracted from public datasets (e.g., data from local governments) when these were available. Alternatively, the area for each of these occupancies was calculated following the approach adopted for the other non-residential building stock.

For airports, a global dataset with airport locations is available from OpenFlights. This dataset contains location attributes such as country, ISO code and region. These data were used to assess the relative size of each airport, from large hub to domestic airport.

A global dataset with port locations is available from worldportsource.com. This dataset includes location attributes such as country, longitude and latitude, and also information about port type and size (see Figure 3-2). These data were used to assess the relative size of the ports, from large to small.

FIGURE 3-2 – DISTRIBUTION OF PORTS IN THE CARIBBEAN

The definition of the number of power facilities, source of energy, geographic location and energy generation capacity was performed considering several sources of information, including the Shift Project Data Portal, OpenStreetMap data, World Bank Development Indicators Database, and local literature concerning the evolution of energy generation in each country. In particular, the location was mostly identified using an algorithm that detects elements (e.g., dams, electrical towers, large transformers, wind fields, solar panels) related with the generation of electricity from OpenStreetMap data. Then, each location was crossed with the latest available data concerning energy generation, or statistically attributed based on the most common source of energy in each country. The final dataset was ultimately verified using Google Earth Imagery.

The development of the exposure database for the road network was performed using data from the Digital Chart of the World, OpenStreetMap Data and the Global Roads Open Access Dataset.

The replacement cost for each type of asset was estimated at country basis by using information from national census and local data. In case of unavailability of local information data from international sources were used. Projects or papers such as Pacific Catastrophe Risk Assessment and Financing Initiative (PCRAFI) Risk Assessment Summary Report, U.S. Energy Information Administration website, the Cost of Road Infrastructure in Developing Countries paper by Collier et al., and Hurricane Mitch Preliminary Damage Assessment Report, developed by the US Army Corps of Engineers among others.

3.1.3 SPATIAL DISTRIBUTION OF EXPOSED ASSETS

With the exception of airports, ports and power facilities for which the exact location was known, it was necessary to spatially distribute all other exposed assets within each administrative division. This distribution was performed considering a wide range of datasets that can be grouped in *Earth observation-based* and *Non-Earth observation-based*. In Earth observation-based databases are included *Night time lights layer* (i.e. data representative of light intensity during the night at a 30 arc-second resolution), particularly useful in distributing commercial and industrial stock, as there is a strong correlation between electrification and industrialization, *Digital Elevation Models (DEM)* were used as a proxy for human activity, as urban settlements tend to exist in relatively flat areas (e.g., valleys and coastlines) as opposed to regions with a steep slope (e.g., mountainsides), *satellite imagery* which plays a fundamental role in the mapping of urban density. The remote sensing imagery leveraged for this module was acquired from the optical 'Landsat-8' satellite. Figure 3-3 shows an example of these data for Belize.

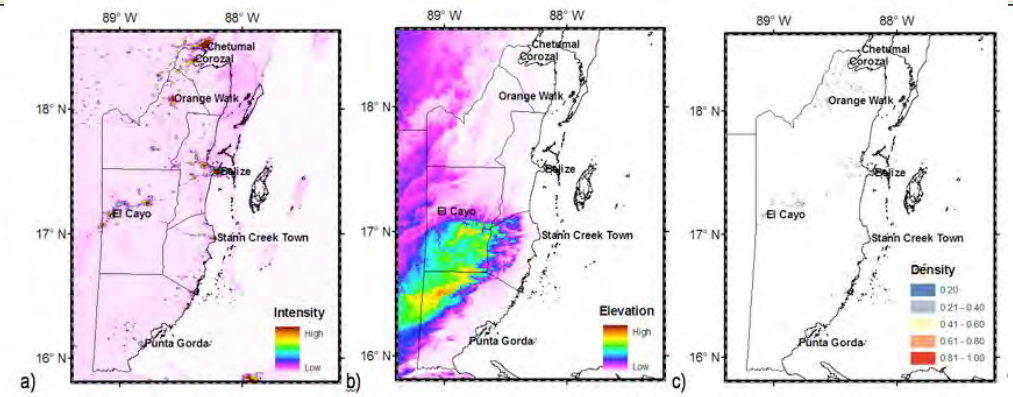

FIGURE 3-3 – A) NIGHT-TIME LIGHTS; B) ELEVATION; AND C) BUILDING DENSITY ACCORDING TO REMOTELY SENSED DATA FOR BELIZE

In Non-earth observation-based datasets are included *land use (LU) maps* which classify the territory of each country according to its use and were used to better estimate the spatial distribution of the SPHERA model's building stock, and to identify areas dedicated to specific types of economic activity; *Roads Datasets* containing the transportation network for each country and used to detect the presence of buildings; *OpenStreetMap (OSM)* which contains a plethora of spatial data such as roads, buildings, land use areas or points of interest; *Rivers and inland water* for detecting areas where no buildings should exist due to the presence of rivers or other inland water bodies (e.g., lakes, lagoons). Figure 3-4 shows an example of the non-earth observation data for Belize.

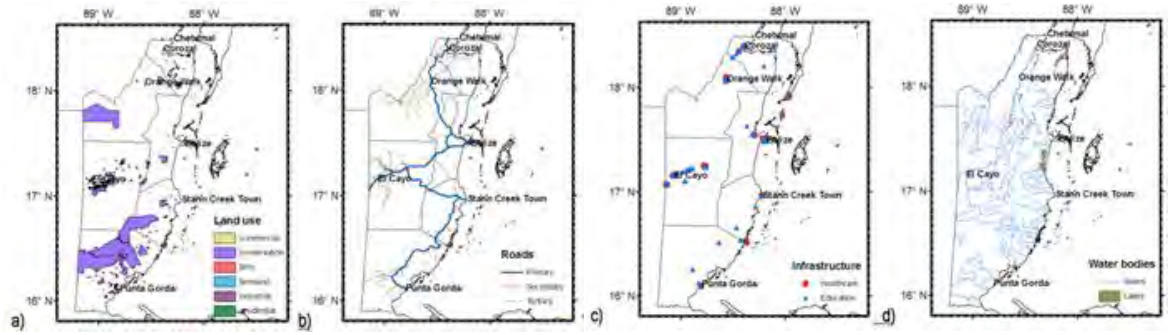

FIGURE 3-4 – A) LAND USE MAPPING; B) TRANSPORTATION NETWORK (ROADS); C) HEALTHCARE AND EDUCATIONAL INFRASTRUCTURE (FROM OSM) AND D) RIVERS AND INLAND WATER BODIES IN BELIZE

3.2 Outputs and validation

This section presents the outcomes of the SPHERA exposure database. It compares the total capital stock of SPHERA countries, and presents examples of how they are distributed between the lines of business. A comparison of key data from SPHERA exposure database is made against the MPRES model (developed by KAC), and UNISDR's GAR15. Finally, some examples are provided to show how the estimated distribution of assets compares with the existing building stock, as observed through satellite imagery. Figure 3-5 shows the total exposure value (without crops) for Group 1 countries.

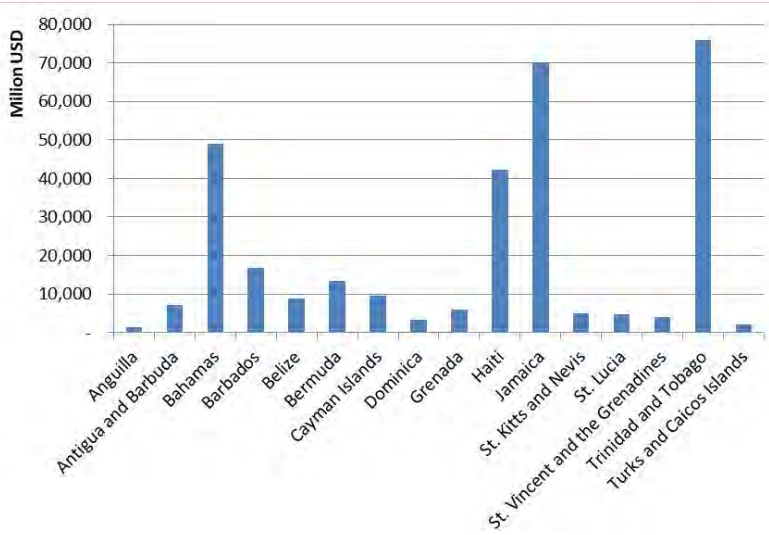

FIGURE 3-5 – COMPARISON OF TOTAL EXPOSURE VALUES FOR GROUP 1 CARIBBEAN COUNTRIES

As explained above, the total number of assets and capital stock (for each building class) are spatially disaggregated leveraging several datasets. An example of the results for Haiti is presented in this section. Figure 3-6 (a) shows the distribution of the total exposed value whereas Figure 3-6 (b) shows the distribution of the exposed value for the residential sector and Figure 3-6 (c) shows the distribution exposed values for roads in Haiti.

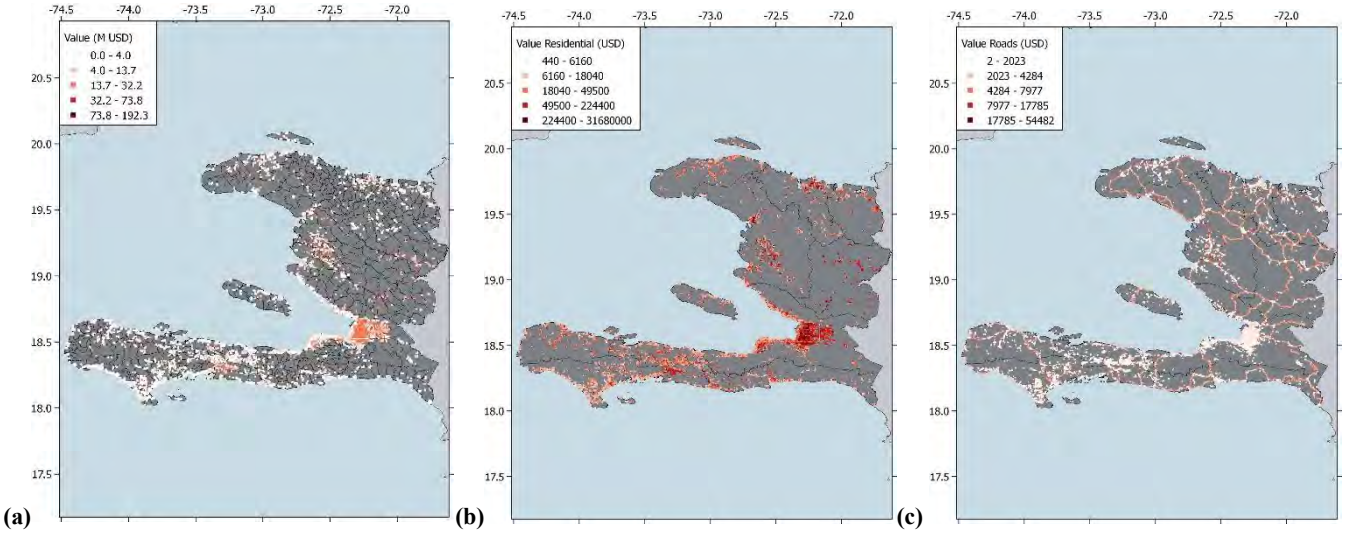

FIGURE 3-6 – (A) DISTRIBUTION OF TOTAL EXPOSED VALUE, (B) RESIDENTIAL EXPOSED VALUE AND (C) ROAD EXPOSED VALUE FOR HAITI

The IED module of SPHERA model was validated against reputable third-party data sources, among which the 2015 Global Assessment Report on Disaster Risk Reduction (GAR15) developed by UNISDR. Figure 3-7 compare the overall exposed value by country derived for the new SPHERA model -with the capital stock value reported in GAR15 and the MPRES (KAC) model. Figure 3-8 shows a comparison of SPHERA, GAR15 and MPRES models with regard to the total replacement cost of the residential sector for Central American countries. Figure 3-9 shows a comparison for the commercial and industrial sectors of group 3 countries. It appears that the SPHERA exposure is in line with the GAR15 values nearly in all the countries.

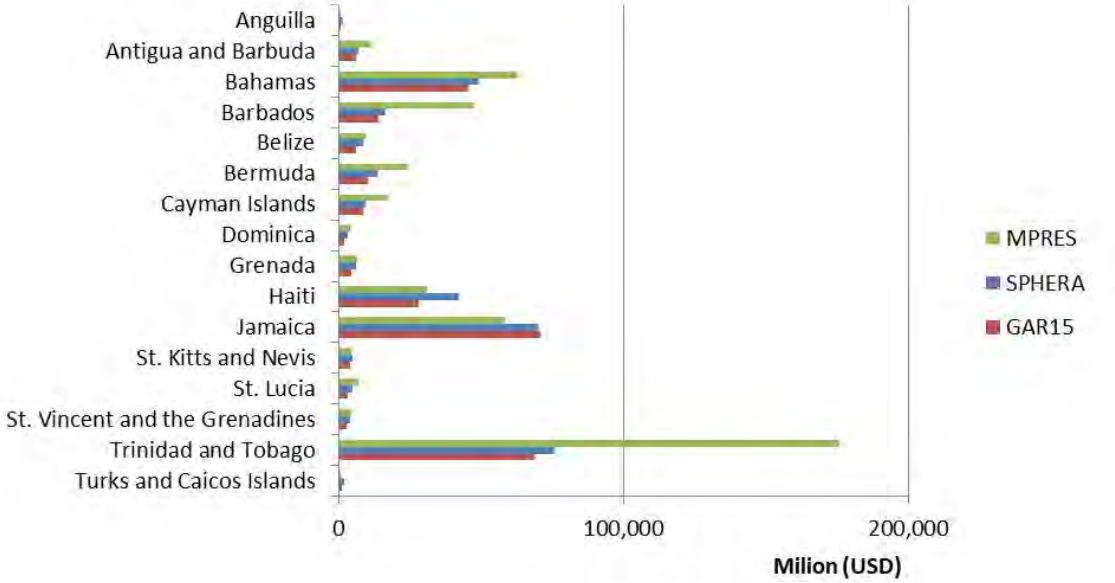

Figure 3-7 – Comparison of the SPHERA exposure (no crops) with MPRES (no Agriculture stock), GAR and XSR2.0 exposure databases for Group 1 countries

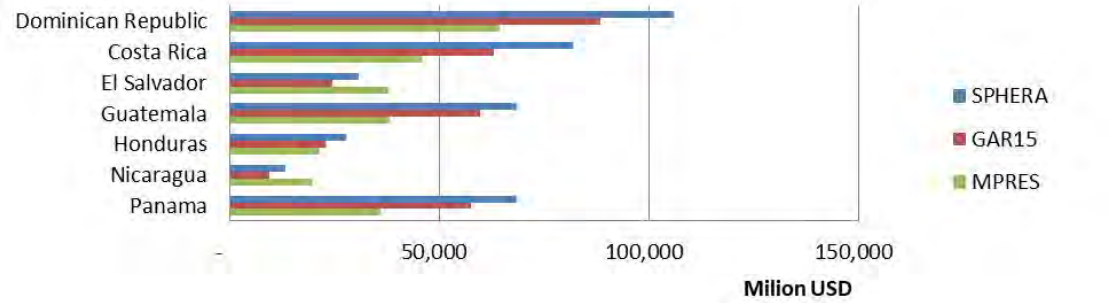

FIGURE 3-8 – COMPARISON OF THE SPHERA RESIDENTIAL EXPOSURE WITH THE MPRES AND GAR RESIDENTIAL EXPOSURE DATABASES FOR GROUP 2 COUNTRIES

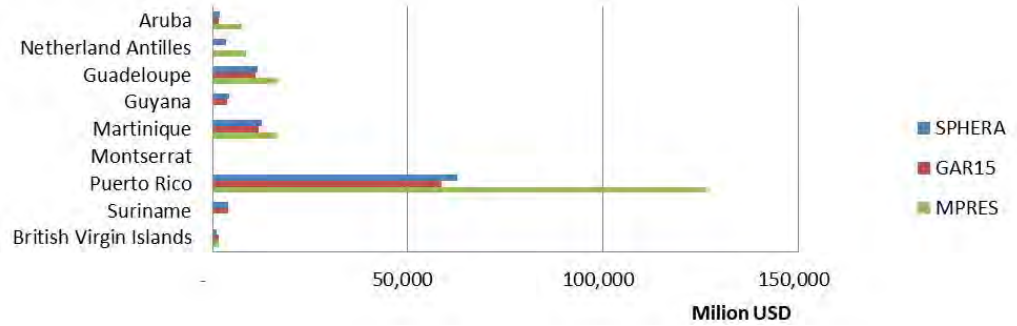

FIGURE 3-9 – COMPARISON OF THE SPHERA COMMERCIAL, HOTEL, RESTAURANT AND INDUSTRIAL EXPOSURE WITH MPRES AND GAR15 COMMERCIAL AND INDUSTRIAL EXPOSURE DATABASES FOR GROUP 3 COUNTRIES

Some other verifications were done to assure the reliability and validity of the obtained SPHERA IED results. Table 3-2 shows the cost per dwelling on GDP per capita, and the number of people per dwelling. Such indicators were used to cross-check the consistency of the results in the region and to verify if the residential exposure depicts a realistic socio-economic condition in the different countries. The results obtained are generally reasonable and the indicators do not show any outlier among the different countries.

Table 3-2 – Socio-economic indicators and conditions used for validation purposes – Group 1 countries

Country	Population (M)	GDP per capita	Ratio (Cost per dwl/Gdp per capita)	Pop per dwl
Anguilla	0.015	21,493	7	3
Antigua and Barbuda	0.105	13,715	13	3
Bahamas	0.391	22,817	11	3
Barbados	0.285	15,429	7	3
Belize	0.367	4,879	6	5
Bermuda	0.065	85,748	4	2
Cayman Islands	0.061	64,105	4	3
Dominica	0.074	7,116	8	2
Grenada	0.107	9,212	10	4
Haiti	10.847	818	11	5
Jamaica	2.881	5,106	11	5
St. Kitts and Nevis	0.055	15,772	10	4
St. Lucia	0.178	7,736	5	4
St. Vincent and the Grenadines	0.11	6,739	7	4
Trinidad and Tobago	1.365	17,322	10	4
Turks and Caicos Islands	0.035	23,615	5	5

Finally, the SPHERA exposure database was validated also in terms of geographic distribution, by comparing it with satellite imagery. Figure 3-10 shows the consistency between the exposure developed for the SPHERA model and satellite images.

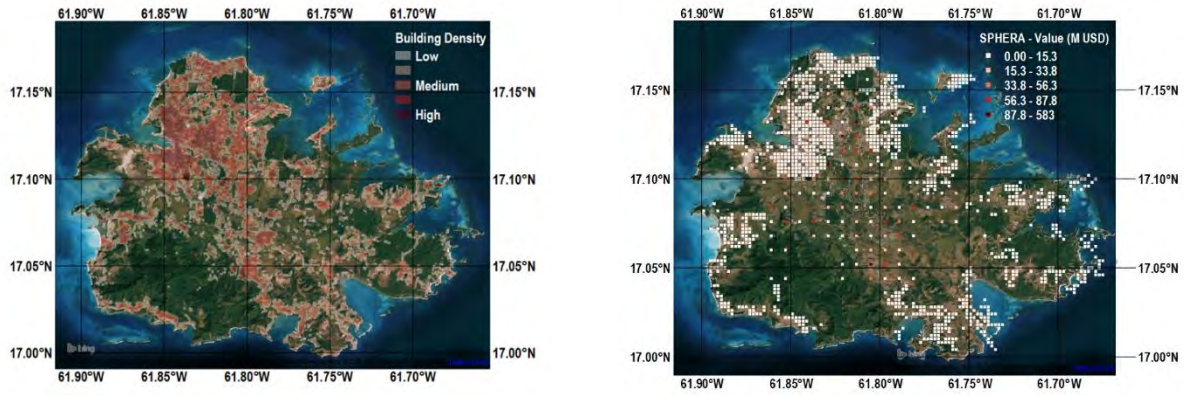

FIGURE 3-10 – (A) ANTIGUA BUILDING DENSITY SATELLITE IMAGE AND (B) SPHERA EXPOSURE DISTRIBUTION IN THE SAME AREA

4 EARTHQUAKE VULNERABILITY

The scope of this section is to describe the earthquake vulnerability modules implemented in the SPHERA model v1.3 for buildings and infrastructure.

The vulnerability model for buildings was developed by means of an analytical procedure that was designed to assess their structural behaviour and their fragility under seismic loading. The use of an analytical methodology allows considering the differences among the several structural typologies and configurations that are common in the Caribbean and Central America. Moreover, it allows accounting for the differences among countries and overcoming the lack of reliable data and scientific studies about the seismic response of buildings in some of the countries covered by the model.

The vulnerability model for infrastructure was derived through a database of fragility and vulnerability functions from the scientific literature. Such functions were used to develop the vulnerability model for the geographic area considered.

4.1 Vulnerability model for buildings

4.1.1 BUILDING TAXONOMY

The development of the vulnerability model for buildings required the definition of a new and updated building taxonomy for the Caribbean and Central America. The definition of building classes was based on an extensive literature review targeting a country-based database of structures. The methodology used in this study accounts for the most common structural typologies in the considered countries. Moreover, it defines a taxonomy based on the parameters that are recognized to have a high influence on the building response under seismic excitation. More specifically, those parameters are: i) structural system configuration, ii) building height (i.e., number of stories), iii) construction material, and iv) design level. The latter is accounted for in the taxonomy that classifies the buildings as "ductile" or "non-ductile". This differentiation reflects, implicitly, the year of construction and, therefore, the building code supposedly adopted for design. A country-by-country investigation allowed assessing the fraction of code-compliant buildings depending on geographic location and age, and the extent to which the adopted regulations are in line with the most recent developments in structural design.

Twenty-five building classes were identified in the exposure model. The definition of those classes is adapted from the GEM taxonomy (Brzev et al., 2013). Tables 4-1 to 4-4 summarize the building classes identified, together with the associated number of stories and a brief description of their structural characteristics.

TABLE 4-1 – BUILDING TAXONOMY FOR REINFORCED CONCRETE CAST-IN-PLACE AND PRE-CAST BUILDINGS.

Class ID	Number of stories	Description
RC+INF+D+LR	1-2	Reinforced concrete infilled frame, ductile, low-rise
RC+INF+D+MR	3-6	Reinforced concrete infilled frame, ductile, mid-rise
RC+INF+D+HR	7+	Reinforced concrete infilled frame, ductile, high-rise
RC+INF+ND+LR	1-2	Reinforced concrete infilled frame, non-ductile, low-rise
RC+INF+ND+MR	3-6	Reinforced concrete infilled frame, non-ductile, mid-rise
RC+INF+ND+HR	7+	Reinforced concrete infilled frame, non-ductile, high-rise
RC+PC+LR	1-2	Pre-cast concrete structure, low-rise
CR+LWAL+LR	1-2	Concrete wall and covintec panel wall structures, low-rise

TABLE 4-2 – BUILDING TAXONOMY FOR MASONRY STRUCTURES (INCLUDING UNKNOWN STRUCTURES).

Class ID	Number of stories	Description
A	1-2	Adobe construction, low-rise
MCF+D+LR	1-2	Confined masonry, ductile, low-rise
MCF+ND+LR	1-2	Confined masonry, non-ductile, low-rise
RM+D+LR	1-2	Reinforced masonry, ductile, low-rise
RM+ND+LR	1-2	Reinforced masonry, non-ductile, low-rise
SM	1-2	Stone masonry, low rise
UFM+LR	1-2	Unreinforced masonry, low-rise
UNK	ND	Unknown and informal construction

TABLE 4-3 – BUILDING TAXONOMY DESCRIPTION FOR WOODEN STRUCTURES

Class ID	Number of stories	Description
WL	1-2	Light wood members, low-rise
WS	1-2	Solid wood members, low-rise
WWD	1-2	Wattle and Daub, low-rise

TABLE 4-4 – BUILDING TAXONOMY FOR STEEL BUILDINGS.

Class ID	Number of stories	Description
S+D+LR	1-2	Steel frame, ductile, low-rise
S+D+MR	3-6	Steel frame, ductile, mid-rise
S+ND+LR	1-2	Steel frame, non-ductile, low-rise
S+ND+MR	3-6	Steel frame, non-ductile, mid-rise
S+INF+D+LR	1-2	Steel frame with masonry infills, ductile, low rise
S+INF+ND+LR	1-2	Steel frame with masonry infills, non-ductile, low rise

4.1.2 METHODOLOGY

Some vulnerability models for the Caribbean and Central America areas, or similar built environments, were already available prior to the inception of this project. However, a series of issues pointed out the need for developing a tailored set of fragility/vulnerability functions. In particular: some of the existing models are too simplistic; most of them underestimate record-to-record variability, uncertainties in the capacity and damage criterion variability; they are not always uniform across different building classes; they are not specific to the characteristics of buildings in Central America and the Caribbean; and they are not specific to the characteristics of the ground motions expected in the region of interest. Nevertheless, the available data were not ignored, but rather used to calibrate and validate the functions obtained herein.

Fragility and vulnerability functions can be derived according to several approaches, namely empirical, analytical, and expert-opinion methods (or a hybrid combination of them). The empirical approach was not considered, mainly because of the lack of building damage/loss and ground motion data in the region of interest. Moreover, even when loss data are available, important limitations still exist, such as: i) post-earthquake damage data are often biased because they are typically collected in the most damaged areas, ii) undamaged structures are usually not included in the dataset and, iii) given that ground motion recordings in the damaged regions are generally not available, relating the level of ground shaking with the observed damage would be a very uncertain exercise. For these reasons, the fragility/vulnerability functions were derived using an analytical approach.

In order to assess the structural performance of the selected case studies and to account for the corresponding uncertainty, an extensive literature review was carried out. For each building class, basic information about a) the elastic or yielding period of vibration, b) the inter-story height, c) the modal participation factor, d) the number of stories, and e) the inter-story drifts for both the yielding and ultimate damage states was collected or inferred from expert judgment. Median capacity curves (in terms of spectral acceleration - Sa - versus spectral displacement - Sd) and their corresponding variance (which allows accounting for building-to-building variability) were then derived for each building class, employing a displacement-based earthquake loss assessment framework (DBELA – Crowley et al. 2004). The median

capacity curves were derived after a comprehensive literature review on the seismic response of the structural types identified in the building taxonomy. For the definition of the capacity curves, priority was given to research studies developed for the countries of study or to scientific works for areas with similar building practices (Villar-Vega et al., 2017). Among the sources considered are: Bal et al., 2008; Crowley, H. and Pinho, 2006; FEMA, 2003; Goda et al., 2014; Oliveira and Navarro, 2010; Tarque et al., 2012; Uchida et al., 2000. Although many of these studies are not strictly related to the region of interest, they are adopted because of similar construction practices and/or structural behaviour.

The building stock quality throughout the considered countries is not homogenous. Consequently, four different vulnerability models were developed, with the objective of representing various levels of vulnerability (i.e., High – VG1, Average – VG2, Low – VG3 and Poor – VG4 building stock quality). Each country was assigned to one of the four classes depending on an analysis of its building stock, on the level of its seismic building code, and on its degree of enforcement (Table 4-5). In particular, in line with this ranking, a set of four capacity curves was developed for each building class of the taxonomy.

Table 4-5 – Vulnerability groups for countries covered by SPHERA model

Vulnerability Group	Countries
VG1 – High Building Stock Quality	Anguilla (AIA), Antigua and Barbuda (ANT), Bahamas (BHS), Barbados (BRB), Bermuda (BMU), Cayman Islands (CYM), St. Kitts and Nevis (KNA), Costa Rica (CRI), Panama (PAN), Guadeloupe (GLP), Martinique (MTQ)
VG2 – Average Building Stock Quality	Dominica (DMA), Grenada (GRD), St. Lucia (LCA), St. Vincent and the Grenadines (VCT), Trinidad and Tobago (TTO), Turks and Caicos Islands (TCA), El Salvador (SLV), Guatemala (GTM), Honduras (HND), Aruba (ABW), Bonaire-Saba-Saint Eustatius (BES), British Virgin Islands (VGB), Curacao (CUW), Dominican Republic (DOM), Puerto Rico (PRI) Sint Maarten (SXM)
VG3 – Low Building Stock Quality	Belize (BLZ), Jamaica (JAM), Nicaragua (NIC), Guyana (GUY), Montserrat (MSR), Suriname (SUR)
VG4 – Poor Building Stock Quality	Haiti (HTI)

Using the GEM OpenQuake Risk Modeler's Toolkit (Silva et al., 2014), a Monte Carlo simulation was performed to produce a synthetic building portfolio based on the median capacity curve (set of capacity curves per building class) allowing, therefore, the propagation of the building-to-building variability in the vulnerability assessment. For each building class, in line with Silva et al. (2014) recommendations, 100 capacity curves were generated achieving statistical convergence within a 5% tolerance (Figure 4-1a).

Each of the 100 capacity curves constituted the backbone of a Single Degree of Freedom system (SDoF) that was later subjected to a set of 294 ground motion records. The set of natural ground motion records was selected to match conditional target spectra (Conditional Spectrum Method by Baker and Cornell, 2005) specific for the region of interest. This approach allows accounting for all the scenarios influencing the seismic hazard in the region of interest by means of the relative contribution established by its disaggregation (Bazzurro and Cornell, 1999).

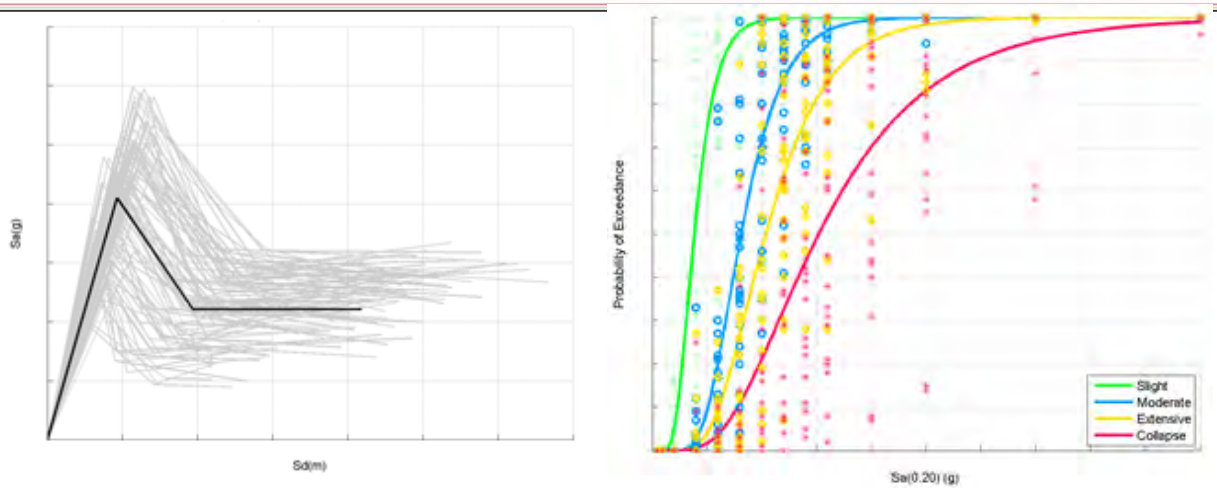

Figure 4-1 – a) Set of synthetic capacity curves and corresponding median for an example capacity curve b) Values of cumulative probability density matrix and associated lognormal fragility curves for one-story stone masonry (SM) building class (medium building quality)

The structural response of each building class and each relative building stock quality group was assessed by means of nonlinear dynamic analysis on 100 single degree of freedom systems. The response obtained from each analysis was used to derive the relationship between ground shaking intensity (Intensity Measure, IM) and structural response (engineering demand parameter, EDP, such as maximum inter-story drift). IM was selected based on the structural dynamic properties of each building class. In particular, the intensity measures considered for the model were spectral accelerations at specified structural periods that are known to correlate well with the structural response and that can be computed directly with all the GMPEs. Then, given a properly defined limit state threshold in terms of EDP, the conditional probability of being in a given damage state or higher was calculated. Finally, the results were fitted using a probability function (e.g. lognormal) obtaining a fragility function (Figure 4-1b).

The vulnerability curves (representing the expected loss for a given level of ground shaking) were later derived combining the fragilities with the so-called consequence function, i.e. damage-to-loss models. The existing damage-to-loss models do not cover all the possible combination of region/country and structural types. Therefore, the consequence functions developed for other regions of the world (Bal et al., 2008; FEMA, 2003; Kappos et al., 2006) were analyzed in order to choose the most suitable for the needs of the current model. For the development of this building vulnerability model an adjusted combination of different consequence function was derived. Such combination was computed considering that the same building damage occurred on similar building types of different countries can be reasonably assumed to cause fairly similar loss ratios.

The main features of the analytical approach followed to derive the vulnerability functions of the SPHERA model are:

1) It accounts for the most important sources of uncertainties, i.e. record-to-record variability and building-to-building variability;
2) it uses ground motions selected to be consistent in terms of hazard with those expected in the region of interest;
3) it propagates the uncertainties at every step of the process;
4) it is based on locally-collected building properties;
5) it provides both damage and loss ratio distributions.

4.1.3 RESULTS

The methodology outlined in the previous section allowed to derive more than 200 vulnerability functions, each specific for a given structural class, building height, design level, and construction quality class.
Figure 4-2 presents the mean vulnerabilities for a particular building typology highlighting the different building stock quality. Figure 4-3 shows the vulnerability curves for different structural typologies that belong to poor quality building stock. The curves were normalized in order to allow their comparison and verify their relative position. The UFM+LR_Sa(0.2s) category was used in all the charts to facilitate the comparison. As can be expected, the adobe structures show the highest propensity to losses while steel and wooden structures appear to be the least vulnerable. Among reinforced concrete structures, the mid-rise non-ductile frames are the most vulnerable ones.

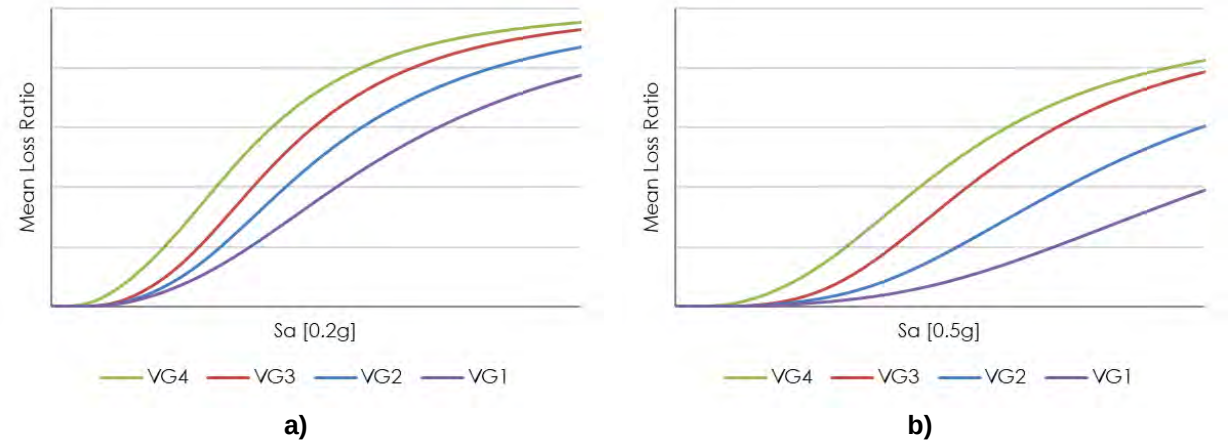

a) **b)**

FIGURE 4-2 – VULNERABILITY CURVES RELATED TO A) UNREINFORCED MASONRY LOW-RISE AND B) REINFORCED CONCRETE LOW-RISE INFILLED FRAMES FOR DIFFERENT QUALITY OF BUILDING STOCK

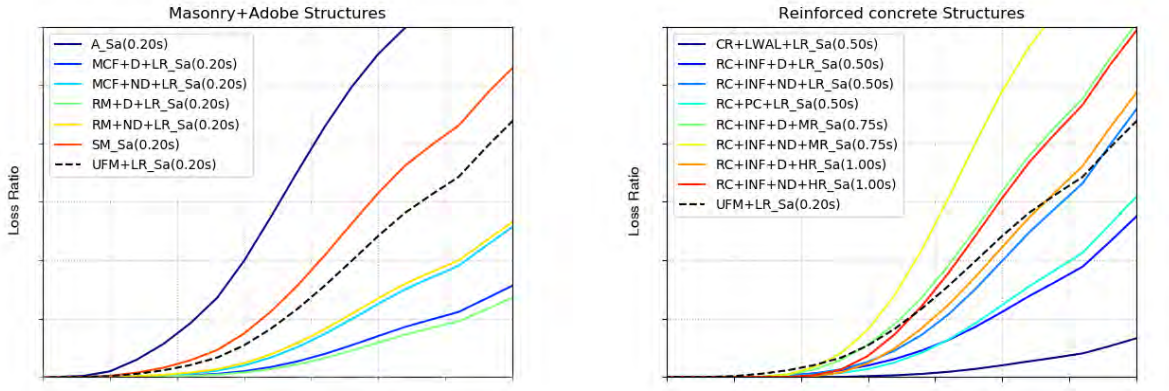

a) **b)**

FIGURE 4-3 – NORMALIZED VULNERABILITY CURVES OF A) ADOBE AND MASONRY STRUCTURES AND B) REINFORCED CONCRETE STRUCTURES BELONGING TO POOR QUALITY BUILDING PORTFOLIO

4.2 Vulnerability model for infrastructures

The vulnerability model for infrastructures was derived constructing a database of fragility and vulnerability functions from the scientific literature. These functions were used to develop the vulnerability model, identifying the main characteristics of the infrastructure in the geographic area considered. It is relevant to note that whilst the general building stock in the Caribbean and Central America differs from that in US and Europe, thus preventing from using the same building vulnerability functions, the infrastructures (e.g. energy generation facilities, ports, airports, etc.) of the Caribbean and

Central American countries are quite similar to the U.S.A. and EU ones in terms of technology and constructions practices. Therefore, the same vulnerability functions are applicable.

The development of fragility functions for infrastructures requires a comprehensive understanding of the different components that integrate each facility. As an example, ports are formed by different components, such as waterfront structures, cranes and cargo handling equipment, fuel facilities, and warehouses, which have different response to seismic action and, therefore, should be treated separately. The vulnerability functions for the different components were derived and then combined to obtain a single function for the whole infrastructure considering the relative economic value of each component type.

An infrastructure taxonomy was defined in order to properly represent the vulnerability of the different infrastructures depending on their main characteristics. Table 4-6 summarizes the infrastructure classes defined together with the data sources considered to construct their fragility/vulnerability functions.

Table 4-6 – Vulnerability classes for infrastructures

Infrastructure Type	Infrastructure Classes	Sources
Power Plants	Gas/Oil Power Plant Coal Power Plant Biomass Power Plant Waste Power Plant Geothermal Power Plant Wind Power Plant Solar Power Plant Hydroelectric Power Plant	(Associates, 2013; Dueñas-Osorio et al., 2007; FEMA, 2003; Ghanaat et al., 2012; Giovinazzi and King, 2009; Hwang and Huo, 1998; Lin and Adams, 2008; USSD, 2009)
Roads	Primary Road Secondary Road Other Roads	(FEMA, 2003; Giovinazzi and King, 2009; Kaynia et al., 2011)
Airports	Airport	(FEMA, 2003)
Ports	Port	(FEMA, 2003; Kakderi and Pitilakis, 2010)

Figure 4-4 shows the mean vulnerabilities for different infrastructure classes. The comparison shows that roads are the less vulnerable infrastructures, this is because their damage is usually correlated with the permanent ground deformation (PGD) and not with peak values of acceleration and depends on likelihood of occurrence of rarer phenomena like liquefaction, landslides and surface fault rupture. On contrary, oil power plants are among the most vulnerable infrastructures given the high damageability of their main components to ground accelerations.

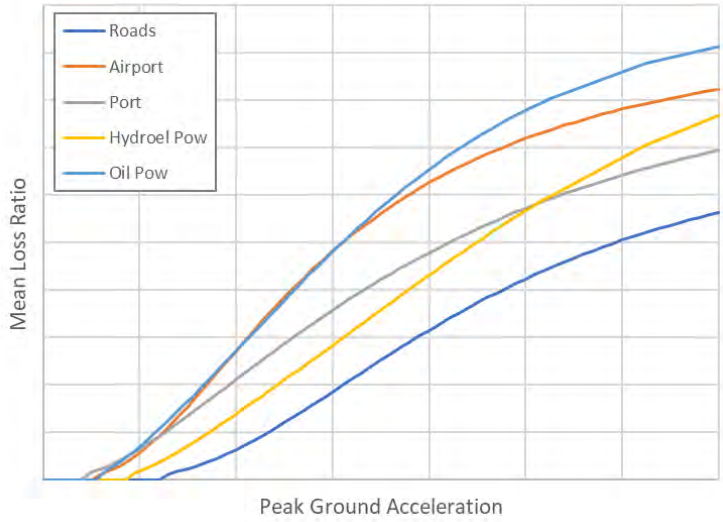

FIGURE 4-4 – COMPARISON OF AVERAGE INFRASTRUCTURE VULNERABILITY CURVES

5 EARTHQUAKE RISK RESULTS

A probabilistic analysis of earthquake risk is intended to estimate the distribution of the probability of losses for a group of exposed assets over a given period of time, as a consequence of the occurrence of future events. This analysis needs to rationally integrate all the uncertainties existing in different parts of the process. The basic question that a probabilistic analysis attempts to answer is: given that there are assets exposed to the effects of earthquakes, how often will losses over a certain value occur?

Given that the frequency of catastrophic events is particularly low, it is not possible to answer this question by analysing the short history of past events. This means that we must develop probabilistic models such as the one described here.

The procedure for probabilistic calculation is therefore an evaluation of losses that will affect a group of exposed assets during each of the scenarios which collectively describe the hazard, and then probabilistically integrating the results obtained using the frequency of occurrence of each scenario.
This chapter describes the methodology used for long-term seismic risk assessment in the Caribbean and Central America. The aim of the long-term seismic risk assessment is to evaluate economic losses due to earthquakes over a sufficiently long time period and to produce the tools needed for the design of a parametric insurance product (event loss tables, exceedance probability curves, etc.) for the countries considered in this study. The “long-term” term refers to the characterization of the economic losses due to earthquakes based on the historical information available, integrated with a stochastically-generated catalogue of seismic events.

Figure 5-1 depicts the general framework of a loss assessment methodology, where a loss module combines the outputs of the hazard, the exposure and the vulnerability modules to derive estimates of the economic losses induced by natural disasters such as earthquakes.
This chapter is structured in the following way:

- The first section describes the approach followed to derive the seismic hazard module.
- The second section describes the methodology implemented for the computation of the losses given a specific level of hazard, using the vulnerability functions and the exposure databases specifically developed for the region.

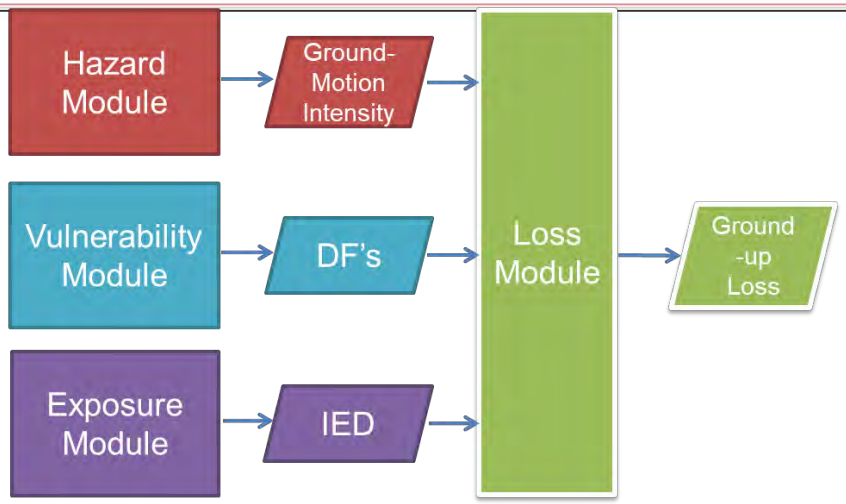

FIGURE 5-1 – FLOWCHART OF THE RISK ASSESSMENT METHODOLOGY

5.1 Risk assessment methodology

The loss module determines the economic losses in all the countries in the IED for each of the possible future events in the stochastic event set. The economic losses for each exposed asset are computed by convolving the ground motion intensity measure distribution at the site with the corresponding damage function. This operation provides a distribution of the mean damage ratio (i.e., repair cost divided by the asset replacement cost). Then, the mean damage ratio is multiplied by the total value of the asset to obtain the distribution of losses for the asset caused by that earthquake. The total loss for each event is then obtained summing up the losses for all the exposed assets. Given that each event has an annual probability of occurrence, the losses for all the scenarios in the stochastic event set can be combined to provide a probabilistic estimate of possible future losses of any amount induced by earthquakes in each country.

The final risk for a set of assets (e.g., the building stock and infrastructure inventory of a country) is usually described in terms of a so-called exceedance probability curve of losses, which provides the annual frequency (or probability) of exceedance of different loss values. The annual loss exceedance rate can be calculated using the following equation:

$$v(p) = \sum_{i=1}^{N} \Pr(P > p \mid Event_i) \cdot F_A(Event_i) \qquad \text{(Eq. 2)}$$

In equation 2, which is one of the many ways the total probability theorem can adopt, *v(p)* is the loss exceedance rate of loss *p*, and $F_A(Event\ i)$ is the annual frequency of occurrence of the *Event i*, while *Pr(P>p(Event i)* is the probability that the loss will be higher than *p,* given that the i^{th} event has occurred. The sum in the equation is made for all potentially damaging events (*N*) included in the stochastic event set. The inverse of the annual rate of the loss corresponds to its expected return period. The loss exceedance curve contains all the necessary information for describing the process of loss occurrence considering the associated uncertainties in the analysis process.

The loss *p* in equation 2 is the sum of the losses that occur to all the assets exposed. The following should be borne in mind:

- The loss *p* is an uncertain quantity whose value, given the occurrence of an event, cannot be precisely known. Therefore, it must be treated as a random variable with a given distribution.

- The loss *p* is calculated as the sum of the losses that occur to each of the exposed assets. All the losses in the sum are correlated random variables since they were caused by the same earthquake and to similar assets.

The approach to derive the loss exceedance curve is the following:

1. For a given event, the probability distribution of losses is determined for each of the assets exposed;
2. Based on the probability distribution of the losses of each asset, the probability distribution of the sum of these losses is computed, considering the correlation between the loss at different sites;
3. Once the probability distribution of the total loss is determined for the event, the probability that the loss exceeds a given value *p* is calculated;
4. The probability determined in (3), multiplied by the annual frequency of occurrence of the event, is the contribution of the event to the rate of exceedance of the loss *p.*

The above calculation repeated for all the events in the stochastic set yields the loss exceedance curve.

5.1.1 TREATMENT OF UNCERTAINTIES

As discussed in the previous sections, the loss computed in a group of exposed assets during a given event is an uncertain quantity, which should be treated as a random variable. Such uncertainty is a combination of several uncertainties, which are all considered in the methodology implemented in the SPHERA model. The model considers the uncertainty in the occurrence of possible future events, the uncertainty related to the estimation of the ground motion intensities caused by an event (via a GMPE) and the uncertainty in the evaluation of damage (and thus of the repair cost) given a certain level of ground motion. Moreover, the model includes a direct evaluation of epistemic uncertainty using a logic tree approach to compute the ground motion fields with different GMPEs.

The probability distribution of the losses due to an earthquake is computed by first determining the distribution of the ground motion intensity at each site and then evaluating the probability distribution of the loss given the level of ground motion. This is a standard approach that simplifies the problem of assessing the loss distribution by dividing it into two steps. This is the methodology that was followed in the development of the SPHERA model. The probability of exceeding the loss *p*, given that an event occurs, is thus expressed as follows:

$$\Pr(P > p \mid Event_i) = \int_I \Pr(P > p \mid I) \cdot f(I \mid Event) dI \qquad \text{(Eq. 3)}$$

In this equation 3, Pr(*P>p*|*I*), P is the probability that the loss will exceed the value *p* given that the local ground motion intensity was *I.* This term represents the vulnerability model and the uncertainty associated with the evaluation of the repair cost given a certain value of ground motion. The term *f(I|Event)* is the probability density function of the ground motion intensity, conditional on the occurrence of the event. This term represents the evaluation of the ground motion, which is uncertain, given the occurrence of an earthquake by means of the GMPE. The probability distribution of the ground motion intensity includes the aleatory uncertainty associated to the use of a GMPE and the epistemic uncertainty due to the use of more than one GMPE to assess the ground motion intensity.

5.1.2 LOSS ASSESSMENT OUTPUTS

The SPHERA model is designed to provide all the loss metrics needed for the design of a parametric insurance product. The main outputs of the long-term seismic risk assessment are the event loss tables (ELTs). The model provides an ELT for each of the countries included in the analysis domain (in some cases the ELTs are provided also for sub-regions within a country, like in the case of The Bahamas), Such a table reports, for each event included in the stochastic event set, the expected value and the corresponding

uncertainty of the economic loss together with its annual frequency of occurrence. The ELTs can then be used to derive the loss exceedance curve (LEC) as previously described. Such a curve contains all the information required to characterize the process of occurrence of losses and is used to the design parametric insurance policies operated by the CCRIF LPC. Figure 5-2 shows an example of a loss exceedance curve derived with SPHERA for Jamaica and Nicaragua.

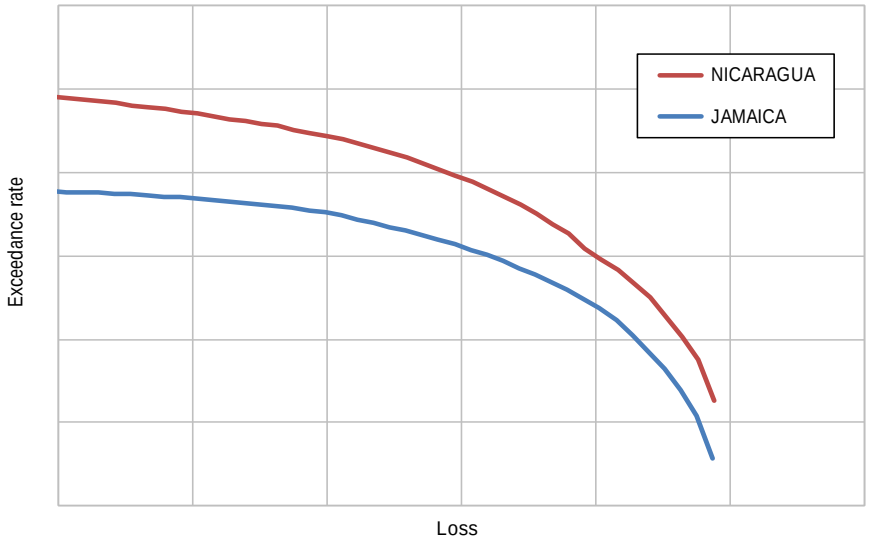

FIGURE 5-2 LOSS EXCEEDANCE CURVES DERIVED WITH SPHERA FOR NICARAGUA AND JAMAICA

Also, and for communication purposes, it is convenient to use specific loss metrics rather than the whole loss exceedance curve. The SPHERA model also provides the two specific risk estimators that are commonly used to communicate risk:

Average annual loss (AAL): this is the expected value of the annual loss. It is an important quantity, since it indicates, assuming that stationarity of the earthquake process holds, the amount of money that is needed every year on average to repair assets due to earthquakes. Therefore, in a simple insurance system, the annual expected loss would be the pure annual premium. Figures 5-3 and 5-4 show the geographic distribution of the AALs computed for unreinforced masonry low-rise buildings in the Caribbean and the Central America regions.

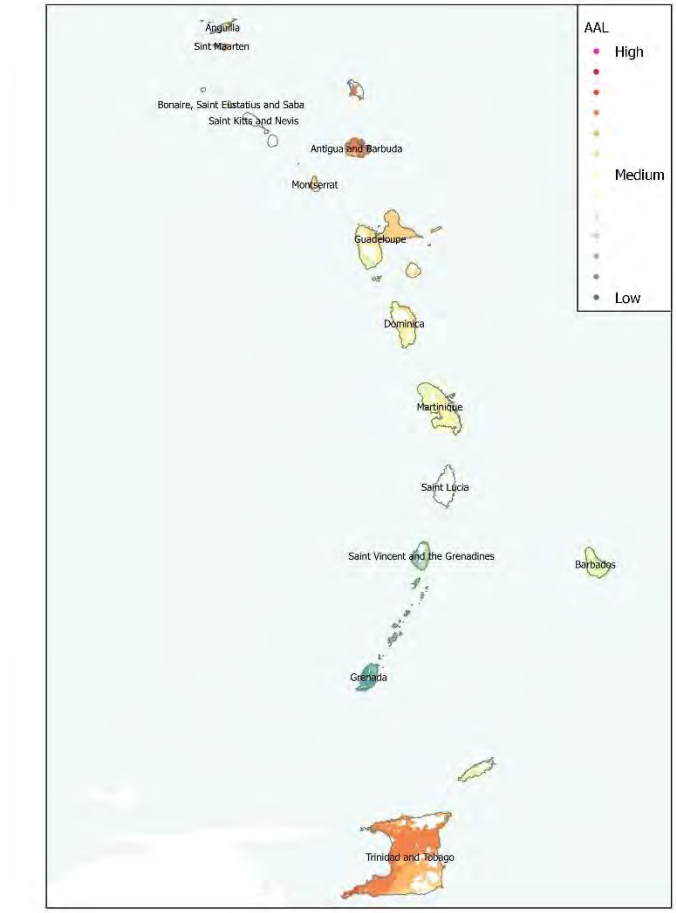

FIGURE 5-3 GEOGRAPHICAL DISTRIBUTION OF AALS (PER MILLE) FOR UNREINFORCED MASONRY LOW-RISE BUILDINGS IN THE CARIBBEAN REGION

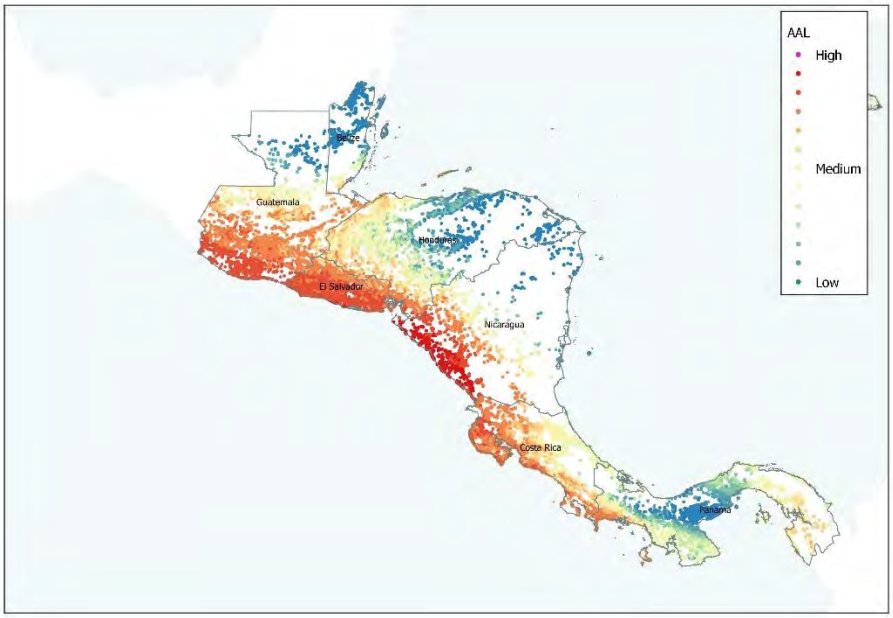

FIGURE 5-4 GEOGRAPHIC DISTRIBUTION OF AALS (PER MILLE) FOR UNREINFORCED MASONRY LOW-RISE BUILDINGS IN THE CENTRAL AMERICA REGION

Probable maximum loss (PML): This is a loss, which does not occur frequently, and it is associated with a quite long return period (or, alternatively, a low exceedance rate). The return period of reference, however, varies. The PML for a given return period is the inverse of *v(p).* Thus, upon definition of a set of representative return periods (e.g. 10, 25, 50, 100, 250, 500, 1000 and 2500 years), the PML values corresponding to such periods and their uncertainty can be read off from the loss exceedance curves.

5.2 Loss validation

5.2.1 VALIDATION OF MODELLED LOSSES AGAINST REPORTED LOSSES

For model validation purposes, reported losses have been collected from a wide variety of sources. These sources include EM-DAT (www.emdat.be/database), ECLAC (https://www.cepal.org/en/datos-y-estadisticas), USGS (https://earthquake.usgs.gov/earthquakes/search), NOAA, GEM Earthquake Consequences Database (https://gemecd.org/), AON (http://catastropheinsight.aonbenfield.com), MunichRe (http://natcatservice.munichre.com/), SwissRe (www.sigma-explorer.com/) and local sources. It should be noted that reported values are, in general, highly uncertain both in the amount and in the content of losses reported (e.g., are only direct losses included? Losses for which lines of business? Are losses to building contents included? Are business interruption losses included? Are emergency costs included?) and often discordant among different and highly reputable sources. Despite being these factors an important source of uncertainty, it is not possible to disaggregate the amounts reported to compare only the direct losses caused by the earthquakes (which is what both MPRES and SPHERA models estimate). In addition to the above-mentioned issues, it should also be noted that seismic instrumentation prior to the 1970s was neither extensive nor as accurate as it is today. Hence, for many events of the first half of the 20th century, even the basic information such as location, depth and event magnitudes of earthquakes, usually varies between different studies and authors.

Reported losses are available for 25 major events in the region, at country scale, since 1907, as shown in Table 5-1 together with the modelled losses by SPHERA. Figure 5-6 shows a graphical comparison of the reported and modelled losses SPHERA. Reported losses in Table 5-2 correspond to the chosen *best reported value*, for each event (see Annex 1 for more details).

Table 5-1 – Comparison of reported and modelled losses for 25 historical earthquakes

Date (YY/MM/DD)	M_w	Depth (km)	Country	SPHERA losses (M USD)	Reported losses (M USD)
1907/01/14	6.5	25	Jamaica	915	715
1931/03/31	6.1	15	Nicaragua	581	524
1951/05/06	6.2	10	El Salvador	214	215
1952/10/27	6.2	25	Haiti	89	180
1965/05/03	5.9	15	El Salvador	265	267
1968/01/04	4.8	5	Nicaragua	10	14
1972/12/23	6.3	10	Nicaragua	1,373	3,471
1973/04/14	6.5	33	Costa Rica	29	1
1976/02/04	7.5	25	Guatemala	3,596	3,307
1982/06/19	7.3	50	Guatemala	19	13
1983/04/03	6.8	20	Costa Rica	86	2
1986/10/10	5.7	7	El Salvador	872	1,478
1990/12/22	6.0	15	Costa Rica	78	38
1991/04/22	7.6	10	Costa Rica	1,108	902
1992/09/02	7.6	30	Nicaragua	48	43
1997/04/22	5.9	25	Trinidad and Tobago	16	37
2001/01/13	7.7	56	El Salvador	1,246	1,141
2001/02/13	6.6	20	El Salvador	185	251
2009/01/08	6.2	20	Costa Rica	141	141
2009/05/28	7.3	20	Honduras	43	42
2010/01/12	7.0	13	Haiti	3,902	4,661
2012/09/05	7.6	30	Costa Rica	209	97
2012/11/07	7.4	21	Guatemala	105	107
2014/04/10	6.1	10	Nicaragua	10	3
2014/07/07	6.9	53	Guatemala	26	25

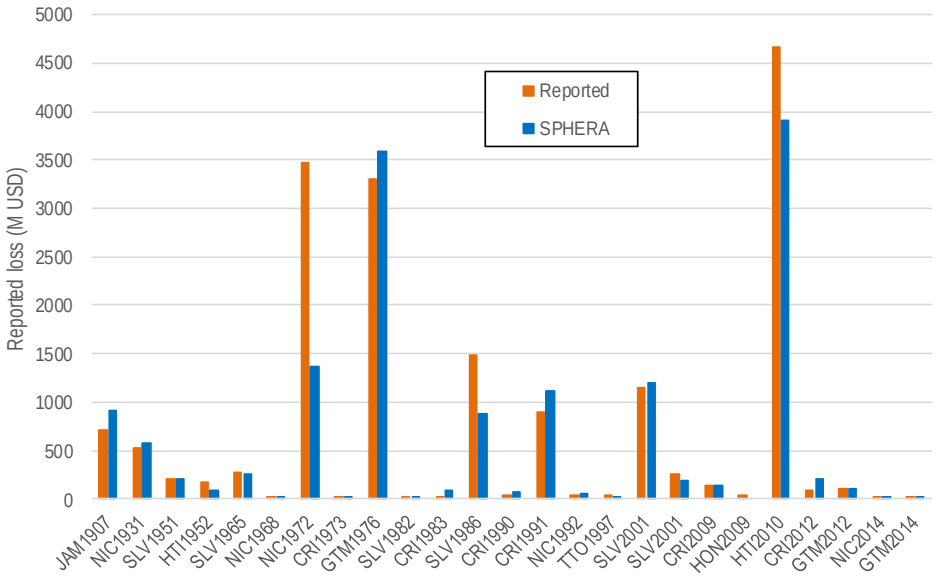

FIGURE 5-5 COMPARISON OF REPORTED AND MODELLED LOSSES FOR 25 EVENTS WITH COUNTRY SCALE REPORTS IN THE REGION OF STUDY

In addition, Figure 5-7 shows the scatter of the modelled losses by SPHERA with respect to the reported ones. From the figure, it can be stated that SPHERA provides accurate results for most of the events. In addition to this plot, logarithmic standard deviations for losses estimated by SPHERA were calculated (for events with losses higher than 10 M USD) obtaining a result of 0.42. It is worth noting that for large events that caused important damages and losses such as the Guatemala 1976, Costa Rica 1991 and Haiti 2010, SPHERA shows a remarkably accurate behaviour.

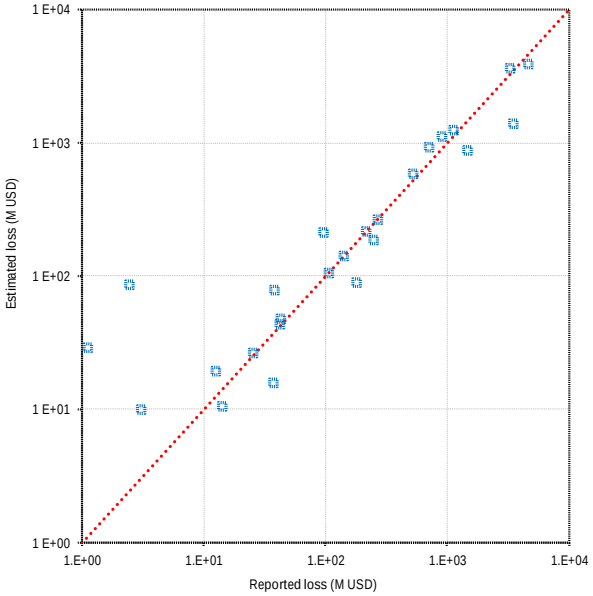

FIGURE 5-6 SCATTERPLOT OF REPORTED LOSSES AND THE ONES MODELLED BY SPHERA FOR HISTORICAL EVENTS

Finally, Figure 5-8 shows the return period of the losses for the 25 earthquakes of Table 5-2 according to the long-term earthquake risk estimations by SPHERA.

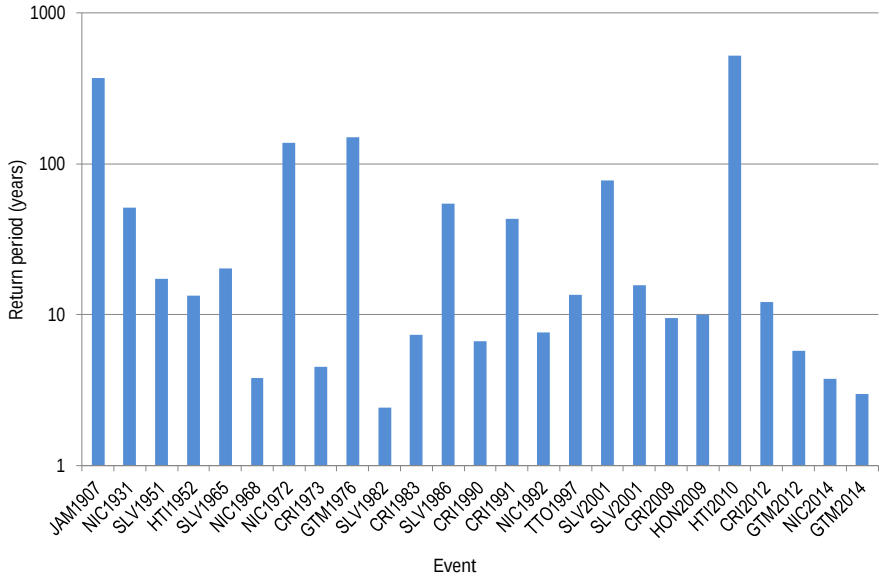

FIGURE 5-7 – LOSS RETURN PERIOD FOR THE MODELLED LOSSES BY SPHERA FOR 25 HISTORICAL EVENTS

5.2.2 VALIDATION OF THE STOCHASTIC CATALOGUE

An additional validation was made in form of a comparison between the loss exceedance probability curves obtained from the historical events and the ones obtained from the stochastic events for countries with seismic activity. A good match means that the synthetic catalogue is able to reproduce correctly the occurrence and intensity of historical earthquakes. Of course, some discrepancies are to be expected due to the vagaries of the short time window observed vis-à-vis the more stable, long-term view of the risk provided by the exceedance probability curve. Results for all countries show a very good fit and the details can be found in the *Earthquake Validation Technical Report*. As an example, Figures 5-9 and 5-10 show the results of the comparison of the historical and stochastic exceedance rates for Costa Rica and Trinidad and Tobago, respectively.

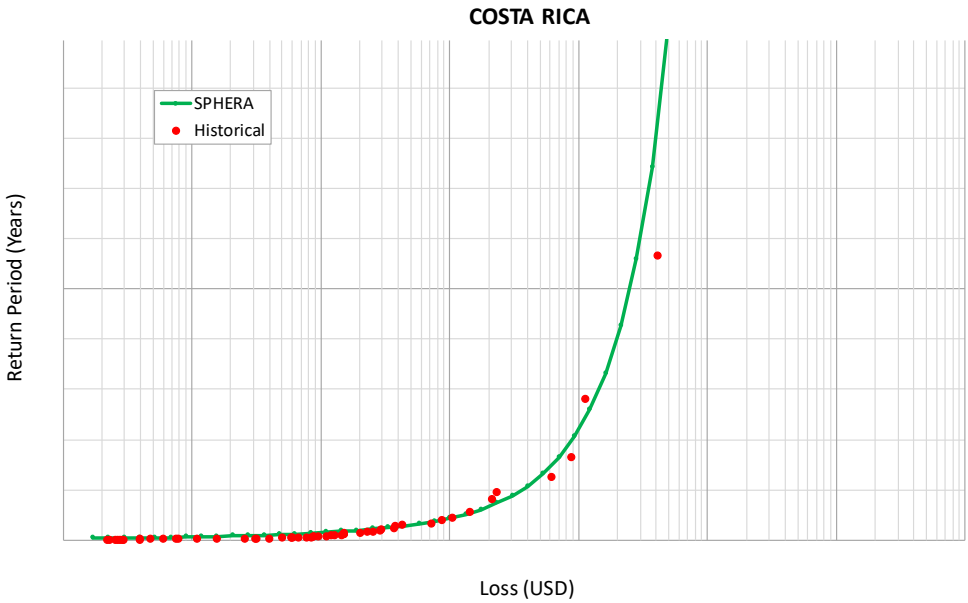

FIGURE 5-8 – EXCEEDANCE RATE OF HISTORICAL AND STOCHASTIC CATALOGUES FOR COSTA RICA

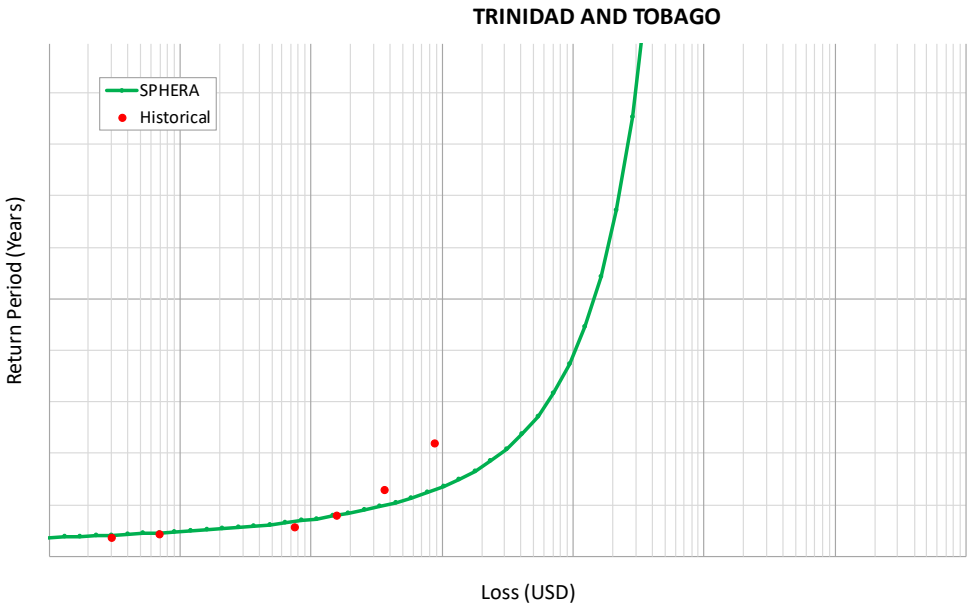

FIGURE 5-9 – EXCEEDANCE RATE OF HISTORICAL AND STOCHASTIC CATALOGUES FOR TRINIDAD AND TOBAGO

6 POST-EVENT LOSS ASSESSMENT

This final chapter describes the methodology used for the near-real time seismic risk assessment in the Caribbean and Central America. The aim of the real-time seismic risk assessment is to evaluate economic losses due to a single earthquake, with the aim of computing whether a payout is due or not, depending on the policy parameters computed in the long-term risk assessment, for the countries considered in this study. The "near-real time" term refers to the characterization of the economic losses due to a single earthquake that has occurred shortly before the beginning of the loss computation.
This chapter is structured in the following way:

- The first section describes how the hazard module is modified for real-time assessment
- The second section describes how the computation of the losses is carried out for a single scenario using the exposure and vulnerability modules

6.1 Hazard footprint generation

The generation of the seismic ground motion intensities has a fundamental role in the post-event rapid loss estimation process. This stage requires the use of some basic data, but also the use of a probabilistic approach which has to be compatible with the framework previously used for the estimation of the physical losses (which is also fully probabilistic).

The seismic ground motion intensity measures need to be well correlated with the damage to exposed assets. In this project, spectral accelerations associated to fundamental periods that range between 0.0s (PGA) and 1.0s were used. All the ground motion intensities generated within this stage must be compatible with the assumptions made during the development of the probabilistic seismic hazard analysis (PSHA) for the study area. This means that the same hazard model components must be used (for example, associated ground motion prediction equations, aspect ratios, and shapes for the ruptures, among others). As a consequence, each future earthquake that occurs within the study area is associated to one (and only one) seismic source of the PSHA model.

Although the USGS seismic hazard intensity maps (shakemaps) are usually a reliable source of information to be used in a rapid loss assessment procedure, they have some drawbacks and cannot be used "as is"

for the purposes of this model. First of all, the pricing process was based on the stochastic event set generated from the R-CRISIS model with around 616,000 stochastic events, which at the same time makes use of a set of assumptions regarding rupture shapes, aspect ratios, rupture orientations (strike and dip values) and attenuation patterns for the seismic waves. The 616,000 ShakeMaps are simply not provided by the USGS. Even if they were, there would not be a consistency between pre- and post-event loss calculations. Another important reason for not using directly the USGS ShakeMaps is the lack of availability for all the spectral ordinates that we utilized in the vulnerability model to estimate building damage from ground motion intensity. To date, the only spectral ordinates reported by the USGS ShakeMaps are 0.0s (PGA), 0.3s, 1.0s and 3.0s (and the last is not available for all earthquakes).

The near-real time loss assessment module of SPHERA relies on a reputable third-party data source to define the main parameters of an earthquake almost immediately after its occurrence. This is the USGS database of real-time earthquake data. The USGS assigns a unique identifier to each event. The identifier allows associating each event with parameters such as its magnitude (M_W), location and depth, as well as, for most of events with moderate-to-high magnitude ($M_W > 5.5$), the moment tensor data. This last parameter allows a more precise identification of the fault plane and modelling of the rupture needed to estimate the ground motion field.

The reported location and hypocentre depth for each event are not only relevant in terms of estimating the event-to-site distance needed in the GMPE but also to identify, in some cases, the seismic source of the hazard model that could have generated such an event. In our model, a geographical overlapping of two or more seismic sources (e.g. a crustal and an intraslab one) is possible, although with different depths. In order to establish which seismic source an earthquake is associated to, a depth range was defined for each of the sources. This was done based on the geometric characteristics and the information included in the historical earthquake catalogue. These ranges allow defining a unique volume, which represents the spatial domain of each of the seismic sources.

A validation of the result with the information of the depth of the event (as reported by the USGS) is also made. Once each event is assigned to a unique seismic source, the process for the generation of seismic hazard intensities makes use of the same assumptions in terms of aspect ratios, rupture shapes and GMPMs used in the PSHA.

Once the earthquake is assigned to a unique seismic source it is not yet defined which fault plane did generate it. If the USGS provides the moment tensor solution for the event, there is information there about two possible nodal (fault) planes and not just one. Hence, a set of rules was developed to choose the most appropriate rupture plane from the two orthogonal ones supported by the tensor solution.
First, each of the 251 seismic sources included in the PSHA model was associated with a set of attributes such as a base azimuth (estimated, when possible, using a statistical procedure based on information contained in the GMTC catalogue), rupture shape (elliptical or rectangular), aspect ratio and associated hybrid GMPM (as per the PSHA model). Additionally, sources where strike-slip mechanisms are predominant were identified, given that this type of rupture mechanisms affects the geographical distribution of the earthquake ground motion intensities. The rules defined allow selecting among the two possible fault planes through the comparison of their strike, dip and rake angles with the base attributes of the source identified.

In the cases in which the rules defined do not allow a clear selection of one of the two possible fault planes or when the moment tensor solution is not provided by the USGS, the geometry of the rupture is modelled using the same approach followed the long-term hazard assessment.

Once the rupture geometry is defined, the ground motion intensity field is computed considering the hybrid GMPE corresponding to the seismic source that was identified for the event.

Earthquakes may occur, although rarely, outside of the defined limits of any of the seismic sources defined in the area under analysis. In those cases, the event is assigned to a background source, using a particular rule for the selection of the fault plane and assuming an elliptical rupture with aspect ratio equal to 1.0. The GMPE assigned to this type of source is then used to estimate the ground motion intensity footprint.

6.2 Loss assessment methodology

When the loss assessment is performed for a single event, equation 2 can be used considering that now *N* takes a value equal to 1 while at the same time, the frequency of occurrence, F_A is set to 1.0. It must be noted, however, that the parametric insurance practice requires that a single number, not a probability distribution, be assigned to the modeled losses. For this purpose, we use the expected value of the loss.

7 REFERENCES

Abrahamson, N.A., Silva, W.J., Kamai, R., 2014. Summary of the ASK14 Ground Motion Relation for Active Crustal Regions. Earthq. Spectra 30, 1025–1055. doi:10.1193/070913EQS198M

Arroyo, D., García, D., Ordaz, M., Mora, M.A., Singh, S.K., 2010. Strong ground-motion relations for Mexican interplate earthquakes. J. Seismol. 14, 769–785. doi:10.1007/s10950-010-9200-0

Associates, J.R.B.&, 2013. Methodology for evaluating the potential for multiple dam failures due to seismic events.

Bal, İ.E., Crowley, H., Pinho, R., Gülay, F.G., 2008. Detailed assessment of structural characteristics of Turkish RC building stock for loss assessment models. Soil Dyn. Earthq. Eng. 28, 914–932. doi:10.1016/j.soildyn.2007.10.005

Bazzurro, P., Cornell, C.A., 1999. Disaggregation of seismic hazard. Bull. Seismol. Soc. Am. 89, 501–520.

Benito, M.B., Lindholm, C., Camacho, E., Climent, A., Marroquin, G., Molina, E., Rojas, W., Escobar, J.J., Talavera, E., Alvarado, G.E., Torres, Y., 2012. A New Evaluation of Seismic Hazard for the Central America Region. Bull. Seismol. Soc. Am. 102, 504–523. doi:10.1785/0120110015

Bernal Granados, G.A., 2014. Metodología para la modelación, cálculo y calibración de parámetros de la amenaza sísmica para la evaluación probabilista del riesgo. Universitat Politècnica de Catalunya.

Bozzoni, F., Corigliano, M., Lai, C.G., Salazar, W., Scandella, L., Zuccolo, E., Latchman, J., Lynch, L., Robertson, R., 2011. Probabilistic Seismic Hazard Assessment at the Eastern Caribbean Islands. Bull. Seismol. Soc. Am. 101, 2499–2521. doi:10.1785/0120100208

Brzev, S., Scawthorn, C., Charleson, A.W., Allen, L., Greene, M., Jaiswal, K., Silva, V., 2013. GEM Building Taxonomy (Version 2.0) (No. 2013-02). GEM Foundation.

Chiou, B.S.-J., Youngs, R.R., 2014. Update of the Chiou and Youngs NGA Model for the Average Horizontal Component of Peak Ground Motion and Response Spectra. Earthq. Spectra 30, 1117–1153. doi:10.1193/072813EQS219M

Cornell, C.A., 1968. Engineering seismic risk analysis. Bull. Seismol. Soc. Am. 58, 1583–1606.

Crowley, H. and Pinho, R., 2006. Simplified equations for estimating the period of vibration of existing buildings., in: First European Conference on Earthquake Engineering and Seismology. pp. 11–22.

Dueñas-Osorio, L., Craig, J.I., Goodno, B.J., 2007. Seismic response of critical interdependent networks. Earthq. Eng. Struct. Dyn. 36, 285–306. doi:10.1002/eqe.626

Engdahl, E., Villasenor, A., 2002. Engdahl, E. and Villasenor, A., 2002. Global seismicity: 1900–1999, international handbook of earthquake and engineering seismology 81A.

Esteva, L., 1970. Regionalización sísmica de México para fines de ingeniería. Instituto de Ingeniería, Universidad Nacional Autónoma de México.

FEMA, 2003. Federal Emergency Management Agency. HAZUS-MH Technical Manual.

Frankel, A., Harmsen, S., Mueller, C., Calais, E., Haase, J., 2011. Seismic Hazard Maps for Haiti. Earthq. Spectra 27, S23–S41. doi:10.1193/1.3631016

Garcia, D., 2005. Inslab Earthquakes of Central Mexico: Peak Ground-Motion Parameters and Response Spectra. Bull. Seismol. Soc. Am. 95, 2272–2282. doi:10.1785/0120050072

Gardner, J.K., Knopoff, L., 1974. Is the sequence of earthquakes in Southern California, with aftershocks removed, Poissonian? Bull. Seismol. Soc. Am. 64, 1363–1367.

Ghanaat, Y., Patev, R., Chudgar, A., 2012. Seismic fragility analysis of concrete gravity dams, in: Proceedings of the 15th World Conference on Earthquake Engineering, Lisbon, Portugal.

Giovinazzi, S., King, A., 2009. Estimating seismic impacts on lifelines: an international review for RiskScape, in: NZSEE Conference, Christchurch, New Zealand.

Goda, K., Yasuda, T., Mori, N., 2014. Sensitivity of Tsunami Profile and Inundation Modeling Considering Stochastic Earthquake Slips, in: Vulnerability, Uncertainty, and Risk. American Society of Civil Engineers, Reston, VA, pp. 2780–2790. doi:10.1061/9780784413609.280

Hwang, H.H., Huo, J.R., 1998. Seismic fragility analysis of electric substation equipment and structures. Probabilistic Eng. Mech. 13, 107–116.

Kakderi, K., Pitilakis, K., 2010. Deliverable 3.9—Fragility Functions for Harbor Elements, SYNER-G Project.

Kanno, T., 2006. A New Attenuation Relation for Strong Ground Motion in Japan Based on Recorded Data. Bull. Seismol. Soc. Am. 96, 879–897. doi:10.1785/0120050138

Kappos, A.J., Panagopoulos, G., Panagiotopoulos, C., Penelis, G., 2006. A hybrid method for the vulnerability assessment of R/C and URM buildings. Bull. Earthq. Eng. 4, 391–413. doi:10.1007/s10518-006-9023-0

Kaynia, A.M., Mayoral, J.M., Johansson, J., Argyroudis, S., Pitilakis, K., Anastasiadis, A., 2011. Fragility functions for roadway system elements. SYNER-G Project Deliverable, 3(7).

Lin, L., Adams, J., 2008. Seismic vulnerability and prioritization ranking of dams in Canada, in: Proceedings of the 14th World Conference on Earthquake Engineering, Beijing, China.

Lin, P.-S., Lee, C.-T., 2008. Ground-Motion Attenuation Relationships for Subduction-Zone Earthquakes in Northeastern Taiwan. Bull. Seismol. Soc. Am. 98, 220–240. doi:10.1785/0120060002

Mueller, C., Frankel, A., Petersen, M., Leyendecker, E., 2010. New Seismic Hazard Maps for Puerto Rico and the U.S. Virgin Islands. Earthq. Spectra 26, 169–185. doi:10.1193/1.3277667

Oliveira, C.S., Navarro, M., 2010. Fundamental periods of vibration of RC buildings in Portugal from in-situ experimental and numerical techniques. Bull. Earthq. Eng. 8, 609–642. doi:10.1007/s10518-009-9162-1

Silva, V., Crowley, H., Yepes, C., Pinho, R., 2014. Silva, V., Crowley, H., Yepes, C. and Pinho, R., 2014, July. Presentation of the OpenQuake-engine, an open source software for seismic hazard and risk assessment, in: Proceedings of the 10th US National Conference on Earthquake Engineering, Anchorage, Alaska.

Storchak, D.A., Di Giacomo, D., Bondár, I., Engdahl, E.R., Harris, J., Lee, W.H., Villaseñor, A., Bormann, 2013. Public release of the ISC–GEM global instrumental earthquake catalogue (1900–2009). Seismol. Res. Lett. 84, 810–815.

Tarque, N., Crowley, H., Pinho, R., Varum, H., 2012. Displacement-Based Fragility Curves for Seismic Assessment of Adobe Buildings in Cusco, Peru. Earthq. Spectra 28, 759–794. doi:10.1193/1.4000001

Tinti, S., Mulargia, F., 1985. An improved method for the analysis of the completeness of a seismic catalogue. Lett. Al Nuovo Cim. Ser. 2 42, 21–27. doi:10.1007/BF02739471

Uchida, A., Kawai, N., Maekawa, H., 2000. Diagnosis method for seismic performance of Japanese traditional timber buildings, in: 6th World Conference on Timber Engineering, Whistler.

USSD, 2009. Managing Our Water Retention Systems, in: 29th Annual USSD Conference Nashville, Tennessee.

Villar-Vega, M., Silva, V., Crowley, H., Yepes, C., Tarque, N., Acevedo, A.B., Hube, M.A., Gustavo, C.D., María, H.S., 2017. Development of a Fragility Model for the Residential Building Stock in South America. Earthq. Spectra 33, 581–604. doi:10.1193/010716EQS005M

Wald, D.J., Worden, B.C., Quitoriano, V., Pankow, K.L., 2006. ShakeMap® manual. Technical Manual, users guide, and software guide Version.

Youngs, R.R., Chiou, S.-J., Silva, W.J., Humphrey, J.R., 1997. Strong Ground Motion Attenuation Relationships for Subduction Zone Earthquakes. Seismol. Res. Lett. 68, 58–73. doi:10.1785/gssrl.68.1.58

Zhao, J.X., 2006. Attenuation Relations of Strong Ground Motion in Japan Using Site Classification Based on Predominant Period. Bull. Seismol. Soc. Am. 96, 898–913. doi:10.1785/0120050122

ANNEX 1. DEFINITION OF THE BEST REPORTED VALUE OF LOSSES FOR HISTORICAL EARTHQUAKES

The validation of SPHERA earthquake model was made with 25 events for which country-scale reported losses were available. Although many more events have caused losses in the region, in most cases the available documentation only includes a qualitative description of the damages instead of a quantification of the final economic losses.

Aiming to define a best reported value for each event, an earthquake database was developed within the framework of this project. The best reported value is estimated to capture the reported direct losses for each event. Several data sources were considered, such as EM-DAT, ECLAC, USGS, NOAA, GEM Earthquake Consequences Database, AON's Catastrophe Insight, MunichRe's NatCat Service and SwissRe's Sigma Explorer, besides local sources and studies. In all cases, the reported values were adjusted using the consumer price index inflation calculator (CPI U.S.) for USD to obtain a present value amount. There are events for which direct economic losses are reported (mostly by ECLAC). In these cases that reported value has been considered as the best reported one.

It is worth noting that the procedure of estimating the best reported values in current money is more complicated for older events given the lack of information and considering that exposure extent and characteristics may differ a lot from current ones.

Next, for each event, a brief description of the estimation of the best reported value is provided:

- **Jamaica 1907 earthquake:** EM-DAT reports 30 M USD as material damages whereas CATDAT reports 13 M USD, at the time of the event. In present USD, these values are equivalent to 715 M USD and 316 M USD, respectively. After reviewing the description of damages reported mostly at Kingston, where around 85% of the buildings suffered considerable damage, the EM-DAT value is considered as more indicative of the direct losses.
- **Nicaragua 1931 earthquake:** Reported economic losses according to EM-DAT, CATDAT and local news are 15 M USD, 30 M USD and 35 M USD, respectively. As per the description of damages (including up to 2,450 fatalities), the highest value is chosen. Adjusted to present value it is equivalent to 524 M USD.
- **El Salvador 1951 earthquake:** The only source for economic losses of this event is EM-DAT that quantifies them in 23 M USD. In present value it is equivalent to 215 M USD.
- **Haiti 1952 earthquake:** The only reported value for economic losses according to EM-DAT is of 20 M USD, which in present value is equivalent to 180 M USD.
- **El Salvador 1965 earthquake:** Only one data source for economic losses of this event is available (EM-DAT), quantifying them in 35 M USD. In present value it is equivalent to 267 M USD.
- **Nicaragua 1968 earthquake:** The only value reported for economic losses is included in EM-DAT, equal to 2 M USD. In present value, it is equivalent to 14 M USD.
- **Nicaragua 1972 earthquake:** Total direct losses reported by ECLAC were quantified in 620 M USD. In present value, it is equivalent to 3,471 M USD.
- **Costa Rica 1973 earthquake:** The only information source for economic losses of this event is EM-DAT, which indicates a value of 0.2 M USD. In present value, it is equivalent to 1.1 M USD.
- **Guatemala 1976 earthquake:** Total direct losses reported by ECLAC were quantified in 748 M USD. In present value it is equivalent to 3,307 M USD.
- **El Salvador 1982 earthquake:** Only EM-DAT provides information about the economic losses of this event, quantifying them in 5 M USD. In present value, it is equivalent to 13 M USD.

- **Costa Rica 1983 earthquake:** Reported losses by EM-DAT are equal to 1 M USD which in present value is equivalent to 2.4 M USD.
- **El Salvador 1986 earthquake:** Total direct losses reported by ECLAC were quantified in 685 M USD. In present value it is equivalent to 1,478 M USD.
- **Costa Rica 1990 earthquake:** Reported losses by EM-DAT are equal to 19.5 M USD, a value that in present money is equivalent to 38 M USD.
- **Costa Rica 1991 earthquake:** Local reports in Costa Rica indicate economic losses of 222 M CRC (equivalent to 328 M USD, in present value). also, EM-DAT quantifies losses in 100 M USD and CATDAT in 902 M USD, in present value. As per the large description of damages in Costa Rica and Panama in housing, roads and bridges, the latter value is considered more representative and it was chosen as best reported value.
- **Nicaragua 1992 earthquake:** The only value reported for economic losses is included in EM-DAT, equal to 25 M USD. In present value, it is equivalent to 43 M USD.
- **Trinidad and Tobago 1997 earthquake:** Reported losses by EM-DAT are equal to 25 M USD, a value that in present money is equivalent to 37 M USD.
- **El Salvador 2001 (January) earthquake:** Total direct losses reported by ECLAC were quantified in 840 M USD. In present value, it is equivalent to 1,141 M USD.
- **El Salvador 2001 (February) earthquake:** Total direct losses reported by ECLAC were quantified in 185 M USD. In present value, it is equivalent to 251 M USD.
- **Costa Rica 2009 earthquake:** Total direct losses reported by UCR were 121 M USD. In present value these losses are equivalent to 141 M USD.
- **Honduras 2009 earthquake:** Reported economic losses by EM-DAT and Wikipedia are 100 M USD and 37 M USD, respectively. After a review of the reported damages and casualties, the second value was used as a reference. In present value it is equivalent to 42 M USD.
- **Haiti 2010 earthquake:** The value of the physical assets destroyed by the ground motion has been quantified in 4,302 M USD by the Post Disaster Needs Assessment (GFDRR). In present money this value is equivalent to 4,661 M USD.
- **Costa Rica 2012 earthquake:** According to Costa Rican National Emergencies Commission, damages to the physical assets were quantified in 50,600 M CRC. In present value, this amount is equivalent to 97 M USD.
- **Guatemala 2012 earthquake:** Several information sources were available for the economic losses caused by this earthquake. Values range between 102 M USD (AON) and 200 M USD (EM-DAT). After reviewing the description of damages and fatalities in several reports, the best reported loss is the one provided by AON, which in present value is of 107 M USD.
- **Nicaragua 2014 earthquake:** The only information source for economic losses of this event is EM-DAT, which indicates a value of 3 M USD.
- **Guatemala 2014 earthquake:** The only information source for economic losses of this event is EM-DAT, which indicates a value of 25 M USD.